

**Michaela Reif, Bsc**

**Development of a high throughput assay for  
esterases and modification of an esterase for  
broadened substrate scope**

**Master's Thesis**

to achieve the university degree of  
Master of Science  
Master's degree programme: Biotechnology

submitted to  
**Graz University of Technology**

Supervisor:  
Univ.-Prof. Dipl.-Ing. Dr.techn. Helmut Schwab  
Dipl.-Ing. Dr.nat.techn. Kerstin Steiner

Institute for Molecular Biotechnology – Graz University of Technology  
Austrian Center for Industrial Biotechnology (acib) – Graz

Graz, 12/2016

**Affidavit**

I declare that I have authored this thesis independently. I have not used other than the declared sources/resources, and that I have explicitly indicated all material, which has been quoted either literally or by content from the sources used. The text document uploaded to TUGRAZonline is identical to the present master's thesis.

-----  
Date

-----  
Signature

## **Acknowledgement**

At this point i want to say thank you to....

...Prof. Helmut Schwab for giving me the chance to do my master's thesis on the institue for molecular biotechnology.

...Kerstin Steiner for supervising me during the whole time of working on my thesis.

...DSM and acib for enabeling the work on this topic.

...Sarah Trunk for instructing me during my project lab.

...the whole team on the 4<sup>th</sup> floor for a great working atmosphere.

...my family and friends for supporting me.

## Abstract

The aim of this study was to develop and optimize a high throughput assay for screening esterase activity in organic solvents. As model reaction the transesterification reaction of vinylbutyrate with *tert*-butanol was chosen. The corresponding product alcohol – vinylalcohol - is transformed to acetaldehyde by keto-enol tautomerization. Hence, the detection of the released acetaldehyde can be the indicator for transesterification activity of esterases. However, the possible background reaction occurring by the hydrolysis of the vinylester has to be considered and excluded. Different aldehyde detection reagents were tested: 4-hydrazino-7-nitro-2,1,3-benzoxadiazole (NBDH), *N*-methyl-benzothiazolon-(2)-hydrazone (MBTH), 4-amino-3-hydrazino-5-mercapto-1,2,4-triazole (Purpald) and 1,3-cyclohexanedione (CHD). In the end aldehyde detection via NBDH turned out to be most suitable for screening purposes. In order to verify the assay different esterases from the strain collection from the institute of molecular biotechnology of the TU Graz were successfully analyzed. However, further tests on the reproducibility of the assay are necessary. In the second part of the study the substrate scope of EstB from *Burkholderia gladioli* should be modified. Eighteen different variants were created successfully via both overlap extension PCR and site-directed mutagenesis. All variants were expressed as soluble protein. With few exceptions all were active in an aqueous environment.

## Kurzfassung

Ziel dieser Arbeit war die Entwicklung und das Optimieren eines Hochdurchsatzverfahrens zum Screenen der Esteraseaktivität in organischen Lösemitteln. Als Modellreaktion diente die Umesterungsreaktion von Vinylbutyrat mit *tert*-Butanol. Der entsprechende Produktalkohol – Vinylalkohol - wird anschließend durch Keto-Enol Tautomerization zu Acetaldehyd umgewandelt. Daher sollte die Messung des freigesetzten Acetaldehyds als Indikator der Syntheseaktivität von Esterasen dienen. Zu beachten sind mögliche Hintergrundreaktionen, die durch Spaltung des Vinylesters durch Hydrolyse auftreten können. In dieser Arbeit wurden verschiedene Reagenzien zur Aldehyddetektion getestet: 4-Hydrazino-7-nitro-2,1,3-benzoxadiazol (NBDH), *N*-Methyl-benzothiazolon-(2)-hydrazon (MBTH), 4-Amino-3-hydrazino-5-mercapto-1,2,4-triazol (Purpald) und 1,3-Cyclohexanedion (CHD). Am Ende erwies sich die Aldehyddetektion mit NBDH als am besten geeignet für das Screening. Zur Überprüfung der Richtigkeit des Assays wurden verschiedene Esterasen einer Stammsammlung des Instituts für Molekulare Biotechnologie der TU Graz erfolgreich gescreent. Trotzdem wurde festgestellt, dass weitere Tests in Bezug auf die Reproduzierbarkeit des Assays notwendig sind. Im zweiten Teil der Arbeit wurde die Substratazeptanz von EstB aus *Burkholderia gladioli* modifiziert. 18 verschiedene Varianten konnten entweder durch Overlap extension PCR und Site-directed mutagenesis erfolgreich hergestellt werden. Alle Varianten konnten als lösliches Protein exprimiert werden. Mit Ausnahme einiger Varianten waren alle in wässrigem Reaktionsmedium aktiv.

# Content

<u>Abstract</u>	<u>III</u>
<u>Kurzfassung</u>	<u>IV</u>
<u>Content</u>	<u>V</u>
<u>1 Introduction</u>	<u>- 1 -</u>
<b>1.1 ENZYMES IN BIOTRANSFORMATIONS</b>	<b>- 1 -</b>
1.1.1 CLASSIFICATION OF HYDROLASES	- 1 -
1.1.2 NATURAL OCCURRENCE AND INDUSTRIAL APPLICATIONS OF CARBOXYLESTERASES	- 2 -
1.1.3 STRUCTURE AND REACTION MECHANISM OF CARBOXYLESTERASES	- 3 -
1.1.4 ENZYMES IN ORGANIC SOLVENT	- 4 -
<b>1.2 PROTEIN ENGINEERING</b>	<b>- 6 -</b>
1.2.1 RATIONAL DESIGN	- 6 -
1.2.2 DIRECTED EVOLUTION	- 6 -
1.2.3 SELECTION AND SCREENING SYSTEMS	- 7 -
<b>1.3 HIGH THROUGHPUT ASSAYS FOR DETERMINING ESTERASE/LIPASE ACTIVITY</b>	<b>- 7 -</b>
<b>1.4 ALDEHYDE DETECTION METHODS FOR DETERMINING ESTERASE SYNTHESIS ACTIVITY</b>	<b>- 8 -</b>
1.4.1 ALDEHYDE DETECTION WITH HYDRAZINES	- 8 -
1.4.2 ALDEHYDE DETECTION WITH <i>N</i> -METHYL-BENZOTHAZOLON-(2)-HYDRAZONE (MBTH)	- 9 -
1.4.3 ALDEHYDE DETECTION WITH HANTZ'SCHE REAGENTS	- 10 -
1.4.4 ALDEHYDE DETECTION WITH 4-AMINO-3-HYDRAZINO-5-MERCAPTO-1,2,4-TRIAZOLE (PURPALD)	- 11 -
<b>1.5 ESTB FROM <i>BURKHOLDERIA GLADIOLI</i></b>	<b>- 12 -</b>
1.5.1 GENERAL INFORMATION ABOUT ESTB FROM <i>BURKHOLDERIA GLADIOLI</i>	- 12 -
1.5.2 STRUCTURE OF ESTB FROM <i>BURKHOLDERIA GLADIOLI</i> AND FUNCTION INVOLVED STRUCTURE SITES	- 13 -
<b>1.6 AIM OF THIS MASTER THESIS</b>	<b>- 14 -</b>
<u>2 Materials and Methods</u>	<u>- 15 -</u>
<b>2.1 MATERIALS AND EQUIPMENT</b>	<b>- 15 -</b>
2.1.1 CHEMICALS	- 15 -
2.1.2 EQUIPMENT	- 16 -
<b>2.2 METHODS</b>	<b>- 17 -</b>
2.2.1 DEVELOPMENT OF A HIGH THROUGHPUT ASSAY FOR SCREENING OF ESTER SYNTHESIS ACTIVITY OF ESTERASES IN ORGANIC SOLVENT	- 17 -
2.2.1.1 Aldehyde detection	- 17 -
2.2.1.1.1 Aldehyde detection with NBD-H	- 17 -

2.2.1.1.2	Measurement of the decrease of the vinyl substrate	- 18 -
2.2.1.1.3	Aldehyde detection with MBTH	- 18 -
2.2.1.1.4	Aldehyde detection with Purpald	- 19 -
2.2.1.1.5	Aldehyde detection with CHD	- 19 -
2.2.1.2	Methanol detection by an AOX/HRP coupled assay	- 19 -
2.2.2	CREATING ESTB VARIANTS FROM <i>BURKHOLDERIA GLADIOLI</i> ESTB	- 20 -
2.2.2.1	GeneJet Plasmid Miniprep	- 20 -
2.2.2.2	Creating EstB variants by overlap extension Polymerase Chain Reaction	- 20 -
2.2.2.3	Promega's Wizard SV gel and PCR clean up system	- 23 -
2.2.2.4	Cutting of the vector pMS470	- 23 -
2.2.2.5	Gibson cloning	- 23 -
2.2.2.6	Transformation of <i>E. coli</i> Top 10F' cells	- 24 -
2.2.2.7	Colony PCR and master plate	- 25 -
2.2.2.8	Sequencing	- 25 -
2.2.2.9	Creating of EstB variants by site-directed mutagenesis	- 25 -
2.2.2.10	Expression of different esterases in deep well plate (DWP) cultivation	- 26 -
2.2.2.11	Glycerol stocks	- 26 -
2.2.2.12	Cell lysis of deep well plate cultivation	- 26 -
2.2.2.13	Expression of EstB variants in shaking flask cultivation	- 27 -
2.2.2.14	Glycerol stocks	- 27 -
2.2.2.15	Cell harvest and cell disruption by sonication	- 27 -
2.2.2.16	Bio-Rad protein assay	- 27 -
2.2.2.17	Sodium Dodecyl Sulfate gel electrophoresis (SDS-PAGE)	- 27 -
2.2.2.18	Quantification of the percentage of EstB within the total protein amount	- 28 -
2.2.2.19	Lyophilization of lysate from <i>E. coli</i> strains	- 28 -
2.2.2.20	Screening for the detection of esterase activity via NBD-H	- 28 -
2.2.2.21	Screening for the detection of esterase activity via pH-shift	- 28 -
<b>3</b>	<b>Results and Discussion</b>	<b>- 30 -</b>
<b>3.1</b>	<b>DEVELOPMENT OF A HIGH THROUGHPUT ASSAY FOR SCREENING THE SYNTHESIS ACTIVITY OF ESTERASES IN ORGANIC SOLVENT</b>	<b>- 30 -</b>
3.1.1	ALDEHYDE DETECTION WITH NBD-H	- 30 -
3.1.2	PHOTOMETRIC DETECTION OF VINYL BUTYRATE AS INDICATOR FOR ENZYME ACTIVITY	- 38 -
3.1.3	ALDEHYDE DETECTION WITH MBTH	- 39 -
3.1.4	ALDEHYDE DETECTION WITH PURPALD	- 42 -
3.1.5	ALDEHYDE DETECTION WITH CHD	- 44 -
3.1.6	METHANOL DETECTION WITH AOX AND HRP	- 45 -
<b>3.2</b>	<b>CLONING EXPERIMENTS FOR CREATING ESTB VARIANTS</b>	<b>- 47 -</b>

---

3.2.1	MUTAGENESIS	- 47 -
3.2.2	EXPRESSION OF ESTERASE VARIANTS	- 50 -
3.2.3	SCREENING OF ESTB VARIANTS WITH THE PH-SHIFT ASSAY	- 53 -
<u>4</u>	<u>Conclusion</u>	<u>- 56 -</u>
<u>5</u>	<u>Tables</u>	<u>- 58 -</u>
<u>6</u>	<u>Figures</u>	<u>- 59 -</u>
<u>7</u>	<u>Literature</u>	<u>- 64 -</u>



# 1 Introduction

## 1.1 Enzymes in Biotransformations

The use of enzymes for catalyzing reactions has increased rapidly over the last decades. Applications can be found in chemical, pharma, cosmetics and food industries inter alia for the production of bulk and fine chemicals (e.g. biodiesel, bioethanol, amino acids, citric acid), pharmaceuticals (e.g. antibiotics, insulin), detergents (e.g. washing powder), food (e.g. beer, wine, cheese) or animal feed. Advantages are due to the availability of the biocatalysts in high yields and purity synthesized via microorganisms as well as to safe, sustainable and environmentally friendly handling. Both isolated enzymes and enzyme systems in living cells as biocatalysts are selective (regio-, chemo-, and enantioselectivity), efficient, fast and operate under mild conditions (low temperatures, low energy consumption) (Buchholz and Kasche, 2006). In comparison to chemical catalyzed processes fewer by-products are produced using biocatalysts. Reusability of enzymes is reached by immobilization strategies. Moreover, enzymes enable a broad range of reactions by different combinations of side chain residues forming the catalytic center, and modifications to improve performance can be made via methods of molecular biology (Beilen and Li, 2002; Buchholz and Kasche, 2006; Gutteridge and Thornton, 2005). In order to differentiate between reaction types enzymes are classified into six big groups: EC1 oxidoreductases, EC2 transferases, EC3 hydrolases, EC4 lyases, EC5 isomerases and EC6 ligases (Buchholz and Kasche, 2006). In the following the hydrolases, especially the esterases, will be described in detail.

### 1.1.1 Classification of hydrolases

Hydrolases (EC3) are defined by catalyzing the reversible cleavage of biochemical bonds in the presence of water. Further classification is due to the kind of bond hydrolyzed (EC3.x, EC3.x.x) and due to the substrate converted (EC3.x.x.x). A short overview of the different hydrolases can be seen in Table 1.

*Table 1: Overview of the enzyme class of hydrolases (EC3)*

Subclass	Acting on	Subclass	Acting on
EC3.1	Ester bonds	EC3.8	Halide bonds
EC3.2	Glycosidic bonds	EC3.9	P-N bonds
EC3.3	Ether bonds	EC3.10	S-N bonds
EC3.4	Peptide bonds	EC3.11	C-P bonds
EC3.5	C-N bonds, other than peptide bonds	EC3.12	S-S bonds
EC3.6	Acid anhydrides	EC3.13	C-S bonds
EC3.7	C-C bonds		

Within the subclass of esterases (EC3.1) sub-subclasses are defined considering the nature of the ester bonds (EC3.1.1 carboxylic ester hydrolases). Therein the group of carboxylesterases (EC3.1.1.1) is assigned amongst others (Bornscheuer, 2002; Boyce and Tipton, 2001; Panda and Gowrishankar, 2005). The reaction catalyzed is the conversion of a carboxylic ester to an alcohol and a carboxylate in the presence of water. In addition to carboxylic esters short chain triglycerides, which are partly soluble in water, can serve as a substrate. In vitro the thermodynamic equilibrium of the catalyzed reaction can be shifted to the formation of ester bonds, in the exclusion of water (Aranda et al., 2014; Bornscheuer, 2002; Faber, 2011). In addition to the carboxylesterases, the structural similar and frequent used triacylglycerol lipases (EC 3.1.1.3) catalyze the hydrolysis and synthesis of water-insoluble long-chain triacylglycerides (Buchholz and Kasche, 2006; Jaeger and Reetz, 1998). Besides different substrate specificities carboxylesterases and triacylglycerol lipases share the same mechanism of reaction for ester hydrolysis or formation (Buchholz and Kasche, 2006). This is described in the chapter 1.1.3.

### 1.1.2 Natural occurrence and industrial applications of carboxylesterases

Carboxylesterases are widely distributed in nature. They can be found in animals, plants, bacteria, fungi, yeast and humans. Naturally the enzyme class is involved in metabolic processes and degradation/detoxification reactions. Considering that, carboxylesterases are attractive tools in biotechnological applications inter alia in synthetic chemistry, food processing, agriculture and pharmaceutical industries (Bornscheuer, 2002; Panda and Gowrishankar, 2005). Examples for industrial applications are the synthesis of optical pure compounds like naproxen via the carboxyl esterase NP (Dröge et al., 2005; Quax and Broekhuizen, 1994) or the production of (+)-*trans*-chrysanthemic acid from (±)-*cis,trans*-ethyl chrysanthemate by a carboxylesterase from *Arthrobacter globiformis* (Nishizawa et al., 1992). Carboxylesterases in the mycelium of *Aspergillus oryzae* and *Rhizopus oryzae* were used for resolution of racemic 2-phenylpropionic acid. The corresponding S and R enantiomers could be produced in high purities of ~90 % and >97 %, respectively (Gandolfi et al., 2001; Romano et al., 2005). Wheelock *et al.* and Li *et al.* described the use of carboxylesterases in environmental monitoring and in situ detoxification of pyrethroids (Li et al., 2008; Wheelock et al., 2008). Human carboxylesterase 1 from the liver is studied intensively as well. Its involvement in the degradation of xenobiotics and endobiotic processing (Fleming et al., 2005) or the activation of the drug capecitabine, used for the treatment of breast cancer (Quinney et al., 2005) is important for pharmaceutical studies. Redinbo and Potter as well as Satoh and Hosokawa wrote a detailed review about carboxylesterases, especially mammalian/human carboxylesterases, and their pharmacological importance (Redinbo and Potter, 2005; Satoh and Hosokawa, 2006).

### 1.1.3 Structure and reaction mechanism of carboxylesterases

In general esterases, including all subclasses, mainly share a  $\alpha/\beta$  fold. In this fold the protein core is surrounded by  $\alpha$ -helices which link eight strands in a central  $\beta$ -sheet (Bornscheuer, 2002; Ollis et al., 1992). Exceptions having a deviant tertiary structure are for example EstB, a carboxylesterase from *Burkholderia gladioli*, which shows a  $\beta$ -lactamase fold, which will be described in more detail in 1.5.2 (Wagner et al., 2002). BioH, a carboxylesterase from *E.coli*, is one more example of a carboxylesterase which does not share the  $\alpha/\beta$  fold (Sanishvili et al., 2003). In the active site the catalytic triad of Ser-His-Asp/Glu, which can also be found in serine proteases, is present for catalyzing enzymatic reactions (Ollis et al., 1992; Romano et al., 2015). Corresponding conserved structures including the active site serine, reviewed by Arpigny and Jaeger, are the GX SXG motif, the GDS(L) motif or the SXXL motif, original found in class C  $\beta$ -lactamases (Arpigny and Jaeger, 1999). The basic mechanism of the catalytic triad is described below and can be seen in Figure 1. Reaction catalyzing actions for transesterification or hydrolysis reactions can be divided into four steps (Aranda et al., 2014; Faber, 2011; Romano et al., 2015):

- (I) activation of the serine hydroxyl group by the catalytic histidine/aspartate ( $H^+$  acceptor) for the nucleophilic attack of the hydroxyl group of serine on the carbonyl group of the substrate to form the first tetrahedral intermediate
- (II) formation of the acyl-enzyme complex with release of the alcohol by proton transfer from the histidine leaving group to the substrate and covalent binding of the substrate to serine
- (III) nucleophilic attack of a water or alcohol molecule (activation via histidine) on the carbonyl carbon of the intermediate to form a second tetrahedral intermediate by hydrolyzing the covalent intermediate
- (IV) release of the ester or acyl product by proton transfer from histidine to serine

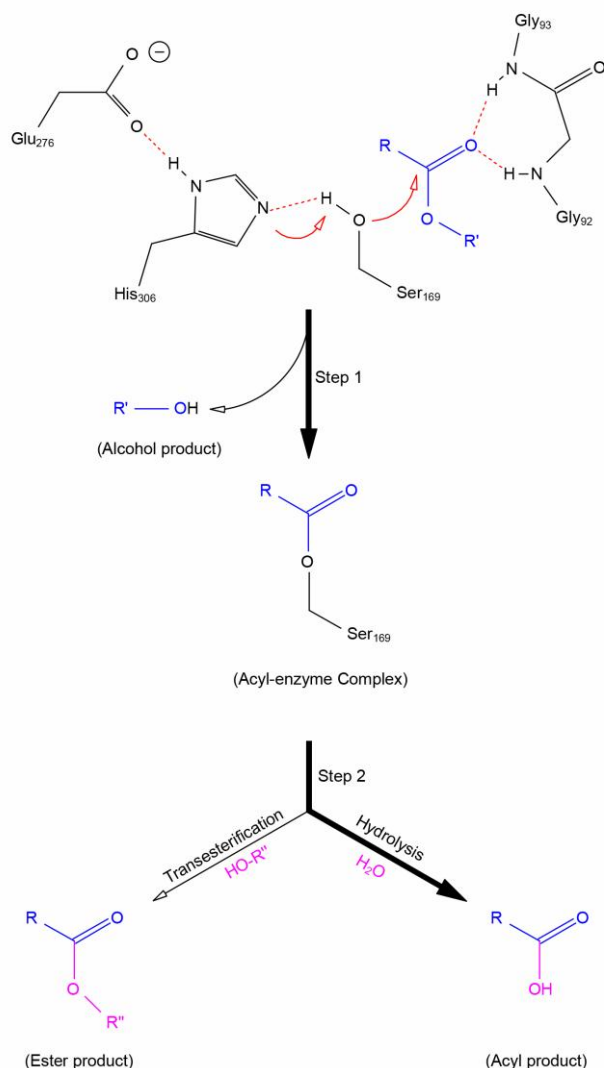


Figure 1: Reaction mechanism of the catalytic triad in the active site of hydrolases (Aranda et al., 2014)

#### 1.1.4 Enzymes in organic solvent

In the research of enzymes predominantly their behavior in their natural environment, an aqueous solution, is examined (Klibanov, 1989). Due to the possibility of shifting the thermodynamic equilibrium to the synthesis instead of hydrolysis reactions, research of alternative media like organic solvents became more important, especially in consideration of lipase or esterase activity. (Ingalls and Squires, 1975; Jakubke et al., 1985; Khmel'nitsky et al., 1988; Konopińska and Muzalewski, 1983). Further advantages of the use of organic solvents are due to insolubility of some substrates and/or products in water and due to minimizing bacterial contamination of the used equipment because of the antibacterial effect of organic solvents (Khmel'nitsky et al., 1988; Patsch and Höhne, 1971). Nevertheless it must be pointed out that enzyme stability and catalytic properties are changed in organic solvents compared to water. Therefore several things have to be considered: the choice of enzyme, the organic solvent, the water content, the drying processes and possible additives. The

enzyme should be readily available and inexpensive (Zaks and Klibanov, 1985). The organic solvent should be compatible with the desired reaction (solubility of substrate/product) and must not be involved in the reaction to avoid side reactions (Dordick, 1989). As both the activity and stability of the enzyme is influenced by the media it should neither inactivate or denature the enzyme nor destroy the enzyme's hydration shell. For correct folding of the enzyme hydrogen bonds and electrostatic and hydrophobic interactions are involved. To ensure these correlations a hydrate shell is needed which must not be destroyed for full catalytic power of the enzyme because otherwise the native conformation and the activity of the enzyme would get lost (Arakawa and Goddette, 1985; Brink and Tramper, 1985; Klibanov, 1989; Kuntz and Kauzmann, 1974; Rupley et al., 1983). To support the right choice of organic solvent Laane *et al.* 1987 correlated the solvents polarity with enzymatic activity via the distribution coefficient  $\log P$  ( $[x_{\text{organic solvent}}]/[x_{\text{water}}]$ ). The higher  $\log P$ , the lower the polarity of the solvent and the higher is the enzyme's activity (Laane et al., 1987; Sangster, 1997). A similar model was introduced by Brink and Tramper 1985 who used the Hildebrand solubility parameter. Low polarity of the solvent and a high molecular weight lead to a high activity of immobilized cells (Brink and Tramper, 1985). According to these results and the assumption that hydrophilic solvents strip essential water molecules from the enzyme, the use of hydrophobic solvents seems advantageous (Klibanov, 1989). Influencing factors are the solvent used and the enzyme structure (Buchholz and Kasche, 2006; Simon et al., 1998). A possibility to improve the activity of enzymes in organic solvents are immobilization or lyophilization (Persson et al., 2002b). Hereby the pH should be kept at the optimum of the enzyme before drying. Ionogenic groups of the protein keep their ionisation state while drying and the enzyme 'remembers' this for activity in organic solvents (Zaks and Klibanov, 1985). Emerging diffusional limitations have to be purged by creating well mixed suspensions of enzyme powder in organic solvent or by prior sonification to demagnify the solid particles (Khmelnitsky et al., 1988; Klibanov, 1989). Other positive effects of drying the enzyme are higher thermo- and storage stability (Klibanov, 1989). The amount of water tolerable in the reaction medium has to be evaluated individually for each enzyme/solvent combination (Carrea et al., 1995; Khmelnitsky et al., 1988; Zaks and Klibanov, 1988). Furthermore polyethylene glykol (PEG), inorganic salts, crown ethers or cyclodextrines can be added before drying to protect the enzyme's aqueous shell and to stabilize it in organic solvents (Inada et al., 1986; Khmelnitsky et al., 1988; Lee and Dordick, 2002; Mine et al., 2003; Persson et al., 2002a, 2002b; Ru et al., 2000; Serdakowski and Dordick, 2008). A review of possible additives for enzyme activation prior to lyophilization was made by Serdakowski and Dordick 2008. In addition to the enzyme's over all activity, its substrate specificity as well as its enantio-, prochiral-, regio- and chemical selectivity change if an organic solvent is used as medium. Detailed effects have to be evaluated for each substrate/enzyme/organic solvent

combination separately (Wescott and Klivanov, 1994). The same applies for the general behavior of different carboxyesterases in organic solvents. Predictions on activity or stability are not possible and have to be evaluated separately for each reaction system. As there are little assays to screen for esterase activity in non-aqueous environment, the development of the same was one aim in the present work. Acetaldehyde, released at transesterification reactions by the use of a vinylsubstrate, should serve as an indicator for enzymatic activity in organic solvents. General different aldehyde detection methods are described in 1.4.

## 1.2 Protein engineering

Two strategies are possible to manipulate the enzyme's properties with molecular biological methods: directed evolution or rational design; the general goal of protein engineering approaches is the overall improvement of the enzyme's properties (activity, selectivity, stability) towards applications of interest. Things to consider are the availability of the gene and its structure, a proper expression host and adequate systems for identifying improved enzyme variants (Bornscheuer and Pohl, 2001; Böttcher and Bornscheuer, 2010; Buchholz and Kasche, 2006; Kazlauskas and Bornscheuer, 2009). Basic information about the course of action of the two possible ways is explained in the next chapters.

### 1.2.1 Rational design

Rational design is defined by the introduction of mutations in a directed way (site-directed mutagenesis). Essentially for the approach is the knowledge about the structure and the relations of sequence, structure and mechanism and function of the protein of interest. X-ray crystallography or NMR structure analysis can report data about the crystal structure. Latter sometimes can give information about protein dynamics as well respectively (Bornscheuer and Pohl, 2001; Buchholz and Kasche, 2006). In addition, the tool of molecular modeling based on sequence homologies helps (1) to understand the behavior of the enzyme (2) to predict effects of changing substrates or reaction condition on the enzyme's performance (3) to anticipate stereoselectivity of enzymatic conversions (Kazlauskas, 2000).

### 1.2.2 Directed evolution

The basic principle of directed evolution is the mutagenesis of the gene of interest in a random way, the creation of mutant libraries and subsequent selection and screening to identify the best variant (Bornscheuer and Pohl, 2001; Buchholz and Kasche, 2006). Random mutagenesis or recombination techniques enable the generation of mutant libraries. First mostly is reached via error prone polymerase chain reaction (epPCR) (Cadwell and Joyce, 1992). The conditions of the PCR protocol are designed to make 'incorrect' sequences per using  $Mn^{2+}$  instead of  $Mg^{2+}$  (the cofactor of the polymerase), per using the Taq polymerase, which does not have a proof reading function or per using imbalanced amounts of deoxynucleotides (dNTPs) (Buchholz and Kasche, 2006). Alternatively to epPCR

the method of sequence saturation mutagenesis (SeSaM (Wong et al., 2004)) can be applied. Second is achieved by homology dependent DNA shuffling (Stemmer, 1994) e.g. via the staggered extension process (StEP (Zhao et al., 1998)) or methods independent of DNA homology e.g. SHIPREC (Sieber et al., 2001), ITCHY (Ostermeier et al., 1999) and SCRATCHY (Lutz et al., 2001). The random introduction of mutations into a gene can involve the complete sequence of the gene or, if some data about structure related functions are available, single parts of the gene e.g. via cassette mutagenesis (Bornscheuer and Kazlauskas, 2011; Buchholz and Kasche, 2006). The next step is to screen the mutant libraries for the best variant. Further details about selection and screening systems can be found in 1.2.3.

### 1.2.3 Selection and screening systems

The most important part in the field of protein engineering is the identification of improved variants. Especially in the approach of directed evolution huge mutant libraries are created which need to be analyzed in a high throughput way. Therefore selection and screening systems are necessary. Things to consider are easy handling of the assay, reproducibility, a high throughput and reaction conditions fitting to process applications (Schmidt and Bornscheuer, 2005). In selection based approaches growing advantages/disadvantages are used to enrich certain microorganisms producing the desired enzyme variant. Even though the system allows high throughput it is limited to enzymatic reactions of the host, whereas screening systems allow analysis of a broad range of reactions. Gas chromatography or high performance liquid chromatography are time consuming. Therefore assays with a spectrometric or fluorescent measurement in microtiter plates are the methods of choice to increase the number of analysis/time (Buchholz and Kasche, 2006).

### 1.3 High throughput assays for determining esterase/lipase activity

For the screening of lipase or esterase activity the corresponding released reaction products (alcohol, acid, ester) can be used to determine enzymatic activity (Romano et al., 2015). Common colorimetric/fluorescent substrates used for the determination of lipase/esterase activity in the presence of water are phenolics like *p*-nitrophenol, umbelliferon or resorufin and their esters. Things to consider here are the instability of some ester substrates at high/low pH and the possibility of false positive results due to the use of non-natural substrates. The enzymatic conversion of an acetate by lipases/esterases can be used as alternative to the before mentioned analysis procedures. The reaction initiates an enzymatic cascade. The hydrolysis of the acetate releases acetic acid. Latter is converted by the acetyl-CoA-synthase to acetyl-CoA. Then further reactions of the citric cycle come into play. ATP, coenzyme A and NAD<sup>+</sup> are required in the reaction cascade. Hence the increasing NADH can be measured spectrometric at 340 nm to determine lipase/esterase activity (Mateos-

Díaz et al., 2012; Schmidt and Bornscheuer, 2005). Possibilities for determining lipase/esterase activity in an anhydrous environment are described in the following.

#### 1.4 Aldehyde detection methods for determining esterase synthesis activity

In transesterification reactions of hydrolases in the absence of water, an ester and an alcohol are converted to their corresponding ester and alcohol. In the case of a vinyl ester as substrate a vinyl alcohol is released. Afterwards keto-enol tautomerization transforms the vinyl alcohol to acetaldehyde, which can be detected as an indicator for enzyme activity. A factor to consider are possible side reactions by hydrolysis of the vinyl ester in the presence of even small amounts of water, which leads to the release of a vinyl alcohol and acetaldehyde, respectively (Konarzycka-Bessler and Bornscheuer, 2003). General methods for aldehyde detection comprise the derivatization of the aldehyde and its detection with spectrometric or fluorescent measurement methods. Derivatizing agents must form a stable product with the analyte which has to fit subsequent analysis methods. In literature derivatizing agents are hydrazines, Hantzsch reagents, MBTH, Purpald, chromotropic acid and parasoaniline. Most of them form a colored/fluorogenic complex via a condensation reaction with the analyte. Detection is carried out with spectrophotometric or fluorescence measurement. In a mixture with more than one aldehyde only the sum of them can be determined. Hence convenient chromatographic separation or a selective detergent reagent, e.g. chromotropic acid for formaldehyde, are required (Vogel and Karst, 2000). Aldehyde detection methods described in literature as well as their possible high throughput applications on screening libraries in an effective way for esterase activity are described below.

##### 1.4.1 Aldehyde detection with hydrazines

Hydrazines are the most used derivatizing agents for aldehyde and ketone detection. The basic reaction mechanism is the coupling of the aldehyde or ketone with the hydrazine forming its corresponding hydrazone. After chromatographic separation of the hydrazines and their derivatives detection of latter is possible via UV/vis or fluorescence measurement (Vogel and Karst, 2000). The most popular hydrazine for aldehyde and ketone detection is 2,4-dinitrophenyl-hydrazine (DNP-H). It is a nitroaromatic hydrazine, which was first mentioned to use for this purpose by Allen *et al.* 1930 and Brady *et al.* 1931. High temperatures and an acidic environment are required for the detection reaction (Allen, 1930; Brady, 1931; Vogel and Karst, 2000). Applications of this method can be found mainly for air samples (Beasley et al., 1980; Grosjean and Fung, 1982). Alternatively hydrazines with benzoxadiazole backbone like 4-hydrazino-7-nitro-2,1,3-benzoxadiazole (NBD-H), 4-aminosulphonyl-7-hydrazino-2,1,3-benzoxadiazole (ABD-H) and 4-(*N,N*-dimethyl-aminosulphonyl)-7-hydrazino-2,1,3-benzoxadiazole (DBD-H) are described in literature



(Uchiyama et al., 2001; Uzu et al., 1990). The reaction mechanism for the detection reaction by NBD-H in a high throughput way, which is applied in this work, based on the method described by Konarzycka-Bessler and Bornscheuer 2003, is shown in Figure 2.

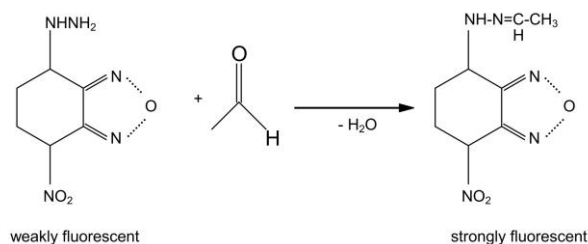


Figure 2: Reaction mechanism of NBD-H with aldehydes to the corresponding hydrazone (Konarzycka-Bessler and Bornscheuer, 2003)

The weakly fluorescent NBD-H undergoes a condensation reaction with the carbonyl group of the aldehyde producing a strongly fluorogenic derivative. The fluorogenic product can be detected at 485 nm excitation and 520 nm emission. As a model reaction transesterification of vinyl laurate with 1-propanol by different freeze-dried esterases and lipases in microtiter plates is described. Solvents tested were isooctane, *n*-hexane and petroleum ether. Fluorescence measurement was carried out at 45° C. A linear range ( $R^2=0.9982$ ) from 0 to 0.02 mM of acetaldehyde was reached for the calibration curve with isooctane as solvent. Enzyme activity was analyzed by measuring the released acetaldehyde. As both the enzymatic and the detection reaction can be carried out in organic solvents an on-line measurement is possible here (Konarzycka-Bessler and Bornscheuer, 2003).

#### 1.4.2 Aldehyde detection with *N*-methyl-benzothiazolon-(2)-hydrazone (MBTH)

The use of MBTH as a detection reagent for aliphatic aldehydes was first described by Sawicki *et al.* 1961. The basic mechanism can be seen in Figure 3.

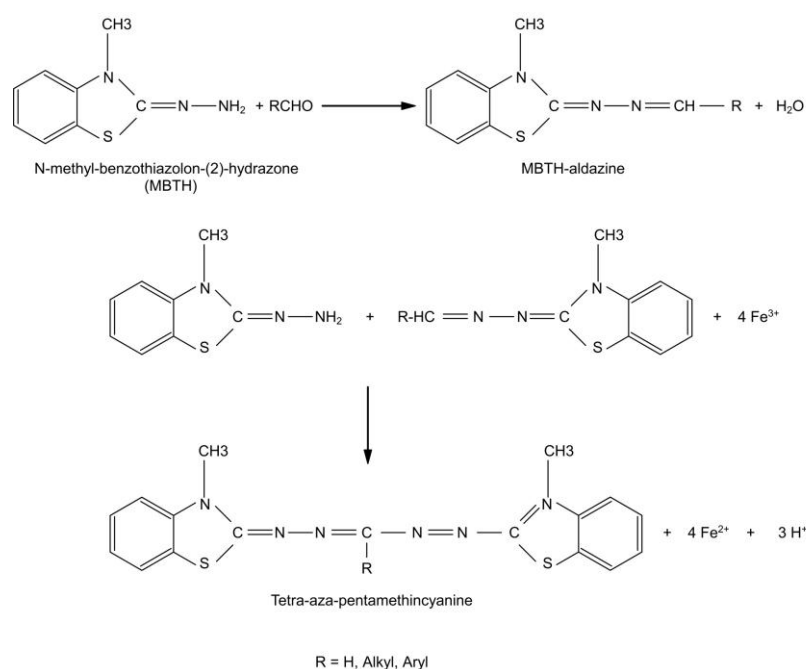


Figure 3: Reaction mechanism of MBTH with aldehydes via the corresponding aldazine to the blue colored tetra-aza-pentamethincyanine (Vogel and Karst, 2000)

The aldehyde and one molecule of MBTH form the corresponding aldazine. Further reaction to the intensive blue colored tetra-aza-pentamethincyanine (TAPMC) occurs by oxidative coupling with another MBTH molecule in the presence of Fe<sup>3+</sup> and H<sup>+</sup> (Hauser and Cummins, 1964; Hünig and Fritsch, 1957; Nebel, 1981; Sawicki et al., 1961). The selectivity of this detection reagents depends on the analytes structure and experimental conditions (Vogel and Karst, 2000). Zheng *et al.* used the just described reaction mechanism for developing a high throughput assay for the screening of lipase synthesis activity in 2014. As a model reaction lipase-catalyzed transesterification between vinylacetate and *n*-butanol in *n*-hexane was chosen. The released acetaldehyde was derivatized by MBTH and the maximum absorption of the corresponding TAPMC was measured at 598 nm. A linear range ( $R^2=0.9994$ ) from 0.001 to 0.15 mM of acetaldehyde dilutions could be reached. Enzymatic reaction was carried out with both immobilized and lyophilized enzymes at 30 °C for 5 min at 200 rpm. The concentration of the acetaldehyde released was measured afterwards. All reactants were pre-dried with molecular sieves (4-Å) (Zheng et al., 2014).

### 1.4.3 Aldehyde detection with Hantz'sche reagents

Aldehyde detection with Hantz'sche reagents was first described by Nash in 1953. This derivatization method is specific for aldehydes. Mechanistically it is based on a cyclization reaction of an aliphatic aldehyde with two  $\beta$ -diketones (e.g. acetylacetone) and ammonia to the yellow colored and fluorescent 3,5-diacetyl-1,4-dihydro-2,6-lutidine (Nash, 1953; Vogel and Karst, 2000). Sawicki and Carnes 1968 described dimedone (5,5-dimethyl-1,3-cyclohexanedione) and 1,3-cyclohexanedione (CHD) as new reagents for  $\beta$ -diketones

(Sawicki and Carnes, 1968). The general reaction mechanism of Hantz'sche reagents is shown in Figure 4. Disadvantageous of this method are the high temperatures necessary for the reaction. Alternatively, acetoacetanilide was introduced in 2007 by Li *et al.* Here mild reaction conditions at room temperature are applicable. Detection can be carried out with both spectrophotometric and fluorescent measurement, whereas latter presumably increases sensitivity (Bailey *et al.*, 1997; Holley *et al.*, 1993; Koizumi and Suzuki, 1988; Li *et al.*, 2007; Nash, 1953; Pickard and Clark, 1984; Sawicki and Carnes, 1968).

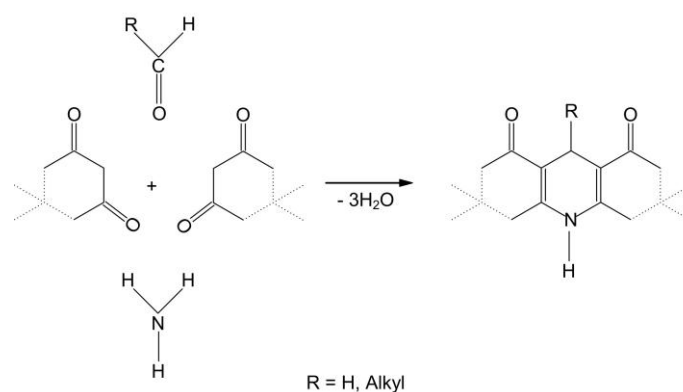


Figure 4: Reaction mechanism of Hantz'sche reagent. Condensation reaction of aldehydes with ammonia and acetylacetone (solid line) or dimedone (dotted line) (Vogel and Karst, 2000)

The paper at the basis for this work was from Vidal *et al.* 2014, who described derivatization for monoaldehydes with CHD. Detection solution was prepared by dissolving 0.4 mg ammonium acetate and 13 mg CHD in 10 mL 100 mM phosphate buffer pH 7.4. Fluorescence measurement was accomplished at 395 nm excitation and 460 nm emission (Vidal *et al.*, 2014). High throughput assays using CHD for aldehyde detection have not been found in literature search for the present work.

#### 1.4.4 Aldehyde detection with 4-amino-3-hydrazino-5-mercapto-1,2,4-triazole (Purpald)

In contrast to the before mentioned detection reagent Purpald needs alkaline conditions to react with aliphatic and aromatic aldehydes. First there is a cyclization step of the two reactants to an aminal. Second the aminal is oxidized to mercapto-triazolo-tetrazine, where the mercapto group is deprotonated to the corresponding anion, which is pink and can be determined via vis spectroscopy (Dickinson and Jacobsen, 1970; Jacobsen and Dickinson, 1974; Quesenberry and Lee, 1996). The basic reaction mechanism is shown in Figure 5.

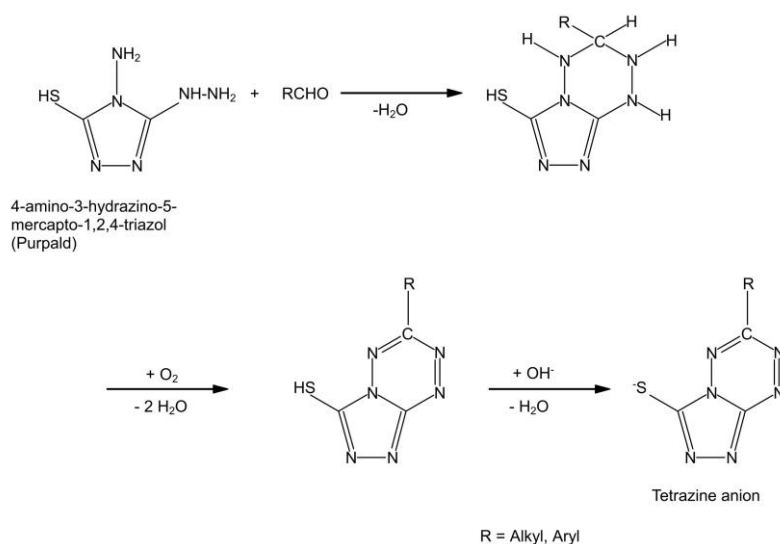


Figure 5: Reaction mechanism of Purpald (Vogel and Karst, 2000)

The procedure for aldehyde detection via Purpald used in the present work was based on the internal report from Petek 2015. The aldehyde detected was benzaldehyde. Different concentrations of Purpald, NaOH and aldehyde were evaluated as well as different incubations times (Petek, 2015). High throughput applications using Purpald as a detection reagent for aldehydes are described for formaldehyde (Jendral et al., 2011; Quesenberry and Lee, 1996; Zurek and Karst, 1997).

## 1.5 EstB from *Burkholderia gladioli*

### 1.5.1 General information about EstB from *Burkholderia gladioli*

EstB was discovered in 1991 from the bacterium *Burkholderia gladioli* via screening of a genomic library of the microorganism (Stubenrauch, 1991). First characterization was done by Schlacher *et al.* 1997 which had a focus on the substrate acceptance of the enzyme (EP6). A high activity on naphthol esters of short chain carboxylic acids (C<sub>2</sub>-C<sub>4</sub>) could be measured. On fluorogenic HPTS-carboxylic acid esters no activity could be determined. Therefore a dependence of the alcohol and the carboxylic acid ester of the esterase on substrate usability was indicated. In addition enantioselective activity as well as activity on bulky substrates like linalyl acetate, which is a ester of a tertiary alcohol and not well accepted by common lipases and esterases, could be observed (Schlacher et al., 1998). Due to the activity on fatty acid esters (C<sub>4</sub>-C<sub>6</sub>) and on triglycerides the water soluble enzyme can be classified as carboxylesterase. What is more is that high deacetylation activity on cephalosporines appeared. This is advantageous for the production of semisynthetic cephalosporin derivatives in industry. Peptidase or β-lactamase activity could not be found although sequence similarities to those hydrolases were shown. The temperature optimum for activity lies at 45 °C but decreases at longer incubation times. The pH optimum is at pH 7. Activity inhibiting substances are inter alia Eserin, NaF and HgCl<sub>2</sub> (Petersen et al., 2001).

Further details about the structure and structure dependent functionalities are described in the next chapter.

### 1.5.2 Structure of EstB from *Burkholderia gladioli* and function involved structure sites

Sequence analysis of EstB by Petersen *et al.* 2001 showed that the enzyme has a size of 392 amino acids and a molecular mass of 41 695 Da. A seven stranded antiparallel  $\beta$ -sheet forms the center of the enzyme's structure. One helix at the N- and three helices at the C-terminus cap the 'front' and the 'back' of the  $\beta$ -sheet. Homologies to  $\beta$ -lactamases, penicillin binding proteins and DD-peptidases could be found by comparison of the amino acid sequences. The serine at position 75, which is part of the  $\beta$ -lactamase motif (S-X-X-K) can be found at the beginning of the second helix. Site-directed mutagenesis (S75->A75) and the crystal structure of the enzyme showed that the hydroxyl group of S75 is the active nucleophile. It attacks the activated ester-carbonyl of the substrate. Activation takes place via hydrogen bonds between the carbonyl oxygen and main-chain NH groups of S75 and V351. Improvement of nucleophilicity is achieved by the general base Y181. The function of EstB was completely lost in the A75 variant. The S149 within the serine hydrolase motif (G-X-S-G), which lipases and esterases have in common, did not influence the enzyme's activity (Petersen *et al.*, 2001; Wagner *et al.*, 2002). Accessibility of the active site in EstB is from the 'front' via a tunnel. A  $\beta$ -sheet (residues 249 to 255) and a loop (residues 314 to 320) narrow the entrance by partly covering it (Wagner *et al.*, 2002). Amino acids presumably important in the catalytic mechanism are S75, K78, Y181 and W348 (Valinger *et al.*, 2007). Studies concerning modification of enantioselectivity of EstB were made via directed and designed evolution by Ivancic *et al.* 2007. Preference for the hydrolysis of the model substrate methyl- $\beta$ -hydroxyisobutyrate was the S-product. Random mutagenesis combined with saturation mutagenesis resulted in both improvement (I152M/L) and impairment (I152S/T/V/A) of S-selectivity as well as in a change to R-selectivity (I152N). Further enhancement of the R-selective variant was achieved by designed evolution at positions S75, K78, Y133, L135, D150, Y181, D186, L249, H253, A256, V257, S272, G274, A275, W348, G349, G350, V351 and M377, which are in the surrounding of S75 in the enzyme's tertiary structure. Resulting best variants had the mutations L135H, H253L and V351A/C/S (Ivancic *et al.*, 2007). Docking experiments by Georg Steinkellner (Group of Karl Gruber) could identify amino acid residues which are involved in building tunnels for the substrate and product entering and leaving the active site of EstB. The entrance of tunnel2 is surrounded by W134, D153, R155 and R258. Possible targets for widening up the access are replacements of Y133, W134, L135, D150, I152, D153, R155, L249, H253, V257, V257, R258, A275, V351 and M377 to smaller amino acids (personal communication with Kerstin

Steiner). Resulting influences of these sequence changes on enzyme's activity still have to be examined.

### 1.6 Aim of this master thesis

In order to screen libraries of esterase or lipase variants in an effective way high throughput assays are needed. Requirements therefore are low costs and an easy to handle time-saving procedure. As there are few high throughput assays for the screening of hydrolases in ester synthesis in organic solvent, the development and optimization of such an assay was one aim of the present work. As model reaction transesterification reaction of vinylbutyrate and *tert*-butanol in organic solvent should be analyzed. Besides the before mentioned aldehyde detection methods via NBD-H, MBTH, CHD and Purpald, measurement of the decline of the vinyl substrate should be evaluated for the application as a screening assay in a high throughput way. In addition, the detection of methanol, released during transesterification reactions with a methylester as substrate, should be investigated.

The aim of the second part of the present work was to create different variants of EstB from *Burkholderia gladioli* via rational design to broaden the enzyme's substrate scope.

## 2 Materials and Methods

### 2.1 Materials and Equipment

#### 2.1.1 Chemicals

Acetaldehyde $\geq 99.5$ % ACS	Sigma Aldrich
Acetonitrile HPLC Gradient Grade $> 99.9$ %	ChemLab
Agarose pegGold universal	Peqlab
Alcohol oxidase (AOX)	Sigma Aldrich
4-amino-3-hydrazino-5-mercapto-1,2,4-triazole (Purpald)	Sigma Aldrich
Ammonium acetate ( $\text{NH}_4\text{CH}_3\text{CO}_2$ )	Carl Roth GmbH
Ampicillin	Carl Roth GmbH
2,2'-azino-bis(3-ethylbenzothiazoline-6-sulphonic acid) (ABTS)	Sigma Aldrich
Benzonase	Merck
<i>tert</i> -Butanol Rotipuran <sup>®</sup> $\geq 99.5$ % p.a. ACS	Carl Roth GmbH
<i>tert</i> -Butylmethylether (tBME) $\geq 99.5$ %	Carl Roth GmbH
Bradford reaction solution	Bio-Rad Laboratories Inc.
Diethylether anhydrous $\geq 99.0$ % ACS	Sigma Aldrich
Dimethylsulfoxide (DMSO) Rotipuran <sup>®</sup> $\geq 99.8$ % p.a.	Carl Roth GmbH
Dimethylformamide (DMF) anhydrous 99.8 %	Sigma Aldrich
Deoxynucleotide triphosphates (dNTPs)	Thermo Fisher Scientific
GeneJet Plasmid Miniprep Kit	Thermo Fisher Scientific
<i>n</i> -Hexane 99 %	LAB Scan
<i>Hind</i> III	NewEngland Biolabs
4-hydrazino-7-nitro-2,1,3-benzoxadiazole (NBD-H)	TCI
Isooctane $\geq 99.5$ % p.a. ACS	Fluka
Isopropyl- $\beta$ -D-1-thiogalactopyranoside (IPTG)	Biosynth
Iron(III)chloride ( $\text{FeCl}_3$ ) hexahydrate	Fluka
Kanamycin	Carl Roth GmbH
Loading dye 6x	Thermo Fisher Scientific
Lysogeny broth (LB) agar 35 g/L Lennox	Carl Roth GmbH
Lysogeny broth medium 20 g/L Lennox	Carl Roth GmbH
Lysozyme from chicken egg $\sim 70000$ U/mL	Fluka
3-methyl-2-benzothialinone (MBTH)	Fluka
Methanol	Carl Roth GmbH
Methylester (MeEst)	DSM
<i>Nde</i> I	NewEngland Biolabs
Horse radish peroxidase (HRP)	Sigma Aldrich
Hydrochloric acid (HCl) 0.1 N stock solution	Carl Roth GmbH
Disodiumhydrogenphosphate ( $\text{Na}_2\text{HPO}_4$ )	Carl Roth GmbH
Sodiumdihydrogenphosphate ( $\text{NaH}_2\text{PO}_4$ )	Carl Roth GmbH

Sodiumhydroxide (NaOH)	Carl Roth GmbH
O'Gene Ruler DNA Ladder Mix (0.1 µL)	Thermo Fisher Scientific
Phenol red sodium salt	Sigma
Phusion Polymerase, 2 U/µL	Thermo Fisher Scientific
Potassium chloride (KCl)	Carl Roth GmbH
Primer	IDT
Dipotassium hydrogen phosphate (K <sub>2</sub> HPO <sub>4</sub> )	Carl Roth GmbH
Potassium dihydrogen phosphate (KH <sub>2</sub> PO <sub>4</sub> )	Carl Roth GmbH
Tetrahydrofuran (THF)	Fluka
Trichlormethane (CHCl <sub>3</sub> )	Carl Roth GmbH
Triton-X 100	Carl Roth GmbH
2xTY medium	Carl Roth GmbH
Vinylbutyrate	Sigma Aldrich
Vinylester (VinEst)	DSM
Wizard SV Gel and PCR Clean up System	Promega

### 2.1.2 Equipment

37 °C/30 °C Incubator	Binder
96 well plates black/transparent	Greiner and Nunc
Centrifuge 5415R	Eppendorf
Centrifuge 5424	Eppendorf
Centrifuge 5810R	Eppendorf
Deepwell plates	Greiner
Desalting membrane	Milipore
Electroporator Micro Pulser™	BioRad
G-Box HR16	SYNGENE
Filter PES 0.45 µm	Agilent Technologies
FLUOstar omega platereader	BMG Labtech
Lyophilisator Christ alpha loc-1m	Braun Biotech International
Magnetic stirrer MR3001K	Heidolph
MicroAmp™ Optical Adhesive Film	Applied Biosystems
Multicanal pipette	Eppendorf
NanoDrop 2000c Spectrophotometer	Thermo Scientific
Plate reader Eon	BioTekR
Plate reader SYNERGYMx	BioTekR
Plate sealer silverseal aluminium	Greiner Bio One GmbH
Scanner Agarosegel Fischer Brand FT-28/312	Herolab GmbH Laborgeräte
Shaker CeromatR BS-1	Sartorius
Thermocycler 2720	Applied Biosystems
Thermomixer comfort	Eppendorf



Scale BL 120 S  
Sonification

Sartorius  
Branson Sonifier S-250

## 2.2 Methods

### 2.2.1 Development of a high throughput assay for screening of ester synthesis activity of esterases in organic solvent

The reaction products from transesterification reactions, acetaldehyde and methanol, depending on the substrate, were used as indicators for measuring enzyme activity. Different methods are described below.

#### 2.2.1.1 Aldehyde detection

##### 2.2.1.1.1 Aldehyde detection with NBD-H

Based on a method described by Konarzycka-Bessler and Bornscheuer (2003) a calibration curve of acetaldehyde was measured by mixing 100  $\mu$ L of acetaldehyde dilutions in organic solvent with 100  $\mu$ L NBD-H in black 96 well polystyrene (PS) plates with transparent bottom. For a blank acetaldehyde was replaced by organic solvent. The NBD-H solution was prepared by dissolving 1 mg in 11 mL of organic solvent for 15 min in a sonication bath. Insoluble particles were removed by centrifugation for 5 min at 3220 g. To avoid evaporation of the acetaldehyde and the organic solvent the plates were sealed with a transparent adhesive film before fluorescence measurement with the FLUOstar Omega platereader.

The influence of following parameters were tested by establishing an acetaldehyde calibration curve:

- organic solvents:  
isooctane:1-propanol 10:1 (v/v), isooctane:1-butanol 10:1 (v/v), isooctane:*tert*-butanol 10:1 (v/v), isooctane:*tert*-butanol 1:10 (v/v), *tert*-butanol, *n*-hexane:*tert*-butanol 1:1 (v/v), dimethylsulfate (DMSO):*tert*-butanol 1:1 (v/v), acetonitrile:*tert*-butanol 1:1 (v/v), *tert*-butylmethylether (tBME):*tert*-butanol 1:1 (v/v), dimethylformamide (DMF):*tert*-butanol 1:1 (v/v) and tetrahydrofuran (THF):*tert*-butanol 1:1 (v/v);
- temperature: 30 - 45 °C
- different intensities of mixing: no mixing, short stirring, shaking step of plate reader at 500 rpm for 1 - 3 s
- batch of acetaldehyde and NBD-H
- acetaldehyde concentration range:  $c_{\text{final}}=0.001$  to 1 mM
- NBD-H concentration range:  $c_{\text{final}}\sim 0.1$  to 0.3 mM

Finally optimized conditions included the mixing of 100  $\mu$ L of acetaldehyde dilutions in the range of  $c_{\text{final}}=0.05$  to 0.8 mM in *tert*-butanol:*n*-hexane 1:1 (v/v) as organic solvent and 100  $\mu$ L of NBD-H solution ( $c_{\text{final}}\sim 0.2$  mM). Measuring parameters for the plate reader FLUOstar (BMG Labtech) are described below.

Excitation 485 nm, Emission 520 nm  
Top Optic  
Flying mode  
Number of flashes per well 1  
Shaking before every cycle step 500 rpm, 1 s  
Gain 1414  
Temperature 30 °C

#### 2.2.1.1.2 Measurement of the decrease of the vinyl substrate

According to Goujard *et al.* 2009 the absorption spectrum of vinylbutyrate at different concentrations ( $c_{\text{final}}=0.25, 0.5, 2.5$  and 5 mM) was measured at 30 °C in different organic solvents (*t*BME, DMSO, *tert*-butanol, isooctane, *tert*-butanol:isooctane 1:5 v/v) at wavelengths from 200 - 600 nm to determine the absorption maximum. The background of *E. coli* lysate on the spectrum was tested by measuring in the presence of different lysate concentrations ( $c_{\text{Protein}_{\text{final}}}=8.3$  mg/mL, 2.6 mg/mL and 0.8 mg/mL) in H<sub>2</sub>O.

For establishing a calibration curve a dilution series of vinylbutyrate in 200  $\mu$ L organic solvent ( $c_{\text{final}}=0.001 - 5$  mM in *tert*-butanol) was measured at 212, 216 and 222 nm at 30 °C in a transparent 96-well Cycloolefin-Copolymere (COC) plate suitable for UV. As blank the organic solvent was used. Before starting the measurement the plate was tape sealed with a transparent adhesive film to avoid evaporation of the organic solvent and the acetaldehyde. The influence of *E. coli* lysate on the measurement was tested by adding 0.2 and 0.5 mg/mL ( $c_{\text{final}}$ ) of protein containing lysate, measurement parameters were the same as described above.

#### 2.2.1.1.3 Aldehyde detection with MBTH

A high throughput way to apply MBTH as a screening agent for hydrolase activity is described by Zheng *et al.* 2014. The absorption maximum of the blue colored TAPMC was determined by recording a spectrum. This was done by mixing 100  $\mu$ L of acetaldehyde ( $c_{\text{final}}=0.1$  mM) in *n*-hexane with 100  $\mu$ L MBTH ( $c_{\text{final}}=0.2$  mM) in H<sub>2</sub>O. The first incubation time was 10 min. 40  $\mu$ L of FeCl<sub>3</sub> (5 mg/mL in 0.05 M HCl) were added and the second incubation lasted for 30 min. For the blank no acetaldehyde was added. The spectrum was measured from 400 - 800 nm after tape sealing the transparent 96 well plates with a transparent adhesive film to avoid evaporation of the acetaldehyde and the organic solvent.

For establishing a standard curve the measurement procedure was analog as described above. Acetaldehyde was used in the range of  $c_{\text{final}}=0.005$  -1 mM, MBTH was used in the concentration of  $c_{\text{final}}=2.4$  mM.

Absorption was measured at 606 nm. The influence of following parameters were tested: incubation time one (0 – 50 min) and two (0 – 90 min), concentration of HCl (0.1 mM – 0.1 M) and application of *E. coli* lysate (0.5 mg/mL; in liquid and lyophilized form). Optimized conditions for establishing the standard curve finally were incubation times of 20 min twice and the HCl concentration was kept at 0.05 M. By using lysate an additional centrifugation step (15 min, 3220 g) and the transfer of the 'reaction mix' to a new microtiter plate were necessary before the detection reaction.

#### 2.2.1.1.4 Aldehyde detection with Purpald

The project lab report from Simone Petek served as basis for the application of the procedure (Petek, 2015). The absorption maximum was determined by mixing 150  $\mu\text{L}$  of acetaldehyde ( $c_{\text{final}}=1$  mM and 10 mM) in *n*-hexane with 50  $\mu\text{L}$  of Purpald ( $c_{\text{final}}=1$  mM) in NaOH (1 M). A spectrum from 400 - 800 nm was measured after an incubation time of 15 min at room temperature. The calibration curve was established in the same course of action. Acetaldehyde was used in the range of  $c_{\text{final}}=0.005$  - 3 mM. Absorption was measured at 540 nm.

#### 2.2.1.1.5 Aldehyde detection with CHD

A calibration curve was established by mixing 100  $\mu\text{L}$  of acetaldehyde dilutions ( $c_{\text{final}}=0.005$  - 10 mM) in DMSO with 100  $\mu\text{L}$  CHD. Latter was prepared by resolving 13 mg with 400 mg ammoniumacetate in 10 mL sodium phosphate buffer (100 mM, pH 7). The reaction mix was incubated for 1 h at 37 °C. To avoid evaporation the black 96 well plate with transparent bottom was tape sealed with a transparent film. Fluorescence measurement was done at 460 nm emission and 395 nm excitation.

#### 2.2.1.2 Methanol detection by an AOX/HRP coupled assay

During transesterifications of a methylester methanol is released, which can be detected to determine enzyme activity. The reaction mix was prepared by mixing 914  $\mu\text{L}$  of ABTS (2 mg/mL in 100 mM KPi pH 7.4) with 6  $\mu\text{L}$  HRP (250 U/mL in ddH<sub>2</sub>O) and 80  $\mu\text{L}$  methanol/methylester/MeEst (DSM) stock (250 mM in ddH<sub>2</sub>O). Thereof 100  $\mu\text{L}$  were mixed with 80  $\mu\text{L}$  lysate (*E. coli*) in 100 mM KPi buffer pH 7.4. 20  $\mu\text{L}$  of AOX (100 mU/mL in buffer) were added immediately before the measurement was started. As blank buffer instead of AOX was added. Absorption was measured at 405 nm.

## 2.2.2 Creating EstB variants from *Burkholderia gladioli* EstB

### 2.2.2.1 GeneJet Plasmid Miniprep

Plasmid DNA was isolated from *E. coli* with the GeneJET plasmid miniprep kit. The general experimental steps are described below:

- Resuspension of the pelleted cells in 250  $\mu$ L resuspension solution in an 1.5 mL reaction tube
- Addition of 250  $\mu$ L lysis solution, mixing thoroughly by inverting the tube 4-6 times until the solution becomes viscous and slightly clear
- Addition of 350  $\mu$ L neutralization solution, mixing thoroughly by inverting the tube 4-6 times
- Centrifugation for 10 min at maximum speed
- Transfer of the supernatant to the GeneJET spin column by pipetting
- Centrifugation for 1 min at maximum speed, the flow through is discarded and the column is reinserted into the same collection tube
- Addition of 400  $\mu$ L wash solution
- Centrifugation for 1 min at maximum speed, the flow through is discarded and the column is reinserted into the same collection tube
- Addition of 400  $\mu$ L wash solution
- Centrifugation for 1 min at maximum speed, the flow through is discarded and the column is reinserted into the same collection tube
- Centrifugation for 1 min at maximum speed to remove residual wash solution
- Transfer of the GeneJET spin column into a fresh 1.5  $\mu$ L reaction tube
- Addition of 40  $\mu$ L water (Fresenius) to elute the plasmid DNA, incubation for 2 min at room temperature, centrifugation for 2 min at maximum speed
- Measurement of the concentration of the plasmid DNA via a spectrophotometric method (Nanodrop)

The purified plasmid DNA was stored at -20 °C.

### 2.2.2.2 Creating EstB variants by overlap extension Polymerase Chain Reaction (PCR)

For the PCR reaction following instructions were used.

PCR-1:

- |                                |                      |
|--------------------------------|----------------------|
| – 31 $\mu$ L deionized water   | Temperature program: |
| – 5 $\mu$ L DMSO (10 %)        | – 1 min 98 °C        |
| – 10 $\mu$ L 5x buffer GC      | – 45 sec 98 °C       |
| – 1 $\mu$ L dNTPs (10 mM each) | – 1 min 57 °C        |

- 1  $\mu$ L forward primer (10 pmol/ $\mu$ L)
- 1  $\mu$ L reverse primer (10 pmol/ $\mu$ L)
- 1  $\mu$ L template DNA (1 ng/ $\mu$ L)
- 0.5  $\mu$ L Phusion polymerase

- 45 sec 72 °C

- 7 min 72 °C

- keep on 4 °C

Number of cycles: 30

dNTPs, primers and template DNA were diluted with deionized water. As a template DNA pMS-EstB-Wildtype was used, outer primers were pMS-EstB-for and pMS-EstB-rev, inner primers as well as the corresponding sequences of all primers can be seen in Table 2.

Table 2: List of primers used with the desired mutation

name of primer	mutation	sequence	PCR 1 [bp]
EstB-Y133A_for	397TAC->GCC	GTCGGGGCTCGGCGCCTGGCTGCTCGAG	849
EstB-Y133A_rev		CTCGAGCAGCCAGGCGCCGAGCCCCGAC	466
EstB-Y133V_for	397TAC->GTC	GTCGGGGCTCGGCGTCTGGCTGCTCGAG	849
EstB-Y133V_rev		CTCGAGCAGCCAGACGCCGAGCCCCGAC	466
EstB-W134A_for	400TGG->GCG	GGCTCGGCTACGCGCTGCTCGAGGG	844
EstB-W134A_rev		CCCTCGAGCAGCGCGTAGCCGAGCC	468
EstB-W134F_for	400TGG->TTC	GGCTCGGCTACTTCCTGCTCGAGGGC	844
EstB-W134F_rev		GCCCTCGAGCAGGAAGTAGCCGAGCC	468
EstB-L135A_for	403CTG->GCG	CTCGGCTACTGGGCGCTCGAGGGCG	842
EstB-L135A_rev		CGCCCTCGAGCGCCCAGTAGCCGAG	470
EstB-D150A_for	448GAC->GCC	CTCGGCATCTCGGCCGGCATCGACCTG	797
EstB-D150A_rev		CAGGTCGATGCCGGCCGAGATGCCGAG	517
EstB-I152A_for	454ATC->GCC	CATCTCGGACGGCGCCGACCTGCGCGAC	792
EstB-I152A_rev		GTCGCGCAGGTCTGGCGCCGTCCGAGATG	523
EstB-D153A_for	457GAC->GCC	CGGACGGCATCGCCCTGCGCGACTTC	787
EstB-D153A_rev		GAAGTCGCGCAGGGCGATGCCGTCCG	526
EstB-R155A_for	463CGC->GCC	GGCATCGACCTGGCCGACTTCGATCTC	782
EstB-R155A_rev		GAGATCGAAGTCGGCCAGGTCGATGCC	542
EstB-R155V_for	463CGC->GTC	CGGCATCGACCTGGTCGACTTCGATCTC	782
EstB-R155V_rev		GAGATCGAAGTCGACCAGGTCGATGCCG	532
EstB-L249A_for	745CTG->GCG	CATCGAGGTGCCGGCGCCGGAAGGCCAC	501
EstB-L249A_rev		GTGGCCTTCCGGCGCCGGCACCTCGATG	814
EstB-H253A_for	757CAC->GCC	CTGCCGGAAGGCGCCGGCGCGGCCGTG	488
EstB-H253A_rev		CACGGCCGCGCCGGCGCCTTCCGGCAG	826
EstB-H253L_for	757CAC->CTC	GCCGGAAGGCCTCGGCGCGGCCG	488
EstB-H253L_rev		CGGCCGCGCCGAGGCCTTCCGGC	824
EstB-V257A_for	769GTG->GCG	CGGCGCGGCCGCGCGTTTCGCG	474
EstB-V257A_rev		CGCGAAACGCGCGGCCGCGCCG	835
EstB-R258A_for	772CGT->GCC	CGGCGCGGCCGTGGCCTTCGCGCCCTCC	474

EstB-R258A_rev		GGAGGGCGCGAAGGCCACGGCCGCGCCG	841
EstB-R258V_for	772CGT->GTG	CGGCGCGGCCGTGGTGTTCGCGCCCTCC	474
EstB-R258V_rev		GGAGGGCGCGAACACCACGGCCGCGCCG	841
EstB-V351A_for	1051GTC->GCC	CAATGGGGCGGCGCCTATGGCCATTC	194
EstB-V351A_rev		GAATGGCCATAGGCGCCGCCCATTTG	1119
EstB-M377A_for	1131ATG->GCG	CCTACGAAGGCGCGTCGGGCCCGC	115
EstB-M377A_rev		GCGGGCCCGACGCGCCTTCGTAGG	1196
pMS-EstB-for		AATAATTTTGTTTAACTTTAAGAAGGAGATAT ACATatgaccgctgcctcgctcg	-
pMS-EstB-rev		TGAAAATCTTCTCTCATCCGCCAAAACAGCC AAGCTTtcagcgcgctagacggcg	-

After the PCR reaction 10  $\mu$ L of loading dye (6x) were added into each tube before performing a preparative agarose gel electrophoresis (1 % Agarose in TAE buffer, 90 V, 1.5 h). Correct sized bands (~800/~500 bp) were cut out of the gel and put into a pre weight 2 mL tube. Purification was done with Promega's Wizard SV gel and PCR clean up system according to the manual with the exception of DNA elution. The experimental steps are described in 2.2.2.3. As standard O'GeneRuler™/Gene ruler 1kb DNA ladder mix was used. To combine the two PCR products a second PCR was made.

#### PCR-2:

- |  |   |
|--|---|
| <ul style="list-style-type: none"> <li>- 36.5 <math>\mu</math>L deionized water</li> <li>- 5 <math>\mu</math>L DMSO (10 %)</li> <li>- 10 <math>\mu</math>L 5x buffer GC</li> <li>- 2.5 <math>\mu</math>L PCR product_for</li> <li>- 2.5 <math>\mu</math>L PCR product_rev</li> <li>- 1 <math>\mu</math>L outer primer_for</li> <li>- 1 <math>\mu</math>L outer primer_rev</li> <li>- 1 <math>\mu</math>L dNTPs (10 mM each)</li> <li>- 0.5 <math>\mu</math>L Phusion polymerase</li> </ul> | Temperature program: <ul style="list-style-type: none"> <li>- 1 min 98 °C</li> <li>- 1 min 98 °C</li> <li>- 1.5 min 57 °C</li> <li>- 45 sec 72 °C</li> <li>- 7 min 72 °C</li> <li>- keep on 4 °C</li> </ul> |
|--|---|

PCR products\_for and rev were the products from PCR 1. Outer primers were pMS-EstB-for and pMS-EstB-rev.

The expected gene size was ~ 1300 bp. The band at this position was cut out of the agarosegel under UV-light and purified as described above.

### 2.2.2.3 Promega's Wizard SV gel and PCR clean up system

The experimental steps for the former are described below as they were applied:

- Addition of 10  $\mu$ L membrane binding solution per 10 mg of gel slice, vortexing, incubation at 60 °C until gel slice is completely dissolved
- Transfer of dissolved gel mixture to SV minicolumn in collection tube, incubation at room temperature for 1 min
- Centrifugation at maximum speed for 1 min, the flow through is discarded and the minicolumn is reinserted into the collection tube
- Addition of 700  $\mu$ L membrane wash solution, centrifugation at maximum speed for 1 min, the flow through is discarded and the minicolumn is reinserted into the collection tube
- Addition of 500  $\mu$ L membrane wash solution, centrifugation at maximum speed for 5 min, the flow through is discarded and the minicolumn is reinserted into the collection tube
- Centrifugation of the column at maximum speed for 1 min to evaporate residual ethanol
- Transfer of the minicolumn to a clean 1.5 ml reaction tube
- Elution of the DNA by adding 30  $\mu$ L of nuclease free water to the minicolumn, incubation at room temperature for 2 min, Centrifugation at maximum speed for 2 min

DNA concentration was measured spectrophotometrically with a Nanodrop spectrophotometer and stored at -20 °C.

### 2.2.2.4 Cutting of the vector pMS470

In order to ligate the mutated DNA sequences with the vector pMS470, the vector had to be cleaved enzymatically. 10  $\mu$ g of vector ( $c=55.6$  ng/ $\mu$ L) were cut with 3  $\mu$ L *Nde*I (20 U/ $\mu$ L) and 3  $\mu$ L *Hind*III (20 U/ $\mu$ L). 21  $\mu$ L cut smart buffer (10x) and 3  $\mu$ L dH<sub>2</sub>O were added. The reaction mix was incubated at 37 °C over night. Afterwards the digested vector was loaded onto a preparative agarose gel (1 %, 90 V, 2.5-3 h) and purified as described above. The expected vector size was 4000 bp.

### 2.2.2.5 Gibson cloning

The insertion of the mutated DNA fragments into the cut vector was accomplished by Gibson cloning. The experimental steps are described below:

- 15  $\mu$ L assembly master mix (composition of assembly master mix is described in Table 3 and Table 4)
- 50 ng of insert (~1300 bp)
- 154 ng of linearized vector (4000 bp)

- incubation 50 °C, 60 min

Table 3: Components of 5x isothermal reaction buffer

component	Stock solution	Volume/amount
25 % (w/v) PEG-8000	PEG-8000	1.5 g
500 mM Tris/Cl pH 7.5	1 M Tris/Cl pH 7.5	3000 $\mu$ L
50 mM MgCl <sub>2</sub>	2 M MgCl <sub>2</sub>	150 $\mu$ L
50 mM DTT	1 M DTT	300 $\mu$ L
1 mM dATP	100 mM dATP	60 $\mu$ L
1 mM dCTP	100 mM dCTP	60 $\mu$ L
1 mM dGTP	100 mM dGTP	60 $\mu$ L
1 mM dTTP	100 mM dTTP	60 $\mu$ L
5 mM NAD	100 mM NAD	300 $\mu$ L
---	sterile ddH <sub>2</sub> O	up to 6000 $\mu$ L
V <sub>tot</sub>	---	6000 $\mu$ L

The PEG-8000 is weight and the stock solutions are added. The mixture is filled up to a total volume of 6 ml with ddH<sub>2</sub>O and vortexed. Aliquots of 100  $\mu$ L are filled into sterile Reaction tubes and stored at -20 °C.

Table 4: Components of Gibson assembly mix

component	Volume to add
5x ISO reaction buffer	320 $\mu$ L
T5 Exonuclease, 10 U/ $\mu$ L	0.64 $\mu$ L
Phusion High-Fidelity DNA Polymerase, 2 U/ $\mu$ L	20 $\mu$ L
Taq DNA Ligase, 40 U/ $\mu$ L	160 $\mu$ L
sterile ddH <sub>2</sub> O	699.36 $\mu$ L
V <sub>tot</sub>	1200 $\mu$ L

The Gibson assembly mix is mixed by inverting and aliquots of 15  $\mu$ L are filled into Reaction tubes and stored at -20 °C.

Afterwards the reaction mixture was desalted and electrocompetent *E. coli* Top10F' cells were transformed with the ligation mix.

#### 2.2.2.6 Transformation of *E. coli* Top 10F' cells

To avoid short circuits during transformation and improve the transformation rate the ligation mix was desalted on a membrane for 15 min. Afterwards 5  $\mu$ L of the ligation mix were added to 80  $\mu$ L cells. Transformation was performed with an electroporator (setting Ec2). 800  $\mu$ L of lysogeny broth medium were added and the cells were incubated at 37 °C for 1 h to



regenerate. 100  $\mu\text{L}$  of the transformed cells were plated onto lysogeny broth agar plates supplemented with ampicillin, which were incubated over night at 37 °C.

#### 2.2.2.7 Colony PCR and master plate

The grown cultures were used for colony PCR to control if the gene was successfully inserted into the vector. At the same time a master plate with all used colonies was made.

PCR:

– 17.5 $\mu\text{L}$ water	Temperature-program:
– 2.5 $\mu\text{L}$ DMSO (10 %)	– 10 min 95 °C
– 2.5 $\mu\text{L}$ Dream Taq buffer	– 30 sec 95 °C
– 0.5 $\mu\text{L}$ dNTPs (10 mM each)	– 30 sec 55 °C
– 0.5 $\mu\text{L}$ for Primer (KST-for)	– 1 min 72 °C
– 0.5 $\mu\text{L}$ rev Primer (KST-rev)	– 7 min 72 °C
– 0.125 $\mu\text{L}$ Dream Taq polymerase	– keep on 4 °C

Number of cycles: 25

After PCR 5  $\mu\text{L}$  loading dye (6x) were added to every sample and the PCR products were analyzed by agarose gel electrophoresis (1 %, 120 V, 1 h). Two colonies of each construct, of which Gibson cloning has been successful, were plated onto lysogeny broth plates with ampicillin. These were incubated over night at 37 °C.

#### 2.2.2.8 Sequencing

The cell material was subsequently used to isolate the plasmids using the GeneJET plasmid miniprep kit as described in 2.2.2.1. Concentrations were measured with a Nanodrop spectrophotometer. 15  $\mu\text{L}$  of each construct were sent for sequencing to Microsynth AG (Switzerland). Sequencing results were evaluated with the program CLC Workbench.

#### 2.2.2.9 Creating of *EstB* variants by site-directed mutagenesis

The protocol for site-directed mutagenesis to create variants of *EstB* is described in the following.

PCR:

– 0.5 $\mu\text{L}$ forward primer (2.5 pmoles/ $\mu\text{L}$ )	Temperature program:
– 0.5 $\mu\text{L}$ reverse primer (2.5 pmoles/ $\mu\text{L}$ )	– 5 min 95 °C
– 0.25 $\mu\text{L}$ dNTPs (10 mM each)	– 50 sec 95 °C
– 1.25 $\mu\text{L}$ Pfu buffer (10x)	– 50 sec 60 °C
– 2 $\mu\text{L}$ template DNA (1 ng/ $\mu\text{L}$ )	– 6 min 68 °C (1 min +
– 0.25 $\mu\text{L}$ Pfu polymerase	1 min/kb template)

- 6.5  $\mu\text{L}$  dH<sub>2</sub>O
- 1.25  $\mu\text{L}$  DMSO (10 %)
- 7 min 68 °C
- Number of cycles: 18

Forward and reverse primer were EstB-M377A\_for and EstB-M377A\_rev respectively. As template pMS-EstB-Wildtype was used.

After PCR 10  $\mu\text{L}$  thereof are mixed with 5  $\mu\text{L}$  Tango buffer (10x), 2  $\mu\text{L}$  *DpnI* and 33  $\mu\text{L}$  H<sub>2</sub>O and incubated at 37 °C for 3 h to digest the methylated parent strain. *DpnI* is inactivated at 70 °C for 30 min. Further experimental steps were analogous to 2.2.2.6, 2.2.2.7 and 2.2.2.8.

#### 2.2.2.10 Expression of different esterases in deep well plate (DWP) cultivation

To be able to calculate protein expression of different esterases in deepwell plate cultivations roughly, five different esterases (pKN27, pKNJ70, pMS-NJ70-M7, pMS-NJ70-J22 and pMS-EstB-WT) were expressed in lysogeny broth and 2xTY medium. Inoculation of the media was from plated *E.coli* cells. Kanamycine (pKN27, pKNJ70) and ampicillin (pMS-NJ70-M7, pMS-NJ70-J22, pMS-EstB-WT) were added respectively. Further experimental steps were done analog to the protocol as described below.

For screening the activity of esterases the enzymes were expressed from *E. coli* strains in deep well plate cultivations. Cells from a gene bank were stamped into 750  $\mu\text{L}$  of lysogeny broth medium with ampicillin for the over-night culture (37 °C, 320 rpm) in deep well plates. Cells with different EstB variants were plated on lysogeny broth plates with ampicillin from a glycerol stock and incubated over night (37 °C). Single colonies were used to inoculate 750  $\mu\text{L}$  of lysogeny broth medium with ampicillin for the over-night culture (37 °C, 320 rpm) in deep well plates. The next day 25  $\mu\text{L}$  thereof were used to inoculate 750  $\mu\text{L}$  of medium of the main culture. The main culture was cultivated for 6h, at 37 °C and 320 rpm. Isopropyl  $\beta$ -D-1-thiogalactopyranoside (IPTG) ( $c_{\text{final}}$  in well=0.1 mM) to the main culture. After 20 h the cells were harvested by centrifugation for 15 min at 4 000 g. The supernatant was discarded and the cell pellet was stored at -20 °C.

#### 2.2.2.11 Glycerol stocks

300  $\mu\text{L}$  of 50 % glycerol were added to 750  $\mu\text{L}$  of the pre-culture in each well of the under sterile conditions. Glycerol stocks were stored at -20 °C.

#### 2.2.2.12 Cell lysis of deep well plate cultivation

300  $\mu\text{L}$  lysis buffer consisting of 0.28 mg/mL lysozyme from chicken egg white (~70 000 U/mg), 4 U/mL Benzonase Nuclease (250 U/ $\mu\text{L}$ ) and 0.2 % Triton-X 100 in 20 mM potassium phosphate buffer pH 7.4 were added to the frozen pellets. The plates were vortexed to resuspend the pellet. Afterwards they were shaken for 1 h at room temperature at 1000 rpm. To separate the crude cell compounds the plates were centrifuged for 15 min at 4000 rpm. The supernatant was used for further analysis.

### 2.2.2.13 Expression of EstB variants in shaking flask cultivation

Shaking flask cultivation of EstB variants was carried out in lysogeny broth medium with ampicillin. For the overnight culture 10 mL of medium were inoculated with one colony of each variant. Incubation was at 37 °C at 120 rpm overnight. The OD<sub>600</sub> was determined the next morning. Before the inoculation was done with 4 mL of the preculture, ampicillin (400 µL) was added to the main culture (400 mL lysogeny broth medium in 1 L baffled flasks). Incubation at 37 °C on the shaking tower (120 rpm) lasted until the cells reached an OD<sub>600</sub> of ~0.8. Afterwards protein expression was induced by adding 200 µL of 0.5 M IPTG (C<sub>final</sub>=0.1 mM). Incubation was at 25 °C at 120 rpm overnight.

### 2.2.2.14 Glycerol stocks

0.5 mL of 50 % glycerol was mixed with 1 mL of preculture of shaking flask fermentation under sterile conditions. Glycerol stocks were stored at -20 °C.

### 2.2.2.15 Cell harvest and cell disruption by sonication

After determination of the final OD<sub>600</sub> of the main culture the cells were harvested by centrifugation for 15 min at 4424 g at 4 °C in a JA-10 rotor.

The supernatant were discarded and the cells were disrupted by sonication. The pellet was transferred in a pre-weight 50 mL tube to determine its weight. To resuspend the pellet 5 mL of 20 mM potassium phosphate buffer pH 7 per gram pellet were added. At least 25 mL have to be added. Sonification was carried out on ice for 6 min (output control 7-8, duty cycle 70-80). The samples were transferred in pre cooled centrifuge tubes and centrifuged at 48384 g for 1 h at 4 °C in a JA 25.50 rotor. Afterward the lysates were filtered with AGILENT filters (PES 0.45 µm) and stored at -20 °C.

### 2.2.2.16 Bio-Rad protein assay

To calculate the protein concentration an eight point calibration curve with BSA-standard (1.5-12 µg/µL) was established. 190 µL of reaction solution (1:5) are incubated with 10 µL of standard/sample for 10 min in a transparent 96-well PS plate (Greiner) at room temperature. Afterwards absorption was measured at 595 nm with the plate reader. The samples were diluted 1:50, and 1:100, 1:200 to be in the linear range of the calibration curve (Absorption 0.3-0.7).

### 2.2.2.17 Sodium Dodecyl Sulfate gel electrophoresis (SDS-PAGE)

The lysates of the EstB protein variants were analyzed on 15 slot NuPAGE 4-12 % Bis-Tris gels. The samples were diluted 1:10. 13 µL of the diluted samples were mixed with 5 µL Novex NuPAGE LDS Sample Buffer (4x) and 2 µL NuPAGE Sample Reducing Agent (10x) and denaturated for 10 min at 95 °C. 10 µL thereof were loaded onto the gel. Running buffer was Novex NuPAGE MES SDS running buffer, as standard PageRuler Prestained protein

ladder was used. The gels were run in an XCell SureLock™ Mini-Cell electrophoresis system with the NuPAGE gel program (120 A, 200 V, 35 min). After gel electrophoresis the gels were stained for 15 min in staining solution (500 mL ethanol, 75 ml acetic acid, 2.5 g Coomassie Brilliant Blue G250, 425 mL deionized water). Afterwards they were destained three times for 20 min in destaining solution (200 mL ethanol, 75 mL acetic acid, 725 mL deionized water).

#### 2.2.2.18 Quantification of the percentage of EstB within the total protein amount

In order to quantify the percentage of expressed EstB within the total of proteins in the lysate the gels from SDS-PAGE were scanned with the G-Box. The software GeneTool by Syngene analyzed the intensity of the protein bands. Calculations for the quantification of EstB within the total of proteins were done by using the volume of the corresponding peaks of the protein bands.

#### 2.2.2.19 Lyophilization of lysate from *E. coli* strains

For the screening assays lysate (*E. coli*, 50 µL) was frozen at -80 °C over night. Lyophilization was carried out in 96-well plates over night. The plates were tape sealed with an aluminium film with small holes in it. The dried lysate was stored completely covered with tape seal at 4 °C in the fridge.

For testing the influence of different additives on the solubility of lyophilized *E.coli* lysates in organic solvent 10 mM, 50 mM, 100 mM and 500 mM of KCl, D-(+)-Galactose, D-(+)-Mannose, Urea and PEG were added to the *E. coli* lysate before the lyophilization process.

#### 2.2.2.20 Screening for the detection of esterase activity via NBD-H

Screening of esterase activity was done in both anhydrous and aqueous conditions. For the first one acetaldehyde detection via NBD-H was used. 50 µL of lysate (*E. coli*) from deepwell plate cultivation was lyophilized over night. 100 µL of organic solvent were added to suspend the lyophilizate, 100 µL of NBD-H with 50 mM vinylbutyrate or a confidential substrate were added respectively. The plate was tape sealed with a transparent adhesive film and fluorescence measurement was started immediately for 60 min as described above to measure the produced acetaldehyde. The only deviation was a shaking step before every cycle for 3 s (500 rpm) instead of 1 s.

#### 2.2.2.21 Screening for the detection of esterase activity via pH-shift

For screening the activity in aqueous conditions a pH-shift was used (Singh et al., 2006). 50 µL of enzyme containing lysate from *E. coli* DWP cultivation were mixed with 50 µL of 20 mM KPi buffer pH 7.4. To start the reaction 100 µL of reaction/detection solution were added immediately before absorption measurement at 432 nm and 556 nm for 15 min at room temperature. The reaction/detection mix was prepared by mixing 80 µL phenol red

(0.025 % in 20 mM KPi buffer pH 7.4,  $c_{\text{final}}=0.01$  %) with 20  $\mu\text{L}$  substrate (50 mM vinylbutyrate in ethanol,  $C_{\text{final vinylbutyrate in well}}=25$  mM).

### 3 Results and Discussion

#### 3.1 Development of a high throughput assay for screening the synthesis activity of esterases in organic solvent

The screening for the ester synthesis activity of esterases is a poorly explored field, especially in a high throughput way. The reaction product of a transesterification reaction of a vinylester with an alcohol is a vinylalcohol, which isomerizes to acetaldehyde. If a methylester instead of a vinylester is used as a substrate, the corresponding reaction product is methanol. Hence the amount of acetaldehyde or methanol produced during transesterification reaction should indicate enzymatic activity of esterases in the absence of water. Side reactions occurring by hydrolysis reactions of the substrate have to be considered. In the following different methods for acetaldehyde and methanol detection were examined.

##### 3.1.1 Aldehyde detection with NBD-H

Due to the applicability as on-line assay of the transesterification activity, the detection of acetaldehyde, which is released during transesterification reactions using vinylester substrates, with NBD-H and fluorescence measurement of the highly fluorogenic product after a coupling reaction of the two components, seemed to be the best way for applying a high throughput screening assay. At first, a standard calibration curve of acetaldehyde was measured as described in the assay from Konarzycka-Bessler and Bornscheuer (2003). Acetaldehyde dilutions were prepared from 0.001 to 0.025 mM, the linear range described in the paper, by mixing the acetaldehyde with isooctane:1-propanol 10:1 (v/v) and in isooctane:1-butanol 10:1 (v/v). Fluorescence was measured at 45 °C (Figure 6). If not otherwise mentioned, triplicates were measured in this section.

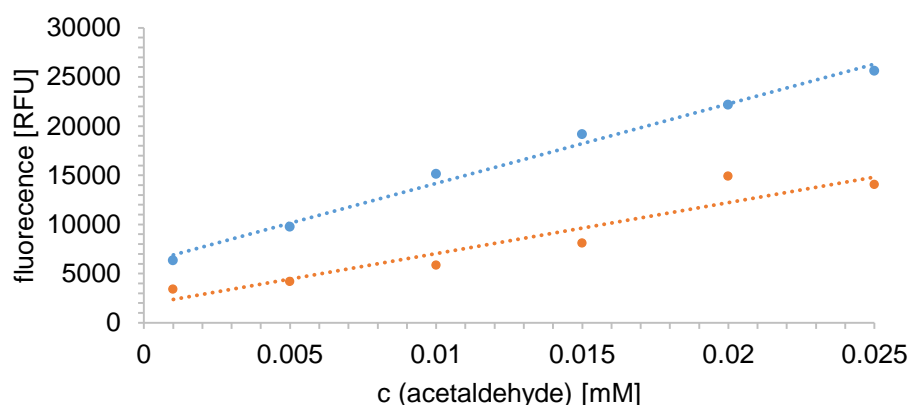


Figure 6: Standard calibration curve of acetaldehyde ( $c_{\text{final}}=0.001-0.025$  mM) detected by NBD-H ( $c_{\text{final}}\sim 0.3$  mM) according to Konarzycka-Bessler and Bornscheuer 2003 with isooctane:1-propanol 10:1 (v/v) resulting in

$R^2=0.9899$  (blue dots) and isooctane:1-butanol 10:1 (v/v) resulting in  $R^2=0.8986$  (orange dots) as solvents; fluorescence measurement was at 485 nm excitation and 520 nm emission at 45 °C, no shaking;

Figure 6 illustrates that the range of 0.001 to 0.025 mM acetaldehyde showed good linearity with  $R^2=0.9899$  for isooctane:1-propanol and  $R^2=0.8986$  for isooctane:1-butanol as solvents. As *tert*-butanol is the alcohol which should react in the transesterification reaction with the vinyl ester 1-propanol and 1-butanol were replaced by that. In combination with NBD-H, the mixture separated into two phases. Therefore, isooctane:*tert*-butanol 10:1 (v/v) seemed to be inappropriate for further investigations. The mixing ratio was changed to 1:10 (v/v) and *tert*-butanol was used as an only solvent for the next measurements. The manageability of latter was difficult due to the melting point of *tert*-butanol (23-26 °C). All used equipment had to be prewarmed at 30 °C in time to avoid solidification of the solvent. Unfortunately, results were not reproducible under the applied conditions. To overcome this problem, the influence of mixing, temperature, incubation times, various batches of acetaldehyde and NBD-H, the use of different multichannel pipettes, the use of a different photometers and the concentration of acetaldehyde and NBD-H were tested but could not improve results satisfactorily. Only a slight improvement of data could be observed by broadening the acetaldehyde concentrations in the range of 0.005 to 0.1 mM, reducing the NBD-H concentrations (~0.1 mM instead of ~0.4 mM) and increasing measurement temperature to 45 °C instead of the aspired 30 °C for the application of the assay. But still data was not reproducible. In literature other mentioned solvents for the NBD-H assay are *n*-hexane, dimethylsulfate (DMSO), acetonitrile, *tert*-butylmethylether (tBME), diethylether, dimethylformamide (DMF) and tetrahydrofuran (THF) (Konarzycka-Bessler and Bornscheuer, 2003; Pohn, 2005). These solvents were mixed with *tert*-butanol 1:1 (v/v) and put into microtiter plates over night to test the stability of the plates. Due to distortion of the microtiter plate, DMF and THF did not come into further consideration as well as diethylether, which is too volatile. Additional experiments were performed with *n*-hexane:*tert*-butanol 1:1 (v/v), DMSO:*tert*-butanol 1:1 (v/v), acetonitrile:*tert*-butanol 1:1 (v/v) and tBME:*tert*-butanol 1:1 (v/v). No fluorescence signal could be measured using these solvent combinations, hence the initial situation allowed the application in the assay. To establish the acetaldehyde calibration curve, microtiter plates were precooled at -20 °C and acetaldehyde dilutions were pipetted on ice to avoid evaporation of the volatile substance. The addition of a second solvent to *tert*-butanol prevents its solidification at temperatures below its melting point. As above described factors seemed to be positive for the measurement, the acetaldehyde concentration range was broadened to 0.005 - 0.8 mM and the NBD-H concentration was reduced from ~0.4 mM to 0.1 mM, measurement temperature was 45 °C and due to the use of lyophilized lysate in the assay later, a shaking step of the photometer was added to the protocol. Figure 7 shows data of resulting standard curves with *n*-hexane:*tert*-butanol 1:1 (v/v), acetonitrile:*tert*-butanol 1:1 (v/v), tBME:*tert*-butanol 1:1 (v/v) and DMSO:*tert*-butanol 1:1 (v/v) which were tested in

parallel. Data shown is after 5 min reaction time, where a linear trend could be observed with all solvents.

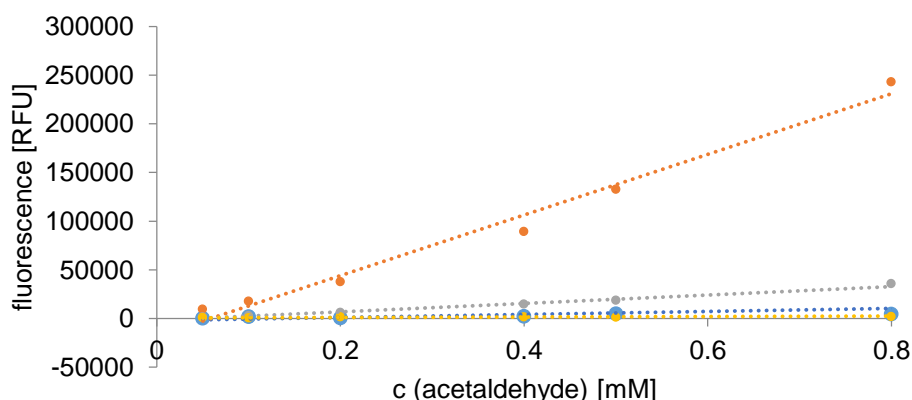


Figure 7: Acetaldehyde standard curves after 5 min reaction time with NBD-H with a previous shaking step (500 rpm, 1 s) in the linear range of 0.05 to 0.8 mM ( $c_{final}$ ) with different solvents; all instruments were precooled before starting the experiment; fluorescence measurement was at 485 nm excitation and 520 nm emission measurement temperature was 45 °C; blue dots: *n*-hexane:*tert*-butanol 1:1 (v/v),  $R^2=0.9763$ ; orange dots: DMSO:*tert*-butanol 1:1 (v/v),  $R^2=0.9831$ ; grey dots: acetonitrile:*tert*-butanol 1:1 (v/v),  $R^2=0.9899$ ; yellow dots: tBME:*tert*-butanol 1:1 (v/v),  $R^2=0.8142$  (yellow dots);

The use of the different solvents for establishing the calibration curve of acetaldehyde resulted in different fluorescent signals. The reason for this might be the different solubility of the NBD-H in the solvents. In acetonitrile:*tert*-butanol 1:1 (v/v) and DMSO:*tert*-butanol 1:1 (v/v) solubility was best, in *n*-hexane:*tert*-butanol 1:1 (v/v) and tBME:*tert*-butanol 1:1 (v/v) it was worse. This is also reflected in the linearity of the curves. Acetonitrile:*tert*-butanol 1:1 (v/v) and DMSO:*tert*-butanol 1:1 (v/v) resulted in curves of the best linearity ( $R^2=0.9899$  and  $R^2=0.9831$ ) compared to the other solvents. Regardless the use of both is inappropriate for high throughput screening due to reaction of the PS microtiter plate in combination with acetaldehyde after 45 min reaction time. These effects were independent of measurement temperature. The same effect could be observed with tBME:*tert*-butanol 1:1 (v/v) ( $R^2=0.8142$ ) as solvent. The use of polypropylene (PP) microtiter plates instead of PS microtiter plates remains to be evaluated. As *n*-hexane:*tert*-butanol 1:1 (v/v) showed quite good linearity as well ( $R^2=0.9763$ ) and no interaction with the microtiter plate could be observed after the addition of acetaldehyde, this solvent combination was used for further investigations if not mentioned differently.

In addition the data for the same measurement over time is shown in Figure 8 for *n*-hexane:*tert*-butanol 1:1 (v/v). After reaching its maximum after ~15 to 25 min, the fluorescence signal remains constant.



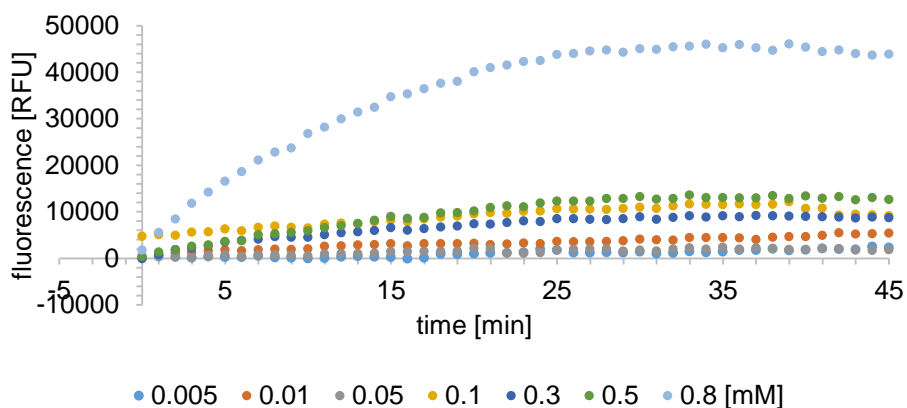


Figure 8: Fluorescence of acetaldehyde standard dilutions [mM] over time (45 min) in *n*-hexane:*tert*-butanol 1:1 (v/v) as organic solvent; all instruments were precooled before starting the experiment; fluorescence measurement was at 485 nm excitation and 520 nm emission; measurement temperature was 45 °C; a shaking step was added to the protocol (500 rpm, 1 s);

As a next step, the influence of the shaking step added was examined by comparing a measurement without and with this step. Shaking of 500 rpm for 1s improved linearity from  $R^2=0.6358$  to  $R^2=0.8723$ , thus shaking was added to the protocol permanently.

Different concentrations of NBD-H (~0.1 mM, 0.2 mM and 0.4 mM) could also influence linearity. 0.2 mM of the detection mix resulted in a curve of better linearity ( $R^2=0.9799$ ) compared to 0.1 ( $R^2=0.9763$ ) and 0.4 mM ( $R^2=0.9033$ ) after 5 min reaction time. Therefore, ~0.2 mM of NBD-H was used in further experiments.

In order to have optimal conditions for the enzyme's activity over time in the assay the temperature could be decreased from 45 °C to 30 °C without losses.

Finally optimized conditions for the measurement of the acetaldehyde standard curve were the precooling of the equipment and the acetaldehyde to avoid evaporation of the volatile substances, the change of the organic solvent to *n*-hexane:*tert*-butanol 1:1 (v/v), the addition of a shaking step which was prolonged (500 rpm, 3 s, before every cycle) with regard to suspending the lyophilized lysate used later in the assay, an NBD-H concentration of ~0.2 mM and a measurement temperature of 30 °C. Data of the standard curve measured with these conditions can be seen in Figure 9 and Figure 10 after 5 min reaction time. The linear range was between 0.05 and 0.5 mM of acetaldehyde during the whole measurement (45 min) and linearity improved with time to  $R^2=0.99$  within this range.

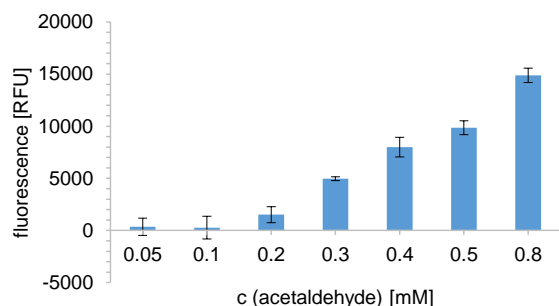


Figure 9: Fluorescence signal of acetaldehyde (0.05-0.5 mM) with standard deviation (triplicates) detected by NBD-H after 5 min reaction time; shaking step: 500 rpm, 3 s, before every cycle; organic solvent: *n*-hexane:*tert*-butanol 1:1 (v/v); all instruments were precooled before starting the experiment; fluorescence measurement was at 485 nm excitation and 520 nm emission; measurement temperature was 30 °C;

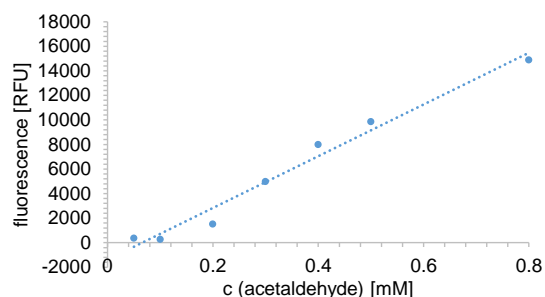


Figure 10: Standard calibration curve of acetaldehyde in the range of 0.05-0.5 mM,  $R^2=0.9774$  (0.1-0.5 mM,  $R^2=0.9771$  respectively) detected by NBD-H after 5 min reaction time; shaking step: 500 rpm, 3 s, before every cycle; organic solvent: *n*-hexane:*tert*-butanol 1:1 (v/v); all instruments were precooled before starting the experiment; fluorescence measurement was at 485 nm excitation and 520 nm emission; measurement temperature was 30 °C;

Since the standard curve with different acetaldehyde dilutions could be established successfully and in a reproducible way with the conditions described above, possible background reactions of the model substrate vinylbutyrate and VinEst (DSM) were tested. Both substrates did not show any hydrolysis background reaction (Figure 11). Due to the good linearity of the standard curve with these solvents the substrate test was performed with acetonitrile:*tert*-butanol 1:1 (v/v) and DMSO:*tert*-butanol 1:1 (v/v) as well. Again, no background hydrolysis reaction could be observed, but still a reaction with the PS microtiter plate occurred.

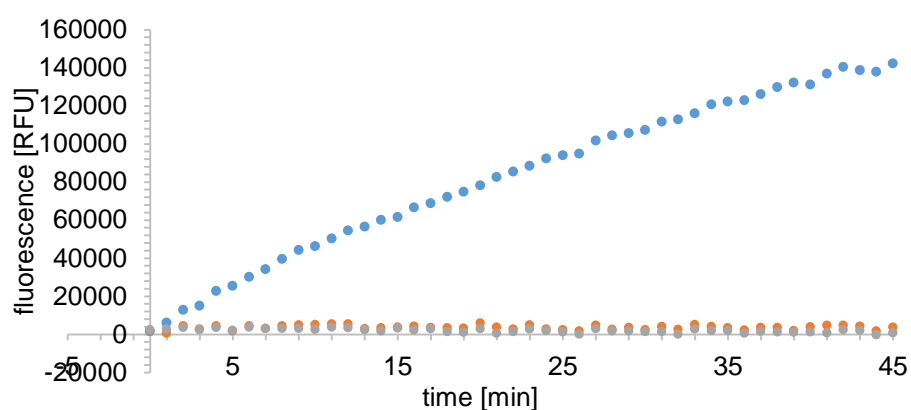


Figure 11: On-line measurement of possible background reactions of different substrates (vinylbutyrate, orange dots; VinEst (DSM), grey dots;  $c_{final}=0.4$  mM) in comparison with the reaction of acetaldehyde ( $c_{final}=0.4$  mM, blue dots) with NBD-H ( $c_{final}\sim 0.2$  mM); organic solvent *n*-hexane:*tert*-butanol 1:1 (v/v); shaking step: 500 rpm, 1 s, before each cycle; fluorescence measurement was at 485 nm excitation and 520 nm emission; measurement temperature 30 °C;

In addition, transparent microtiter plates and black microtiter plates with transparent bottom were compared. As linearity is as good as with the black ones ( $R^2=0.9329$  after 5 min of

reaction, improving with time, acetaldehyde range: 0.05 to 0.8 mM) the use of both is possible.

As a next step the influence of lyophilized lysate (*E. coli*; 0.5 mg/mL) in general was examined to test any interference. The standard curve did not show as good linearity as without the lysate, but still in an acceptable range ( $R^2=0.8675$  after 15 min reaction time, improving with time, acetaldehyde range from 0.05 to 0.8 mM). Testing different additive to improve solubility of the lyophilized *E.coli* in organic solvents did not lead to any results. The influence on enzymatic activity remains to be evaluated. Further optimizations of the lyophilization process could not be made. The freeze-drier was broken during working on this thesis.

To verify the usability of the assay for screening, the synthesis activity of five different esterases was tested. Results can be seen in Figure 12. Differences in activities of the enzymes can be observed very well after a minimum reaction time of 30 min. The longer the reaction time, the clearer are the differences. In addition, the enzymes seem to be stable in the organic solvent mix even after the reaction time of 60 min.

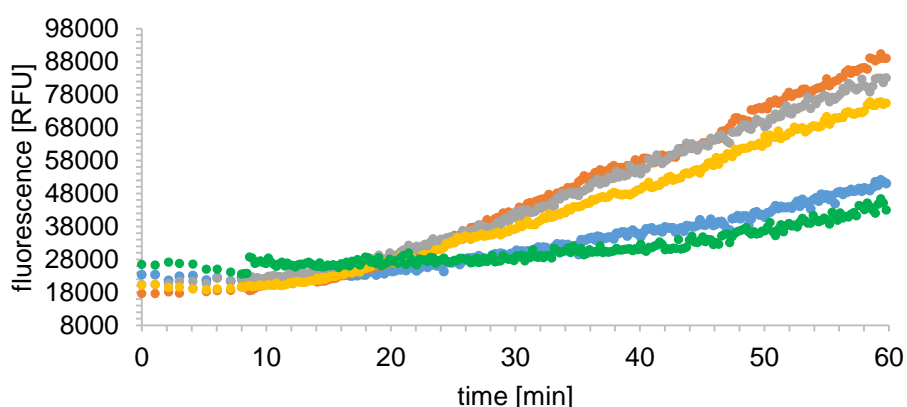


Figure 12: Verification of the NBD-H assay by comparison of the activity of different esterase variants (triplicates): pKN27 (blue dots), pKNJ70 (orange dots), pMS-NJ70-M7 (grey dots), pMS-NJ70-J22 (yellow dots) and pMS-EstB-WT (green dots); organic solvent: *n*-hexane:*tert*-butanol 1:1 (v/v); shaking step: 500 rpm, 3 s, before each cycle; fluorescence measurement was at 485 nm excitation and 520 nm emission; measurement temperature 30 °C; cell free lysate from shaking flask cultivation of *E. coli* was used; Vinylbutyrate  $c_{final}=10mM$ ;

For further verification, active known esterases were chosen from the strain collection of the institute for molecular biotechnology. *E. coli* lysates of two different DWP cultivations were used. The blank subtracted from data was a lysate containing the pMS vector without any esterase. Results of screening via the pH shift assay were compared with results of the developed NBD-H assay afterwards. Figure 13 shows results of the pH shift assay after 15 min of absorption measurement. The tested esterases are shown with decreasing activity. Measurement of the two different cultivations concurred well. Slight differences can be

observed e.g. for pMSH81. This can arise from different growing behavior of the *E. coli* cells in the two DWPs or due to the variability of the assay itself.

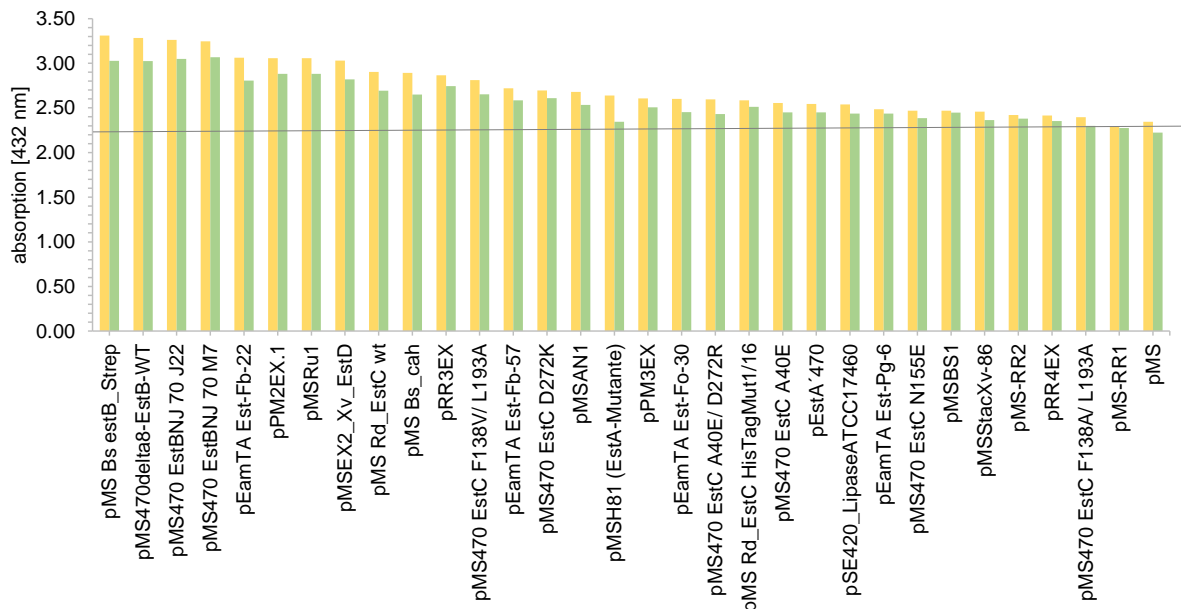


Figure 13: pH-shift in aqueous reaction medium of liquid *E. coli* lysate (50  $\mu$ L) from DWP cultivations of different esterases; vinylbutyrate ( $C_{final}=25$  mM) was used as substrate; the pH shift was detected with phenolred ( $C_{final}=0.01$  %); the yellow and the green bars indicate the lysate of two different *E. coli* DWP cultivations; reaction time: 15 min; end point measurement at 432 nm at 30  $^{\circ}$ C; measurement of duplicates;

The NBD-H assay was applied with *n*-hexane:*tert*-butanol 1:1 (v/v) as solvent first (Figure 14, data after 60 min of reaction). Again the two different cultivations concurred well, with the exception of a view outliers. Since the activity of those esterases fit better in the pH shift assay different growing behavior can be excluded as a reason for these variations. Most likely the variability of the assay itself as well as influences of the lyophilization process might be the explanation. In general EstC variants seem to be most active/stable under the applied reaction conditions. The comparison of activity measured with the pH shift assay and with the NBD-H assay is not possible due to completely different results. This might be on the basis of aqueous and organic reaction environment for the enzymes and corresponding stability of the proteins.

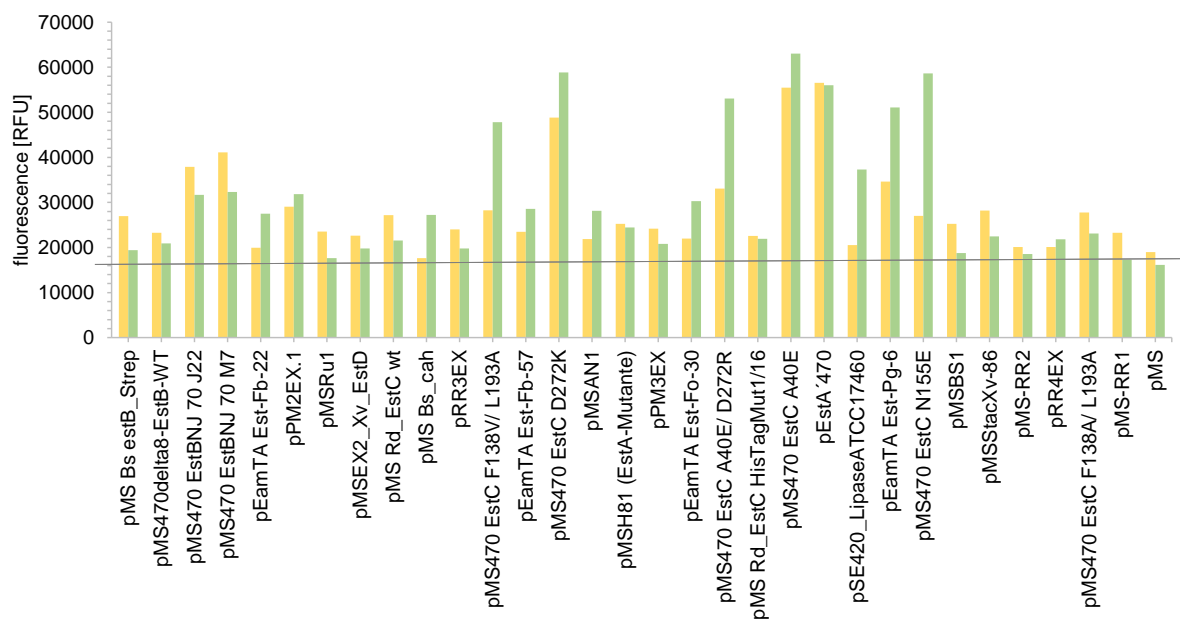


Figure 14: Acetaldehyde detection via on-line measurement with NBD-H in organic solvent; transesterification reaction of different esterases (duplicates) in the absence of water was analyzed with *n*-hexane:*tert*-butanol 1:1 (v/v) as solvent; the yellow and the green bars indicate the lysate of two different DWP cultivations; reaction time: 60 min; fluorescence measurement was at 485 nm excitation and 520 nm emission; measurement temperature: 30 °C; shaking step: 500 rpm, 3 s, after each cycle; lysate of *E. coli* (50  $\mu$ L) was lyophilized over night; Vinylbutyrate was used as substrate ( $c_{\text{final}}=25$  mM);

In addition the assay was made with DMSO:*tert*-butanol 1:1 (v/v) as organic solvent. A high background signal could be observed using this reaction system. The remaining fluorescence signal representing enzymatic activity is rather low. Hence it indicates instability or limited activity of the enzymes in this solvent. But since the before mentioned reaction with the PS microtiter plate could be observed which only occurs if acetaldehyde is released in DMSO:*tert*-butanol 1:1 (v/v) a complete inactivation of the enzymes can be excluded. Most active/stable enzymes are EstC variants again. Further comparison of these results with the pH shift or the other NBD-H assay is inefficient due to the presumably limiting activity of the enzymes.

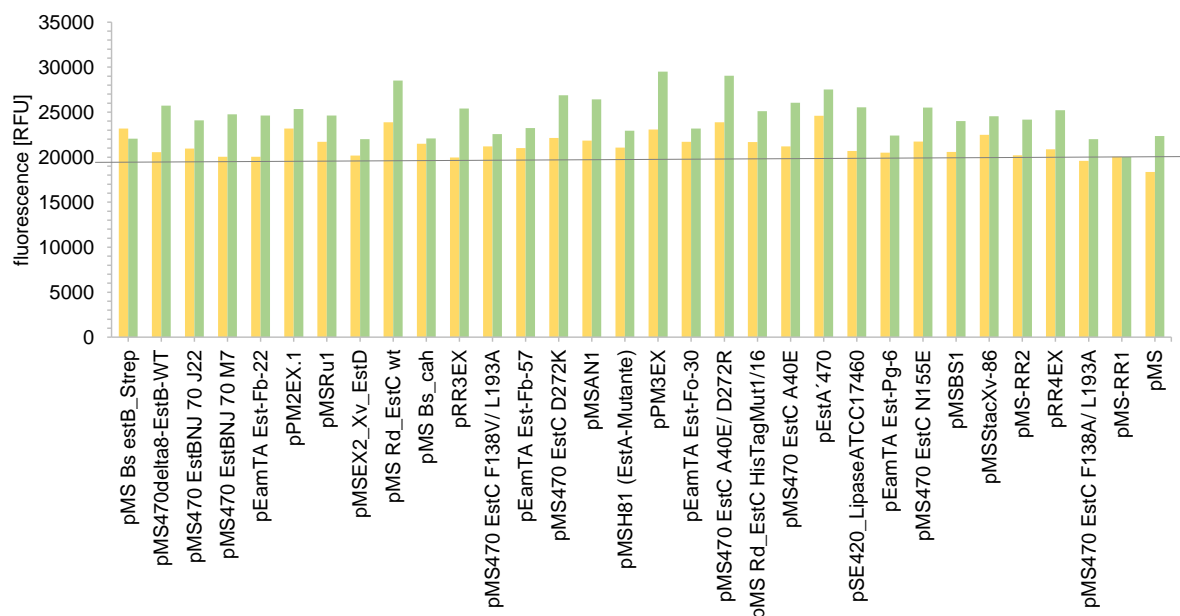


Figure 15: Acetaldehyde detection via on-line measurement with NBD-H; transesterification reaction of different esterases (duplicates) in the absence of water was analyzed with DMSO:tert-butanol 1:1 (v/v) as solvent; the yellow and the green bars indicate the lysate of two different DWP cultivations; reaction time: 60 min; fluorescence measurement was at 485 nm excitation and 520 nm emission; measurement temperature: 30 °C; shaking step: 500 rpm, 3 s, after each cycle; lysate of *E. coli* was lyophilized over night (50  $\mu$ L); Vinylbutyrate was used as substrate ( $C_{final}=25$  mM);

Due to problems of reproducibility of acetaldehyde detection via NBD-H mentioned earlier, further possibilities for developing a high throughput assay to screen for the esterase activity in non-aqueous environment were tested. These are described in the following.

### 3.1.2 Photometric detection of vinylbutyrate as indicator for enzyme activity

Since acetaldehyde shows a lower absorbance than vinyl esters at UV wavelengths Goujard et al. 2009 described a UV/Vis spectrophotometric method to determine enzyme activity of hydrolases via the decrease of the vinylsubstrate during transesterification reaction. In order to determine the absorption maximum of vinylbutyrate as well as possible background signals of organic solvents and lysate, a UV/Vis spectrum from 200 to 600 nm was measured. Figure 16 shows that the absorption maximum of vinylbutyrate increases with higher concentrations. 0.25 mM of vinylbutyrate show a maximum at 212 nm, 0.5 mM at 216 nm and 2.5 mM at 222 nm, therefore the measurement of different vinylbutyrate dilutions to establish a standard curve was performed at these three wavelengths. Due to instability of the UV microtiterplate with *n*-hexane, tBME and isooctane, *tert*-butanol was the organic solvent of choice. Due to the low melting point of *tert*-butanol all used equipment had to be prewarmed for further investigations. Neither acetaldehyde nor the organic solvents caused any background signal at the absorption maximum of vinylbutyrate. In contrast to that the empty UV suitable microtiter plate and liquid lysate did.

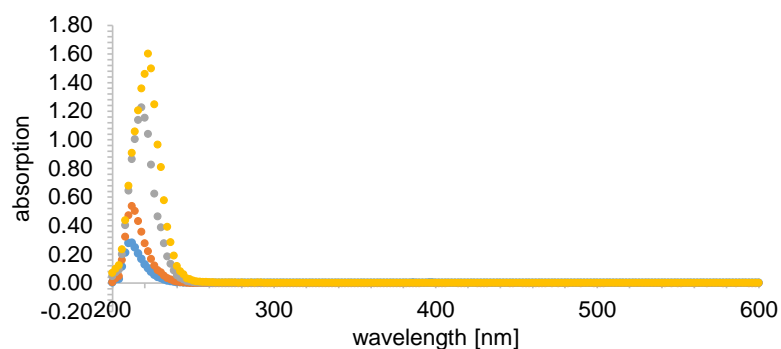


Figure 16: UV/Vis spectrum of different vinylbutyrate concentrations ( $c_{final}$ ) in *tert*-butanol: 0.25 mM (blue dots), 0.5 mM (orange dots), 2.5 mM (grey dots) and 5 mM (yellow dots); organic solvent: *tert*-butanol; measurement temperature: 30 °C;

To establish a calibration curve different vinylbutyrate concentrations in *tert*-butanol were measured at 212, 216 and 222 nm. A standard curve of good linearity of vinylbutyrate concentration in the range of 0.001-0.5 mM ( $R^2=0.9792$ ) was reached at 212 nm, higher concentrations were determined at 222 nm (0.05-10 mM,  $R^2=0.8832$ ) and at 216 nm best linearity over a broad concentration range from 0.001 to 1 mM was reached (Figure 17, Figure 18).

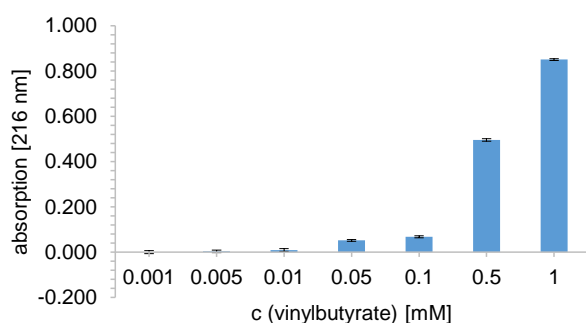


Figure 17: Standard calibration curve of vinylbutyrate (0.001-1 mM) in *tert*-butanol with standard deviations (triplicates); measured at 216 nm at 30 °C; prewarmed equipment;

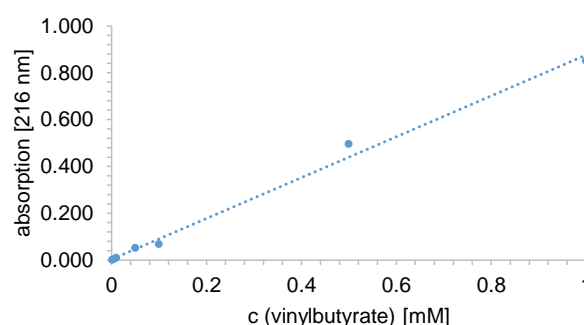


Figure 18: Standard calibration curve of vinylbutyrate in *tert*-butanol in the range of  $c_{final}=0.001-1$  mM ( $R^2=0.9934$ ) measured at 216 nm at 30 °C; prewarmed equipment;

As a next step the influence of lysate on establishing the standard calibration curve was determined. Due to the high background and precipitating of liquid lysate in organic solvent only concentrations of 0.2 mg/mL protein were possible to use to get a linear curve. Considering above mentioned results this method is inappropriate for screening.

### 3.1.3 Aldehyde detection with MBTH

For photometric detection of aldehydes MBTH is another suitable reagent. In the presence of an acidic environment and  $FeCl_3$  the blue colored complex TAPMC is formed during detection reaction of acetaldehyde with MBTH. The protocol used is based on Zheng *et al.* 2014. In the beginning a spectrum was measured in the range of 400 to 800 nm to identify the maximum absorption of the blue TAPMC. As can be seen in Figure 19 this is at 606 nm.

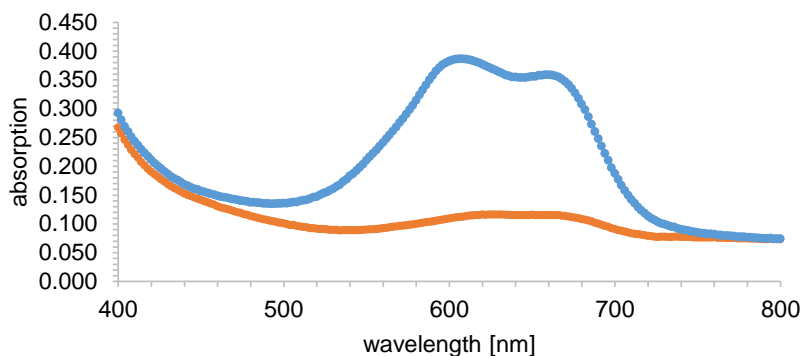


Figure 19: UV spectrum of TAPMC from aldehyde detection with MBTH ( $c_{\text{final}}=0.2$  mM) in the presence of  $\text{FeCl}_3$  (5 mg/mL in 0.05 M HCl); acetaldehyde (0.1 mM) in *n*-hexane (blue dots), *n*-hexane (orange dots); the first incubation time was 10 min, the second one 30 min; measurement temperature: 30 °C;

Afterwards a standard curve was established as described in the paper. Good linearity ( $R^2=0.9566$ ) was reached by this protocol as can be seen in Figure 20 and Figure 21.

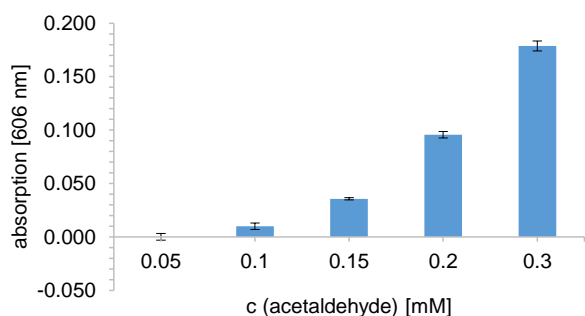


Figure 20: Standard calibration curve of acetaldehyde (0.05-0.3 mM) with standard deviations (triplicates) detected by MBTH ( $c_{\text{final}}=2.4$  mM) in the presence of  $\text{FeCl}_3$  (5 mg/mL in 0.05 M HCl) according to Zheng et al. 2014; the first incubation time was 10 min, the second one 30 min; measurement temperature: 30 °C; organic solvent: *n*-hexane;

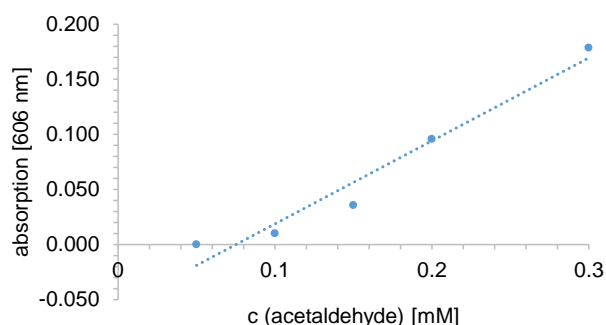


Figure 21: Standard calibration curve of acetaldehyde (0.05-0.3 mM)  $R^2=0.9566$  detected by MBTH ( $c_{\text{final}}=2.4$  mM) in the presence of  $\text{FeCl}_3$  (5 mg/mL in 0.05 M HCl) according to Zheng et al. 2014; the first incubation time was 10 min, the second one 30 min; measurement temperature: 30 °C; organic solvent: *n*-hexane;

Since different incubation times were described in literature (Anthon and Barrett, 2004; Eberhardt and Sieburth, 1985; Zheng et al., 2014) the influence was examined on the standard curve. An increase of the first incubation time from 10 to 20 min and a decrease of the second incubation time from 30 to 20 min resulted in a curve with better linearity as can be seen in Figure 22 ( $R^2=0.9914$ ). In addition Figure 23 shows the color reaction of the standard curve. According to this results the optimized incubation times were used for further investigation.



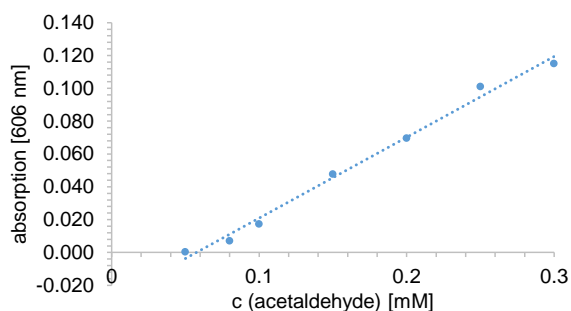


Figure 22: Standard calibration curve of acetaldehyde (0.05-0.3 mM,  $R^2=0.9914$ ) detected by MBTH ( $C_{final}=2.4$  mM) in the presence of  $FeCl_3$  (5 mg/mL in 0.05 M HCl) according to 2.2.1.1.3; the first incubation time was 20 min, the second one 20 min; measurement temperature: 30 °C; organic solvent: n-hexane;

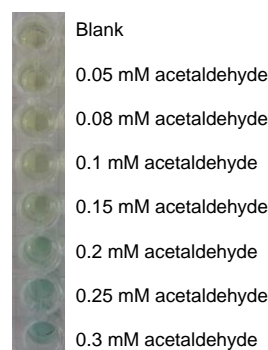


Figure 23: Color reaction of the standard calibration curve of acetaldehyde detected by MBTH ( $C_{final}=2.4$  mM) in the presence of  $FeCl_3$  (5 mg/mL in 0.05 M HCl); the first incubation time was 20 min, the second one 20 min; measurement temperature: 30 °C; organic solvent: n-hexane;

As the detection takes place in an acidic environment the influence of HCl concentration in a range of 0.1 mM to 0.1 M on the reaction was tested as well. This allows adaption, if hydrolytic activity occurs in the substrate test. A reaction can be observed at low concentrations, but it is more intense at higher concentrations. Hence, if not needed HCl concentration should not be lowered to very small molarity. An additional point is that  $FeCl_3$  should always be solved right before usage, otherwise the signal of detection reaction decreases due to oxidation of the  $FeCl_3$  with time. In contrast to that solvation time of MBTH did not influence results.

In the next step the assay was tested with addition of liquid and lyophilized lysate. The liquid one precipitated in organic solvent, thus the microtiter plate was centrifuged for 15 min at maximum speed and acetaldehyde dilutions were transferred to a new plate for detection. The same procedure was applied with lyophilized lysate, because the solid particles would disturb absorption measurement. Resulting standard curves showed a low linearity considering single measurements, duplicates did not fit together quite good. A change in the color of the detection from green to blue could also be observed. This might be an indicator that aldehydes and ketons in the lysate react with the MBTH. Furthermore, after incubation of the acetaldehyde dilutions at room temperature, which should simulate the time of the enzymatic reaction, both the acetaldehyde and the organic solvent volatilize. As cover during incubation time a transparent plastic film and aluminium film were tested, but both could not stop vaporization. Cooling or freezing of the plate after incubation at room temperature also did not work out to condensate the acetaldehyde or organic solvent. Hence evaporation seems to go through the cover. What is more are possible metabolizing reactions of the acetaldehyde by the *E. coli* lysate as additional reason for the disappearance of the same in the presence of lysate over longer incubation periods. Up to now the two different actions can not be separated completely due to evaporation happening as there is no dense cover.

Further investigations on identifying possible metabolizing reactions of the acetaldehyde by *E. coli* lysate clearly remain to be made.

In parallel the best way to suspend the lyophilized lysate in organic solvent in the microtiter plates was figured out. The placing on a shaker as well as in a sonification bath did not lead to satisfactory results. Hence the best option was to stir every well with small magnetic stirrers.

For the sake of completeness background reactions of the substrate (vinylbutyrate and VinEst (DSM)) were tested. As can be seen in Figure 24 none of them showed was hydrolyzed under the chosen reaction conditions in the absence of enzyme.

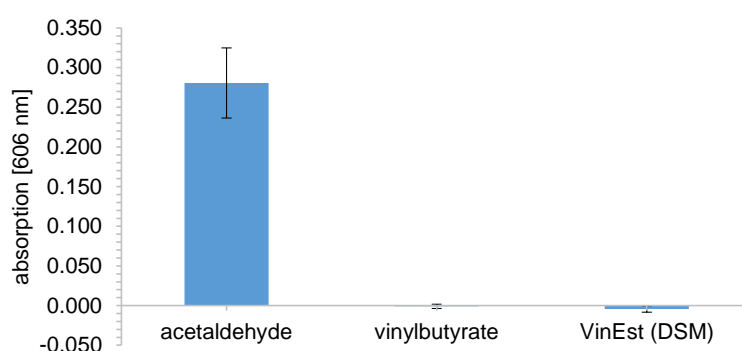


Figure 24: Comparison of the background reaction of different substrates ( $c_{final}=0.1$  mM) in the MBTH assay;  $c_{final}$  (MBTH): 2.4 mM,  $FeCl_3$ : 5 mg/mL in 0.05 M HCl; incubation time 1: 20 min; incubation time 2: 20 min; measurement temperature: 30 °C; organic solvent: *n*-hexane;

As the application of the assay is only possible for detection at the end of the reaction and not as online assay as the reaction conditions would harm the enzyme, but acetaldehyde evaporates during extended incubation times, the MBTH assay is not suitable for high throughput screening of transesterification reaction of esterases with a vinyl ester substrate.

### 3.1.4 Aldehyde detection with Purpald

Purpald is another aldehyde detection reagent. In contrast to MBTH, the reaction takes place under basic conditions; a pink colored complex is formed. To determine the absorption maximum a spectrum was measured in the range of 400 to 800 nm. As a result Figure 25 shows that Purpald's maximal absorption is at a wavelength of 540 nm.

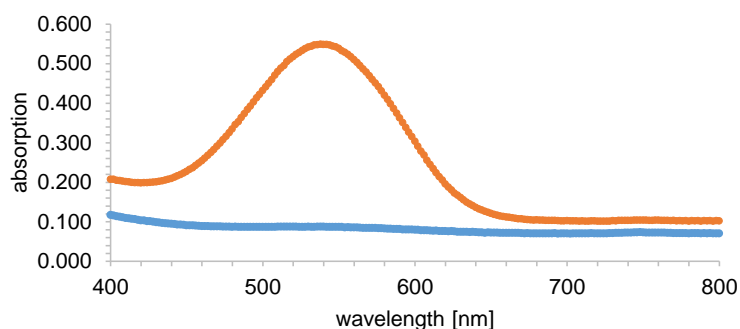


Figure 25: UV spectrum of the acetaldehyde Purpald complex; acetaldehyde  $c_{final}=1$  mM in *n*-hexane are shown with orange dots, *n*-hexane with blue dots;  $c_{final}$  (Purpald)=1 mM; NaOH: 1 M; incubation time: 15 min; measurement temperature: 30 °C;

A standard curve with acetaldehyde dilutions in *n*-hexane was established. As visible in Figure 26 and Figure 27, good linearity ( $R^2=0.9843$ ) is reached in the range of 0.4 to 3 mM. In addition Figure 28 shows the color reaction of the acetaldehyde standard curve detected by Purpald.

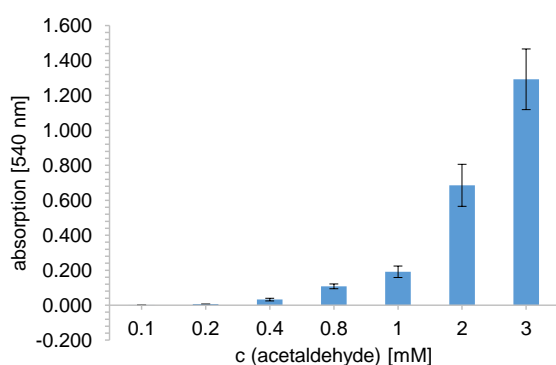


Figure 26: Standard calibration curve of acetaldehyde (0.1-3 mM) with standard deviations (triplicates) detected by Purpald ( $c_{final}=1$  mM) according to 2.2.1.1.4. NaOH: 1 M; incubation time: 15 min; measurement temperature: 30 °C; organic solvent: *n*-hexane;

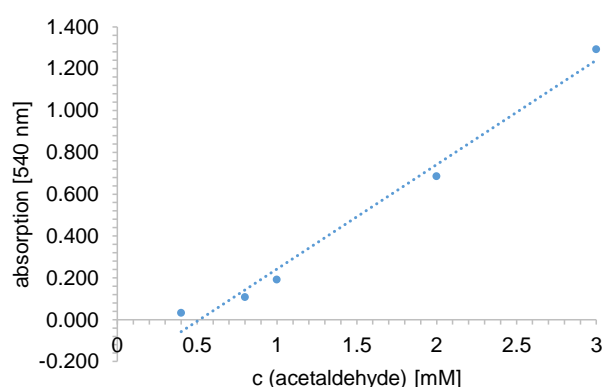


Figure 27: Standard calibration curve of acetaldehyde (0.1-3 mM,  $R^2=0.9843$ ) detected by Purpald ( $c_{final}=1$  mM) according to 2.2.1.1.4; NaOH: 1 M; incubation time: 15 min; measurement temperature: 30 °C; organic solvent: *n*-hexane;

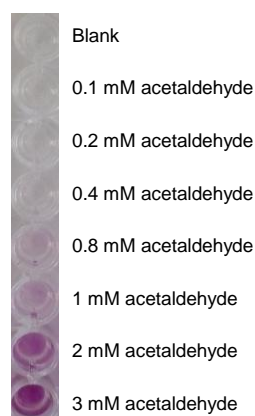


Figure 28: Color reaction of the standard calibration curve of acetaldehyde detected by Purpald ( $c_{final}=1$  mM); NaOH: 1 M; incubation time: 15 min; measurement temperature: 30 °C; organic solvent: *n*-hexane;

In the substrate test, background reaction with vinylbutyrate and VinEst (DSM) appeared (Figure 29).

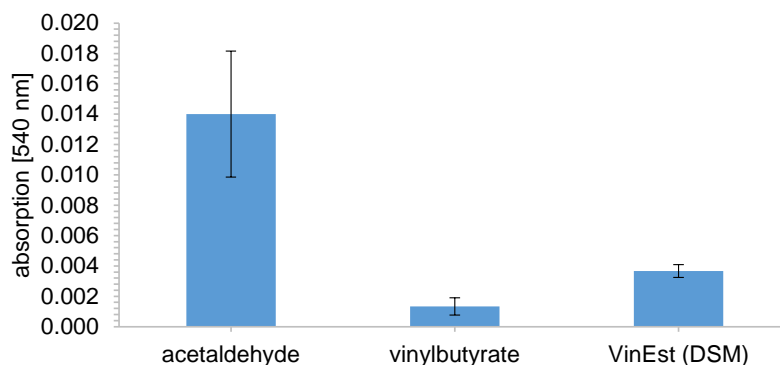


Figure 29: Comparison of the background reaction of different substrates ( $c_{final}=0.4$  mM) in aldehyde detection by Purpald;  $c_{final}$  (Purpald)=1 mM; NaOH: 1 M; incubation time: 15 min; measurement temperature: 30 °C; organic solvent: n-hexane;

No further optimizations of the protocol were made for this method. The alkaline reaction conditions resulted in high background reactions. A possibility to reduce these would be the reduction of NaOH concentration. The minimal concentration for solving the Purpald was 0.01 M of NaOH (sonication bath, 15 min). Analysis using 0.01 M of NaOH were not made. Beyond that on-line measurement is not possible under the applied conditions and the problem of evaporation or metabolizing reactions of the acetaldehyde by *E. coli* lysate needs to be solved. All in all the method is inappropriate for using it for the screening assay.

### 3.1.5 Aldehyde detection with CHD

The second fluorimetric assay for aldehyde detection in this work is the use of CHD as detection reagent. According to the protocol of Vidal *et al.* 2014, a standard curve of acetaldehyde dilutions was measured. It showed good linearity in the range of 0.005 and 1 mM ( $R^2=0.9962$ ) as can be seen in Figure 30 and Figure 31.

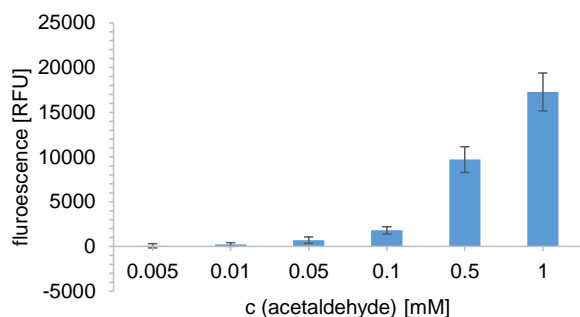


Figure 30: Standard calibration curve of acetaldehyde (0.005-1 mM) with standard deviations (triplicates) detected by CHD in the presence of ammonia acetate after incubation for 1 h at 37 °C; measurement temperature 30 °C; organic solvent: DMSO; emission 460 nm; excitation 395 nm;

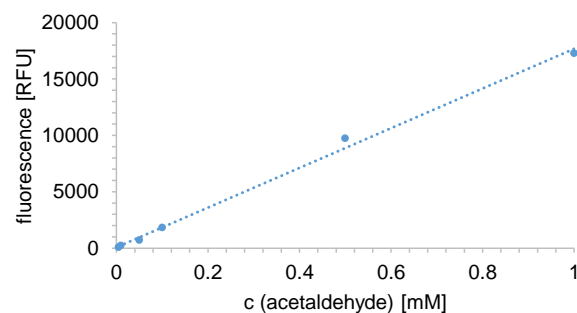


Figure 31: Standard calibration curve of acetaldehyde (0.005-1 mM,  $R^2=0.9962$ ) detected by CHD in the presence of ammonia acetate after incubation for 1 h at 37 °C; measurement temperature 30 °C; organic solvent: DMSO; emission 460 nm; excitation 395 nm;

Afterwards the influence of temperature (30 °C instead of 37 °C) and the minimal incubation times at these temperatures were examined. Measurement at 30 °C needed an incubation time of ~90 min to get a linear curve (0.1-1 mM,  $R^2=0.9893$ ), at 37 °C a minimum of ~30 min was needed (0.05-1 mM,  $R^2=0.9736$ ), but at both temperatures the range of linearity increased with rising reaction time. The substrate test looked similar to that of Purpald. Even higher background reactions with vinylbutyrate and VinEst (DSM) can be seen by using CHD for aldehyde detection (Figure 32).

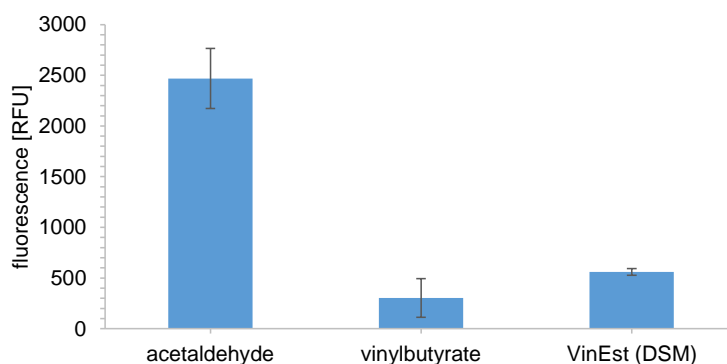


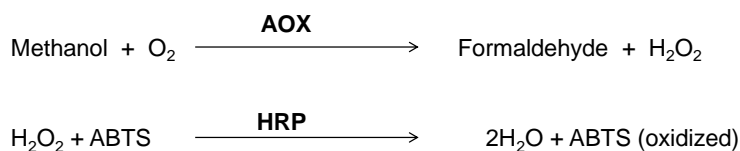
Figure 32: Comparison of the background reaction of different substrates ( $C_{final}=0.1$  mM) detected by CHD in the presence of ammonia acetate after incubation for 1 h at 37 °C; measurement temperature 30 °C; organic solvent: DMSO; emission 460 nm; excitation 395 nm;

Volatilization of the acetaldehyde and the organic solvent as well as possible metabolizing reactions of the acetaldehyde by *E. coli* lysate presumably are problems as well, therefore the method is inappropriate if applied in the described way. Research for the possibility of on-line measurement in non-aqueous environment remains to be made.

### 3.1.6 Methanol detection with AOX and HRP

Besides the detection of acetaldehyde produced via transesterification of a vinylester with an alcohol, methanol can be detected if a methylester is the substrate for the reaction. For that enzymatic reactions with alcohol oxidase (AOX) and horseradish peroxidase (HRP) were

used. In the presence of oxygen the methanol is converted to formaldehyde and hydrogen peroxide by an AOX. Latter is converted with 2,2'-azino-bis-(3-ethylbenzothiazole-6-sulfonic acid (ABTS) by the HRP to water and ABTS (oxidized) (Janssen and Ruelius, 1968; Keeseey, 1987). The scheme of reaction can be seen in Figure 33.



ABTS: 2,2'-azino-bis-(3-ethylbenzothiazoline-6-sulfonic acid),  $c_{\text{final}}=4$  mM  
 HRP: Horse raddish peroxidase,  $c_{\text{final}}=1.5$  U/mL  
 AOX: Alcoholoxidase,  $c_{\text{final}}=50$  U/mL  
 Methanol:  $c_{\text{final}}=20$  mM

Figure 33: Reaction of enzymatic methanol detection with AOX and HRP

Figure 34 shows the conversion of methanol via the AOX/HRP system over time.

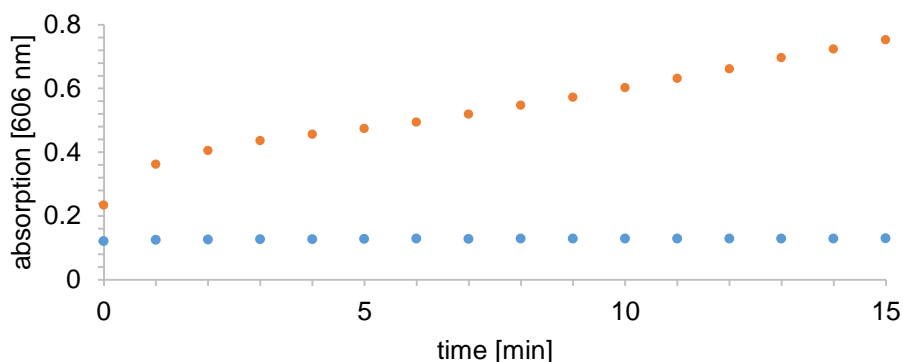


Figure 34: Methanol detected by AOX and HRP according to 2.2.1.2; blank (blue dots) methanol 250 mM orange dots; measurement temperature: 30 °C;

The addition of liquid lysate of *E. coli* did not disturb the measurement, as the curve looked similar to that of Figure 34. Even an incubation time of the methanol over-night did not affect its detection e.g. by evaporating through the tape seal or metabolizing reactions by *E. coli* lysate. Results of testing possible background reactions of methylbutyrate or MeEst (DSM) are shown in Figure 35.

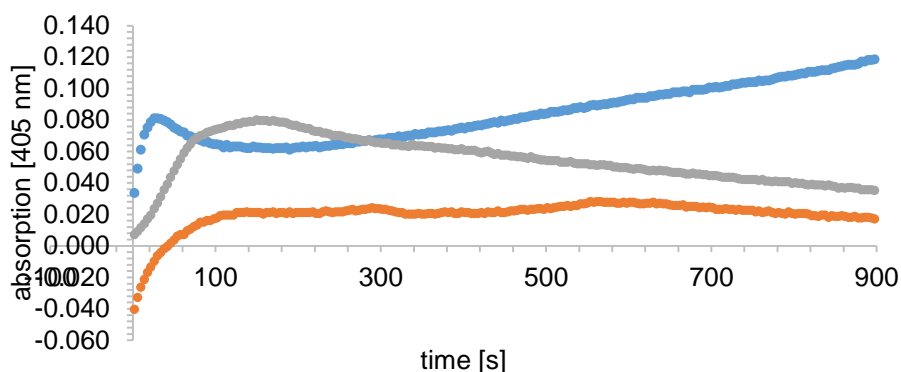


Figure 35: Comparison of the background reaction of different substrates in enzymatic methanol detection via AOX and HRP; 250 mM, methanol (blue dots), methylbutyrate (orange dots) and MeEst (DSM) (grey dots); measurement temperature: 30 °C;

There is a signal for both the methylbutyrate and MeEst (DMS). This indicates hydrolysis of these substrates in aqueous solution. Due to this background signal the method seems to be inappropriate for screening esterases concerning their transesterification activity.

## 3.2 Cloning experiments for creating EstB variants

### 3.2.1 Mutagenesis

The enzyme of choice for mutagenesis is the hydrolase EstB from *Burkholderia gladioli*. Eighteen different variants were created to enlarge the space for substrates/products entering and leaving the enzyme. Thus the conversion of bigger substrates should be possible. Variants were created by overlap extension PCR and site-directed mutagenesis. The preparative agarosegel of PCR 1 showed bands at a size of ~800 and ~500 bp for the two fragments of each gene. The exact length of the PCR 1 products with overhangs for ligation with the pMS vector can be seen in Table 2. With exception of the gene fragments for the EstB-M377A variant PCR 1 products could be used for further processing. After PCR 2 most of the lines of the preparative agarosegel were smeared and some additional bands could be seen. The correct sized band at ~1300 bp was not there at all or very light. As the sequence for EstB is rich in G and C, three different additives, DMSO, betaine and MgCl<sub>2</sub>, which were described in literature to use for GC rich sequences (Frackman et al., 1998), were tested to improve PCR 2 results. The addition of 0.5 and 1 mM MgCl<sub>2</sub> alone (data not shown) and the combination of MgCl<sub>2</sub> with 5 % DMSO did not enhance PCR reaction at all. No or a very light correct sized bands can be seen in addition to unspecific bands (Figure 36). Betaine in the concentrations of 0.125 and 0.25 M and 2.5 and 5 % of DMSO as well as the combination of betaine (0.25 M) and DMSO (5 %) could improve the intensiveness of the band at ~1300 bp, but there were still unspecific bands (Figure 36). Due to least additional bands and an intensive correct sized band 10 % of DMSO were added to PCR 2 reactions.

As smeary other small bands could be seen in PCR 1 too, 10 % DMSO were added in the left reactions as well to reduce unspecific binding of the primers.

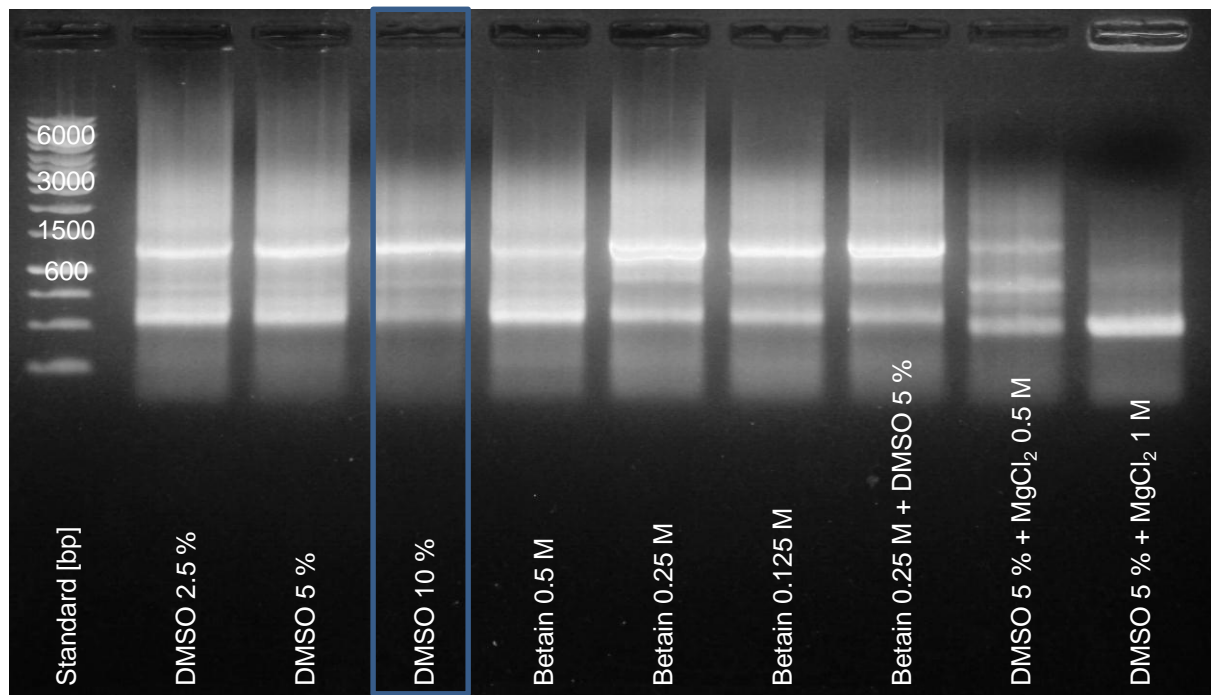


Figure 36: Agarosegel after PCR 2 of *EstB* variant genes with the three different additiva DMSO, betaine and  $MgCl_2$  recommended for GC rich sequences

DNA concentrations after gel purification of the gene fragments and the complete gene can be seen in Table 5.

Table 5: DNA concentrations of PCR 1 and PCR 2 products after gel purification

Gene fragment	c [ng/ $\mu$ L]	Gene fragment	c [ng/ $\mu$ L]	Gene	c [ng/ $\mu$ L]
EstB-Y133A_for	41.3	EstB-R155V_for	64.4	EstB-Y133A	16.4
EstB-Y133A_rev	33.8	EstB-R155V_rev	78.4	EstB-Y133V	48.9
EstB-Y133V_for	52.9	EstB-L249A_for	36.2	EstB-W134A	11.1
EstB-Y133V_rev	52.7	EstB-L249A_rev	57.8	EstB-W134F	27.2
EstB-W134A_for	17.8	EstB-H253A_for	21.5	EstB-L135A	11.5
EstB-W134A_rev	35.8	EstB-H253A_rev	36.1	EstB-D150A	22.2
EstB-W134F_for	39.3	EstB-H253L_for	35.6	EstB-I152A	10.1
EstB-W134F_rev	52.2	EstB-H253L_rev	27.1	EstB-D153A	10.3
EstB-L135A_for	35.1	EstB-V257A_for	12.7	EstB-R155A	18.4
EstB-L135A_rev	31.0	EstB-V257A_rev	51.6	EstB-R155V	21.3
EstB-D150A_for	58.6	EstB-R258A_for	65.8	EstB-L249A	16.9
EstB-D150A_rev	26.8	EstB-R258A_rev	8.7	EstB-H253A	18.5
EstB-I152A_for	14.4	EstB-R258V_for	31.3	EstB-H253L	16.3
EstB-I152A_rev	15.8	EstB-R258V_rev	21.5	EstB-V257A	22.1
EstB-D153A_for	35.1	EstB-V351A_for	15.8	EstB-R258A	14.4



EstB-D153A_rev	56.9	EstB-V351A_rev	69.0	EstB-R258V	38.3
EstB-R155A_for	59.3	EstB-M377A_for	-	EstB-V351A	18.5
EstB-R155A_rev	81.4	EstB-M377A_rev	-	EstB-M377A	-

As vector backbone pMS470 was used. After cutting with *NdeI* and *HindIII* a correct sized band appeared at ~4000 bp at the preparative agarosegel. Gibson cloning was applied to combine inserts and the digested vector. The plasmid of the Est-B-M377A variant was the only one created by following the procedure of site-directed mutagenesis. *E. coli* Top10F' cells were transformed with the plasmids afterwards. In order to determine the success of the cloning a colony PCR was made. Figure 37 exemplary shows the results of it for the EstB-W134F variant. Positive hits with a band at ~1300 bp can be seen in the blue squares. As control the pMS vector was used, which has a 1600 bp fragment in the cloning site which can also be seen on the gel.

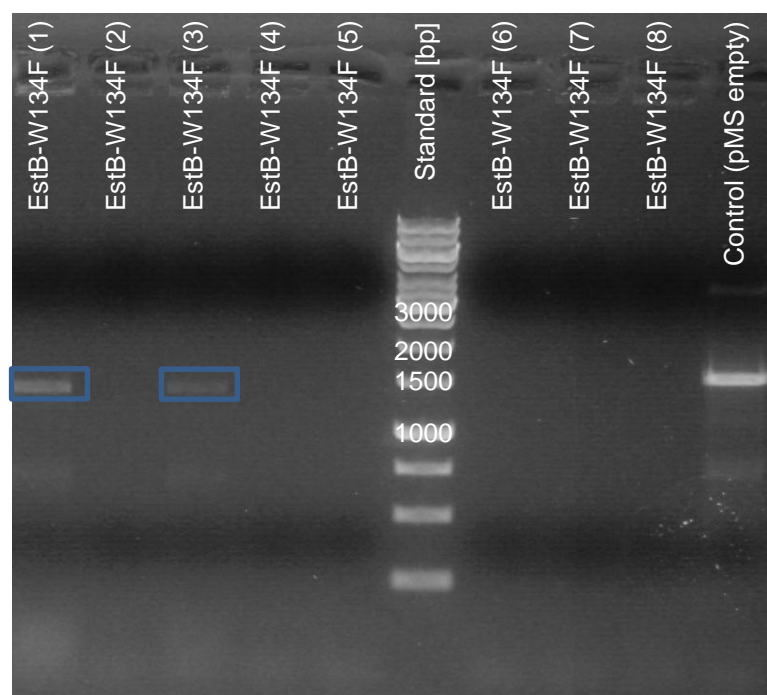


Figure 37: Agarosegel colony PCR from pMS470-EstB-W134F

Several positive colonies of each construct were streaked out to isolate their plasmid DNA for sequencing. As soon as a colony with the correct sequence was found without any additional mutations it could be used for further processing. DNA concentration of plasmids containing the EstB gene with correct sequences can be seen in Table 6.

Table 6: DNA concentrations [ng/μL] of plasmid DNA of the different EstB variants with correct sequence

variant	DNA concentration [ng/μL]
EstB-Y133A	192.0

EstB-Y133V	175.9
EstB-W134A	100.6
EstB-W134F	82.5
EstB-L135A	196.8
EstB-D150A	71.1
EstB-I152A	178.7
EstB-D153A	186.5
EstB-R155A	123.4
EstB-R155V	155.9
EstB-L249A	180.6
EstB-H253A	96.0
EstB-H253L	223.8
EstB-V257A	272.0
EstB-R258A	140.4
EstB-R258V	86.9
EstB-V351A	162.7
EstB-M377A	120.9

All plasmids, except the I152A and the M377A variants, which had still additional mutations at this time, were used for transformation of *E.coli* Top10 F' cells for cultivation and protein expression.

### 3.2.2 Expression of esterase variants

The EstB variants were expressed by shake flask cultivation to analyze their expression. Single colonies were used to inoculate the precultures. OD<sub>600</sub> measurements at different timepoints can be seen in Table 7.

Table 7: OD<sub>600</sub> measurement of shake flask cultivation of *E.coli* Top10F'-pMS-EstB variants and weight of the cell pellet after cell harvest [g]

variant	OD <sub>600</sub>				cell pellet [g]
	preculture	inoculation	induction	cell harvest	
EstB-Y133A	0.47	0.005	0.76	6.83	2.3
EstB-Y133V	0.51	0.005	0.83	6.39	2.1
EstB-W134A	0.76	0.008	0.81	6.57	2.2
EstB-W134F	0.37	0.004	0.76	1.51	2.2
EstB-L135A	0.92	0.009	0.76	6.15	2.1
EstB-D150A	0.92	0.009	0.76	6.76	2.0
EstB-D153A	0.36	0.004	0.72	6.25	2.2
EstB-R155A	0.65	0.007	0.72	7.02	2.0
EstB-R155V	0.47	0.005	0.74	6.04	2.2
EstB-L249A	2.59	0.026	0.93	4.71	2.3

EstB-H253A	1.86	0.019	0.77	3.62	2.0
EstB-H253L	2.62	0.026	0.90	5.11	2.3
EstB-V257A	2.23	0.022	0.83	4.52	2.3
EstB-R258A	2.45	0.025	0.90	4.71	2.4
EstB-R258V	2.09	0.021	0.90	4.95	2.4
EstB-V351A	2.11	0.021	0.80	4.53	2.3
Wild type	2.44	0.024	1.1	5.87	2.5
pMS control	2.91	0.030	0.75	4.55	2.0

As not all variants could be expressed in the same cultivation differences in growing of the precultures could be observed due to a longer incubation time. After harvesting the cells were disrupted by sonification. The protein content of the cell free lysate was determined by Bio-Rad protein assay. Figure 38 shows the corresponding BSA standard curve which was used to calculate protein concentrations (Table 8).

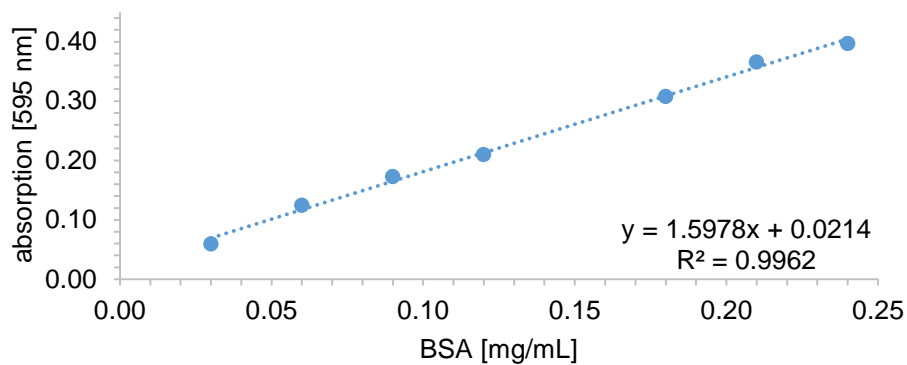


Figure 38: Bio-Rad protein assay BSA standard calibration curve

Table 8: Protein concentrations of the cell free lysate from EstB variants from shaking flask fermentation after Bio-Rad protein assay [mg/mL]

variant	mean [mg/mL]	standard deviation
EstB-Y133A	13.50	0.98
EstB-Y133V	14.34	0.29
EstB-W134A	11.69	0.97
EstB-W134F	11.64	0.64
EstB-L135A	11.17	0.75
EstB-D150A	11.65	0.89
EstB-D153A	11.40	0.87
EstB-R155A	11.11	0.99
EstB-R155V	12.30	1.15
EstB-L249A	12.31	0.74

EstB-H253A	10.42	0.46
EstB-H253L	13.48	0.31
EstB-V257A	13.56	0.69
EstB-R258A	16.14	0.51
EstB-R258V	12.49	0.62
EstB-V351A	11.77	0.69
Wild type	16.18	0.62
pMS empty	13.74	0.38

With the exception of the wildtype and the R258A variant with a protein content of ~16 mg/mL in the cell free lysate, protein expression in the other variants was quite similarly between 11 and 14 mg/mL.

In the following the SDS-PAGE gel of the different lysate fractions can be seen in Figure 39.

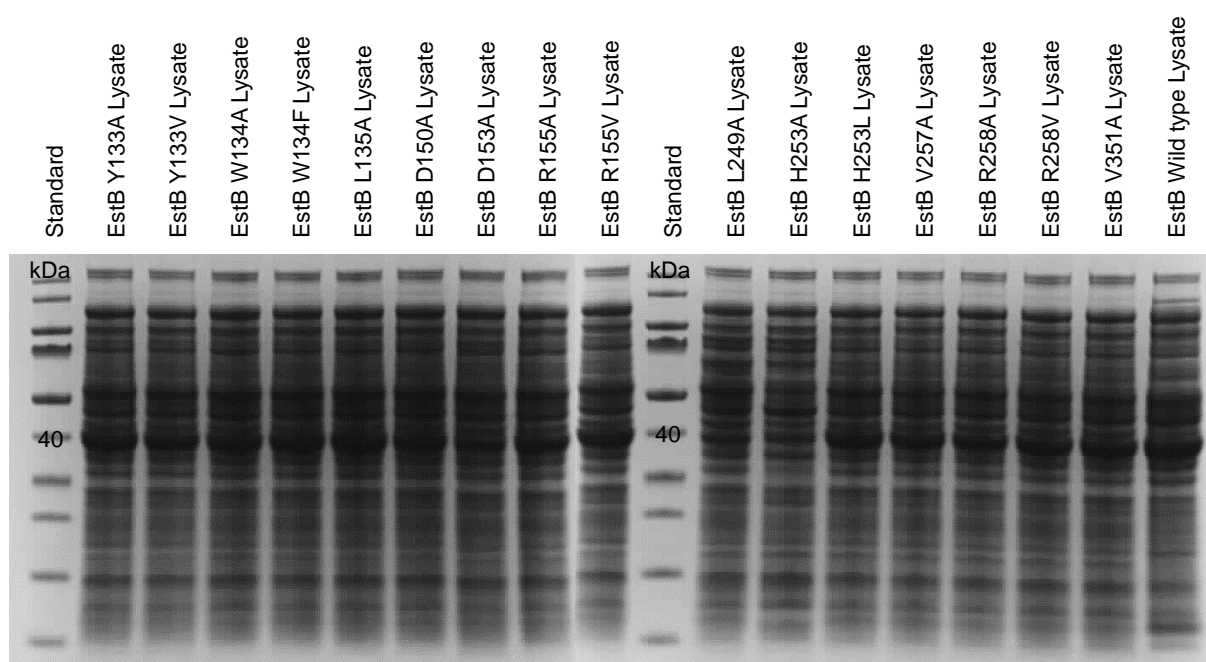


Figure 39: SDS-PAGE of the lysate fraction (2.5 µg protein) of shake flask cultivation

Almost all variants showed a visible and intensive band at 42 kDa, which represents the size of EstB, in the lysate fraction. The less intensive bands of the L249A and the H253A variant might be due to the formation of inclusion bodies. These can not be analyzed in detail in the pellet fraction, because outer membrane proteins have the same size as EstB. Nevertheless all created variants are expressed and soluble. The exact percentage of EstB variants of total protein in the cell free lysate is shown in Table 9. Quantitative analysis was made with computer software (GeneTool by Syngene). Rather low calculations for some variants

(L135A, D150A, D153A) do not match with visual observations. Hence normalizing of data to the wildtype was not possible due to obviously wrong analysis of the computer software.

Table 9: Percentage of EstB variants of total protein in the cell free lysate

EstB variant	Y133A	Y133V	W134A	W134F	L135A	D150A	D153A	R155A	R155V
[%] total protein	13	12	10	11	6	9	8	12	13
EstB variant	L249A	H253A	H253L	V257A	R258A	R258V	V351A	WT	
[%] total protein	5	5	12	11	12	12	12	14	

For the sake of completeness the plasmids pMS-EstB-I152A and pMS-EstB-M377A transformed *E.coli* Top10F' later. Protein expression showed that these variants were expressed and soluble as well.

In addition to the shake flask cultivation a DWP cultivation of esterases from a reference stock was made to estimate protein expression in two different media via Bio-Rad protein assay. As can be seen in Table 10 protein expression in lysogeny broth medium resulted in ~5 mg/mL protein, whereas protein expression in 2xTY medium resulted in a higher protein concentration (~7 mg/mL) for all different esterases. A reason for this might be the rich composition of 2xTY medium, which contains 1.5 fold more trypton and doubled amount of yeast extract compared to lysogeny broth medium. It is presumably that growing of bacteria is enhanced thereby and therefore total protein content in the cell free lysate is higher.

Table 10: Protein concentration [mg/mL] of cell free lysate from DWP cultivation of different esterases in lysogeny broth and 2xTY medium

variant	lysogeny broth medium		2xTY medium	
	mean [mg/mL]	standard deviation	mean [mg/mL]	standard deviation
pKN27	5.89	2.057	6.58	0.942
pKNJ70	4.28	0.569	6.42	0.885
pMS-NJ70M7	5.04	0.655	6.77	0.735
pMS-NJ70J22	4.69	0.381	6.61	1.047
pMS-EstB-WT	4.64	0.743	6.97	1.954

The created EstB variants were expressed by shaking flask and DWP cultivation for further analysis by the pH-shift assay.

### 3.2.3 Screening of EstB variants with the pH-shift assay

At first the pH-shift assay was made with a defined amount of protein with cell free lysate derived from shake flask fermentation to get a comparable impression of the activity of the EstB variants in an aqueous environment. Figure 40 shows that almost all variants show comparable or slightly more activity than the wild type. Exceptions thereof are the inactive

EstB-L249A variant and the less active EstB-H253A variant. Low expression (0.4 fold compared to the WT for both) might be the reason (3.2.2). In addition a  $\beta$ -sheet which contains the residues 249 to 255 partly covers the entrance to the active site of the enzyme (Wagner et al., 2002). The change of L to A and of H to A at positions 249 and 253 respectively might lead to conformational changes which deteriorate the accessibility of the active site serine, hence enzyme activity is limited.

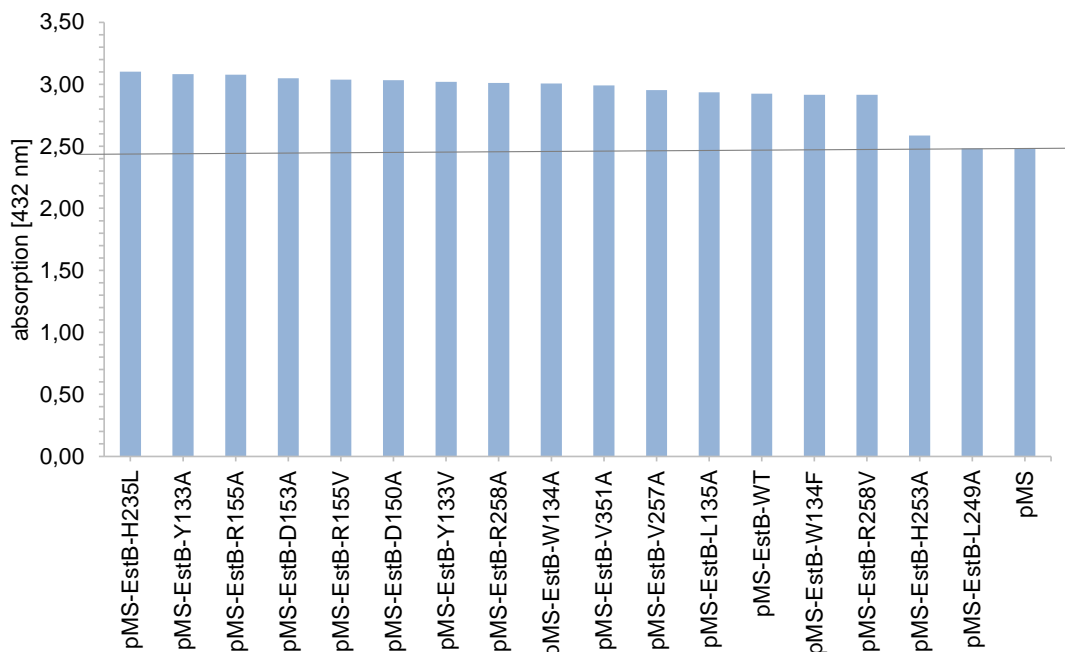


Figure 40: pH-shift assay of EstB variants with *E. coli* lysate (5 mg/mL) from shaking flask cultivation; the black line marks the activity of the wild type EstB; vinylbutyrate ( $C_{final}=25$  mM) was used as substrate; the pH shift of enzymatic reaction of hydrolases in the presence of water was detected with phenol red ( $C_{final}=0.01$  %); reaction time: 15 min; end point measurement at 432 nm at 30 °C; measurement of duplicates;

As second the pH-shift assay was applied with lysate (*E. coli* TOP10F'-pMS) from DWP cultivations. Two different cultivations were measured two times. Results can be seen in Figure 41.

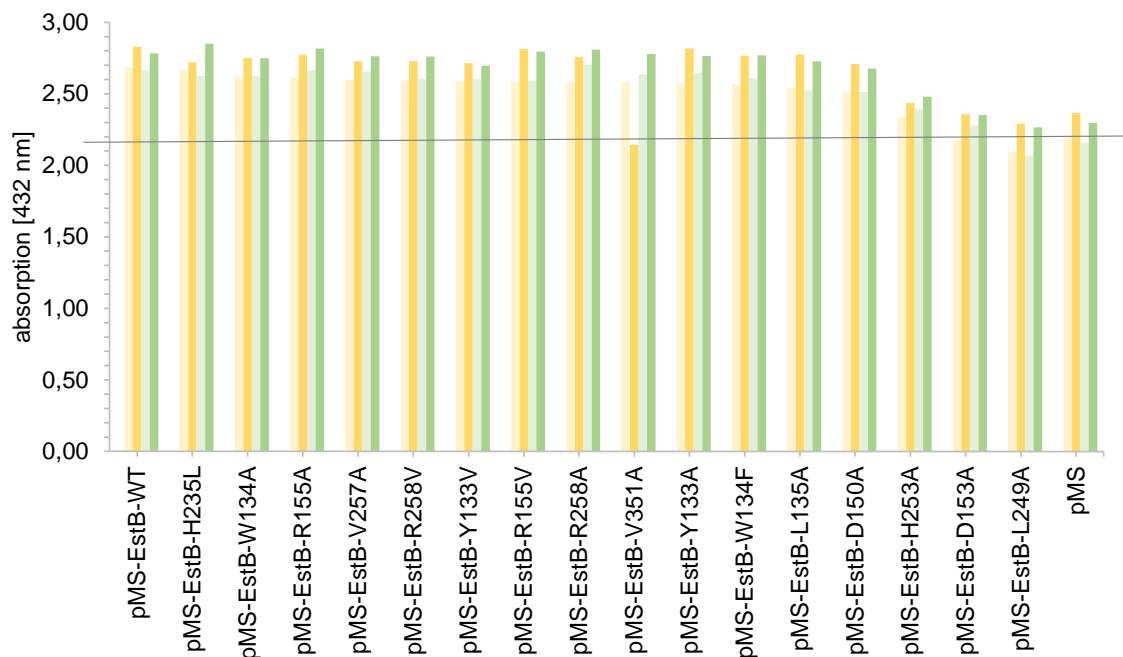


Figure 41: pH-shift in aqueous reaction medium of liquid *E. coli* lysate (50  $\mu$ L) from DWP cultivations of EstB variants; vinylbutyrate ( $C_{final}=25$  mM) was used as substrate; the pH shift was detected with phenol red ( $C_{final}=0.01$  %); the yellow and the green bars indicate the lysate of two different *E. coli* DWP cultivations; reaction time: 15 min; end point measurement at 432 nm at 30  $^{\circ}$ C; measurement of duplicates;

In general both the two cultivations and the doubled measured lysate fit together. Except EstB-H253A and EstB-L249A all variants showed similar or slight better activity compared to the wild type. In contrast to the results above the EstB-D153A variant did not show good activity as well. Differences in doubled measured lysate can be explained via variability of the assay itself. The growing behavior of *E. coli* cells, which is variable in cultivations, explains the differences between the lysate of the two measured DWPs. Limited growth also could ascribe the huge difference of activity of the EstB-D153A variant in the pH-shift assay from DWP cultivation and in the pH-shift assay with lysate from shaking flask cultivation, where a defined amount of protein was used. For the sake of completeness the I152A and the M377A variant were expressed later and showed activity in the pH-shift assay as well.

## 4 Conclusion

To sum up the first part of the present work the establishing of a high throughput assay for screening for transesterification activity partly worked. After modifying the protocol of Konarzycka-Bessler and Bornscheuer (2003) an acetaldehyde standard curve with good linearity ( $R^2=0.9763$ ) could be measured. Optimizations were made concerning the general handling (pre-cooling of equipment and acetaldehyde), the organic solvent (*n*-hexan:*tert*-butanol 1:1 v/v), the acetaldehyde concentration range (0.05 to 0.8 mM) and measurement conditions (shaking step 500 rpm, 3 s, before every cycle, measurement temperature 30 °C). Applying the assay by measuring the activity of different esterases in an organic environment lead to the verification of the assay. What remains for further investigations is the process of lyophilization (attitude, variability within the 96-well plate, time, addition of additives), the choice of organic solvents or their mixing ratio respectively (stability and activity of enzymes), the drying of the solvents before using them in the assay, the determination of optimal amounts of enzyme and substrate as well as the effect of using PP microtiter plates instead of PS microtiter plates. Since the detection reaction of aldehydes via MBTH and Purpald require acidic or alkaline conditions on-line measurement is not possible. Evaporation of the acetaldehyde and the organic solvents or metabolizing reactions of the acetaldehyde by the *E. coli* lysate during transesterification reaction are limiting problems and still have to be identified clearly. Therefore a suitable dense cover for the microtiter plates is necessary. The applicability of aldehyde detection with CHD is not suitable for the screening assay as well if executed as described. Background reactions occur by the hydrolysis of the vinylbutyrate and the MeEst (DSM). On-line measurement in non-aqueous environment remains to be evaluated. Due to the need of solvent stable, UV suitable microtiter plates, which are very expensive as well as due to the high background of both, the liquid lysate and the empty UV microtiter plates, measuring the decrease of the vinylsubstrate is not appropriate for the assay. Last but not least methanol detection by the enzymatic AOX and HRP combination is not eligible as well. High background signals due to hydrolysis of the methylester and the MeEst (DSM) do not enable the determination of the enzymes synthesis activity reliably. Hence the on-line detection of the produced acetaldehyde released during transesterification reactions of a vinyl substrate with an alcohol by NBD-H is the best way to screen for esterase synthesis activity in a high throughput way. However, further improvements, already mentioned above, are still necessary to enhance reproducibility of the assay in practical applications to get reliable results and to rule out enzyme catalyzed hydrolysis of the ester in the presence of trace amounts of water. In the second part of the present work creation of EstB variants was successful via overlap extension PCR and site-directed mutagenesis. PCR conditions were optimized by adding 10 % DMSO for the GC rich sequences. Defined amounts of the expressed variants were analyzed for their hydrolysis activity in aqueous



solution by analyzing the occurring pH shift. Almost all variants were active, most of them in equivalent levels of the wild type. Exceptions due to low expression were EstB-L249A and EstB-H253A. In addition lysate from DWP cultivations was examined for high throughput screening. The variants EstB-L249A and EstB-H253A, EstB-D153A showed low activity. The reason might be low expression in the DWP cultivation. The application of the screening assay with NBD-H was not possible here due to missing reproducibility. Further investigations have to be made.

## 5 Tables

Table 1: Overview of the enzyme class of hydrolases (EC3) .....	- 1 -
Table 2: List of primers used with the desired mutation .....	- 21 -
Table 3: Components of 5x isothermal reaction buffer.....	- 24 -
Table 4: Components of Gibson assembly mix.....	- 24 -
Table 5: DNA concentrations of PCR 1 and PCR 2 products after gel purification .....	- 48 -
Table 6: DNA concentrations [ng/ $\mu$ L] of plasmid DNA of the different EstB variants with correct sequence.....	- 49 -
Table 7: OD <sub>600</sub> measurement of shake flask cultivation of E.coli Top10F'-pMS-EstB variants and weight of the cell pellet after cell harvest [g].....	- 50 -
Table 8: Protein concentrations of the cell free lysate from EstB variants from shaking flask fermentation after Bio-Rad protein assay [mg/mL].....	- 51 -
Table 9: Percentage of EstB variants of total protein in the cell free lysate .....	- 53 -
Table 10: Protein concentration [mg/mL] of cell free lysate from DWP cultivation of different esterases in lysogeny broth and 2xTY medium .....	- 53 -

## 6 Figures

- Figure 1: Reaction mechanism of the catalytic triad in the active site of hydrolases (Aranda et al., 2014) ..... - 4 -
- Figure 2: Reaction mechanism of NBD-H with aldehydes to the corresponding hydrazone (Konarzycka-Bessler and Bornscheuer, 2003) ..... - 9 -
- Figure 3: Reaction mechanism of MBTH with aldehydes via the corresponding aldazine to the blue colored tetra-aza-pentamethincyanine (Vogel and Karst, 2000)..... - 10 -
- Figure 4: Reaction mechanism of Hantz'sche reagent. Condensation reaction of aldehydes with ammonia and acetylacetone (solid line) or dimedone (dotted line) (Vogel and Karst, 2000)..... - 11 -
- Figure 5: Reaction mechanism of Purpald (Vogel and Karst, 2000)..... - 12 -
- Figure 6: Standard calibration curve of acetaldehyde ( $c_{\text{final}}=0.001-0.025$  mM) detected by NBD-H ( $c_{\text{final}}\sim 0.3$  mM) according to Konarzycka-Bessler and Bornscheuer 2003 with isooctane:1-propanol 10:1 (v/v) resulting in  $R^2=0.9899$  (blue dots) and isooctane:1-butanol 10:1 (v/v) resulting in  $R^2=0.8986$  (orange dots) as solvents; fluorescence measurement was at 485 nm excitation and 520 nm emission at 45 °C, no shaking; ..... - 30 -
- Figure 7: Acetaldehyde standard curves after 5 min reaction time with NBD-H with a previous shaking step (500 rpm, 1 s) in the linear range of 0.05 to 0.8 mM ( $c_{\text{final}}$ ) with different solvents; all instruments were precooled before starting the experiment; fluorescence measurement was at 485 nm excitation and 520 nm emission measurement temperature was 45 °C; blue dots: n-hexane:tert-butanol 1:1 (v/v),  $R^2=0.9763$ ; orange dots: DMSO:tert-butanol 1:1 (v/v),  $R^2=0.9831$ ; grey dots: acetonitrile:tert-butanol 1:1 (v/v),  $R^2=0.9899$ ; yellow dots: tBME:tert-butanol 1:1 (v/v),  $R^2=0.8142$  (yellow dots);..... - 32 -
- Figure 8: Fluorescence of acetaldehyde standard dilutions [mM] over time (45 min) in n-hexane:tert-butanol 1:1 (v/v) as organic solvent; all instruments were precooled before starting the experiment; fluorescence measurement was at 485 nm excitation and 520 nm emission; measurement temperature was 45 °C; a shaking step was added to the protocol (500 rpm, 1 s);..... - 33 -
- Figure 9: Fluorescence signal of acetaldehyde (0.05-0.5 mM) with standard deviation (triplicates) detected by NBD-H after 5 min reaction time; shaking step: 500 rpm, 3 s, before every cycle; organic solvent: n-hexane:tert-butanol 1:1 (v/v); all instruments were precooled before starting the experiment; fluorescence measurement was at 485 nm excitation and 520 nm emission; measurement temperature was 30 °C;..... - 34 -
- Figure 10: Standard calibration curve of acetaldehyde in the range of 0.05-0.5 mM,  $R^2=0.9774$  (0.1-0.5 mM,  $R^2=0.9771$  respectively) detected by NBD-H after 5 min reaction time; shaking step: 500 rpm, 3 s, before every cycle; organic solvent: n-hexane:tert-butanol 1:1 (v/v); all instruments were precooled before starting the experiment; fluorescence

measurement was at 485 nm excitation and 520 nm emission; measurement temperature was 30 °C;..... - 34 -

Figure 11: On-line measurement of possible background reactions of different substrates (vinylbutyrate, orange dots; VinEst (DSM), grey dots;  $c_{\text{final}}=0.4$  mM) in comparison with the reaction of acetaldehyde ( $c_{\text{final}}=0.4$  mM, blue dots) with NBD-H ( $c_{\text{final}}=0.2$  mM); organic solvent n-hexane:tert-butanol 1:1 (v/v); shaking step: 500 rpm, 1 s, before each cycle; fluorescence measurement was at 485 nm excitation and 520 nm emission; measurement temperature 30 °C; ..... - 34 -

Figure 12: Verification of the NBD-H assay by comparison of the activity of different esterase variants (triplicates): pKN27 (blue dots), pKNJ70 (orange dots), pMS-NJ70-M7 (grey dots), pMS-NJ70-J22 (yellow dots) and pMS-EstB-WT (green dots); organic solvent: n-hexane:tert-butanol 1:1 (v/v); shaking step: 500 rpm, 3 s, before each cycle; fluorescence measurement was at 485 nm excitation and 520 nm emission; measurement temperature 30 °C; cell free lysate from shaking flask cultivation of E. coli was used; Vinylbutyrate  $c_{\text{final}}=10$  mM; ..... - 35 -

Figure 13: pH-shift in aqueous reaction medium of liquid E. coli lysate (50  $\mu$ L) from DWP cultivations of different esterases; vinylbutyrate ( $c_{\text{final}}=25$  mM) was used as substrate; the pH shift was detected with phenolred ( $c_{\text{final}}=0.01$  %); the yellow and the green bars indicate the lysate of two different E. coli DWP cultivations; reaction time: 15 min; end point measurement at 432 nm at 30 °C; measurement of duplicates; ..... - 36 -

Figure 14: Acetaldehyde detection via on-line measurement with NBD-H in organic solvent; transesterification reaction of different esterases (duplicates) in the absence of water was analyzed with n-hexane:tert-butanol 1:1 (v/v) as solvent; the yellow and the green bars indicate the lysate of two different DWP cultivations; reaction time: 60 min; fluorescence measurement was at 485 nm excitation and 520 nm emission; measurement temperature: 30 °C; shaking step: 500 rpm, 3 s, after each cycle; lysate of E. coli (50  $\mu$ L) was lyophilized over night; Vinylbutyrate was used as substrate ( $c_{\text{final}}=25$  mM); ..... - 37 -

Figure 15: Acetaldehyde detection via on-line measurement with NBD-H; transesterification reaction of different esterases (duplicates) in the absence of water was analyzed with DMSO:tert-butanol 1:1 (v/v) as solvent; the yellow and the green bars indicate the lysate of two different DWP cultivations; reaction time: 60 min; fluorescence measurement was at 485 nm excitation and 520 nm emission; measurement temperature: 30 °C; shaking step: 500 rpm, 3 s, after each cycle; lysate of E. coli was lyophilized over night (50  $\mu$ L); Vinylbutyrate was used as substrate ( $c_{\text{final}}=25$  mM); ..... - 38 -

Figure 16: UV/Vis spectrum of different vinylbutyrate concentrations ( $c_{\text{final}}$ ) in tert-butanol: 0.25 mM (blue dots), 0.5 mM (orange dots), 2.5 mM (grey dots) and 5 mM (yellow dots); organic solvent: tert-butanol; measurement temperature: 30 °C; ..... - 39 -

- Figure 17: Standard calibration curve of vinylbutyrate (0.001-1 mM) in tert-butanol with standard deviations (triplicates); measured at 216 nm at 30 °C; prewarmed equipment; . - 39 -
- Figure 18: Standard calibration curve of vinylbutyrate in tert-butanol in the range of  $c_{\text{final}}=0.001-1$  mM ( $R^2=0.9934$ ) measured at 216 nm at 30 °C; prewarmed equipment; .... - 39 -
- Figure 19: UV spectrum of TAPMC from aldehyde detection with MBTH ( $c_{\text{final}}=0.2$  mM) in the presence of  $\text{FeCl}_3$  (5 mg/mL in 0.05 M HCl); acetaldehyde (0.1 mM) in n-hexane (blue dots), n-hexane (orange dots); the first incubation time was 10 min, the second one 30 min; measurement temperature: 30 °C; ..... - 40 -
- Figure 20: Standard calibration curve of acetaldehyde (0.05-0.3 mM) with standard deviations (triplicates) detected by MBTH ( $c_{\text{final}}=2.4$  mM) in the presence of  $\text{FeCl}_3$  (5 mg/mL in 0.05 M HCl) according to Zheng et al. 2014; the first incubation time was 10 min, the second one 30 min; measurement temperature: 30 °C; organic solvent: n-hexane; ..... - 40 -
- Figure 21: Standard calibration curve of acetaldehyde (0.05-0.3 mM)  $R^2=0.9566$  detected by MBTH ( $c_{\text{final}}=2.4$  mM) in the presence of  $\text{FeCl}_3$  (5 mg/mL in 0.05 M HCl) according to Zheng et al. 2014; the first incubation time was 10 min, the second one 30 min; measurement temperature: 30 °C; organic solvent: n-hexane;..... - 40 -
- Figure 22: Standard calibration curve of acetaldehyde (0.05-0.3 mM,  $R^2=0.9914$ ) detected by MBTH ( $c_{\text{final}}=2.4$  mM) in the presence of  $\text{FeCl}_3$  (5 mg/mL in 0.05 M HCl) according to 2.2.1.1.3; the first incubation time was 20 min, the second one 20 min; measurement temperature: 30 °C; organic solvent: n-hexane;..... - 41 -
- Figure 23: Color reaction of the standard calibration curve of acetaldehyde detected by MBTH ( $c_{\text{final}}=2.4$  mM) in the presence of  $\text{FeCl}_3$  (5 mg/mL in 0.05 M HCl); the first incubation time was 20 min, the second one 20 min; measurement temperature: 30 °C; organic solvent: n-hexane; ..... - 41 -
- Figure 24: Comparison of the background reaction of different substrates ( $c_{\text{final}}=0.1$  mM) in the MBTH assay;  $c_{\text{final}}$  (MBTH): 2.4 mM,  $\text{FeCl}_3$ : 5 mg/mL in 0.05 M HCl; incubation time 1: 20 min; incubation time 2: 20 min; measurement temperature: 30 °C; organic solvent: n-hexane; ..... - 42 -
- Figure 25: UV spectrum of the acetaldehyde Purpald complex; acetaldehyde  $c_{\text{final}}=1$  mM in n-hexane are shown with orange dots, n-hexane with blue dots;  $c_{\text{final}}$  (Purpald)=1 mM; NaOH: 1 M; incubation time: 15 min; measurement temperature: 30 °C; ..... - 43 -
- Figure 26: Standard calibration curve of acetaldehyde (0.1-3 mM) with standard deviations (triplicates) detected by Purpald ( $c_{\text{final}}=1$  mM) according to 2.2.1.1.4. NaOH: 1 M; incubation time: 15 min; measurement temperature: 30 °C; organic solvent: n-hexane; ..... - 43 -
- Figure 27: Standard calibration curve of acetaldehyde (0.1-3 mM,  $R^2=0.9843$ ) detected by Purpald ( $c_{\text{final}}=1$  mM) according to 2.2.1.1.4; NaOH: 1 M; incubation time: 15 min; measurement temperature: 30 °C; organic solvent: n-hexane; ..... - 43 -

- Figure 28: Color reaction of the standard calibration curve of acetaldehyde detected by Purpald ( $c_{\text{final}}=1$  mM); NaOH: 1 M; incubation time: 15 min; measurement temperature: 30 °C; organic solvent: n-hexane; ..... - 43 -
- Figure 29: Comparison of the background reaction of different substrates ( $c_{\text{final}}=0.4$  mM) in aldehyde detection by Purpald;  $c_{\text{final}}$  (Purpald)=1 mM; NaOH: 1 M; incubation time: 15 min; measurement temperature: 30 °C; organic solvent: n-hexane; ..... - 44 -
- Figure 30: Standard calibration curve of acetaldehyde (0.005-1 mM) with standard deviations (triplicates) detected by CHD in the presence of ammonia acetate after incubation for 1 h at 37 °C; measurement temperature 30 °C; organic solvent: DMSO; emission 460 nm; excitation 395 nm; ..... - 45 -
- Figure 31: Standard calibration curve of acetaldehyde (0.005-1 mM,  $R^2=0.9962$ ) detected by CHD in the presence of ammonia acetate after incubation for 1 h at 37 °C; measurement temperature 30 °C; organic solvent: DMSO; emission 460 nm; excitation 395 nm;..... - 45 -
- Figure 32: Comparison of the background reaction of different substrates ( $c_{\text{final}}=0.1$  mM) detected by CHD in the presence of ammonia acetate after incubation for 1 h at 37 °C; measurement temperature 30 °C; organic solvent: DMSO; emission 460 nm; excitation 395 nm; ..... - 45 -
- Figure 33: Reaction of enzymatic methanol detection with AOX and HRP..... - 46 -
- Figure 34: Methanol detected by AOX and HRP according to 2.2.1.2; blank (blue dots) methanol 250 mM orange dots; measurement temperature: 30 °C;..... - 46 -
- Figure 35: Comparison of the background reaction of different substrates in enzymatic methanol detection via AOX and HRP; 250 mM, methanol (blue dots), methylbutyrate (orange dots) and MeEst (DSM) (grey dots); measurement temperature: 30 °C;..... - 47 -
- Figure 36: Agarosegel after PCR 2 of EstB variant genes with the three different additives DMSO, betaine and  $\text{MgCl}_2$  recommended for GC rich sequences..... - 48 -
- Figure 37: Agarosegel colony PCR from pMS470-EstB-W134F ..... - 49 -
- Figure 38: Bio-Rad protein assay BSA standard calibration curve..... - 51 -
- Figure 39: SDS-PAGE of the lysate fraction (2.5  $\mu\text{g}$  protein) of shake flask cultivation .... - 52 -
- Figure 40: pH-shift assay of EstB variants with *E. coli* lysate (5 mg/mL) from shaking flask cultivation; the black line marks the activity of the wild type EstB; vinylbutyrate ( $c_{\text{final}}=25$  mM) was used as substrate; the pH shift of enzymatic reaction of hydrolases in the presence of water was detected with phenol red ( $c_{\text{final}}=0.01$  %); reaction time: 15 min; end point measurement at 432 nm at 30 °C; measurement of duplicates;..... - 54 -
- Figure 41: pH-shift in aqueous reaction medium of liquid *E. coli* lysate (50  $\mu\text{L}$ ) from DWP cultivations of EstB variants; vinylbutyrate ( $c_{\text{final}}=25$  mM) was used as substrate; the pH shift was detected with phenol red ( $c_{\text{final}}=0.01$  %); the yellow and the green bars indicate the lysate

---

of two different E. coli DWP cultivations; reaction time: 15 min; end point measurement at 432 nm at 30 °C; measurement of duplicates; ..... - 55 -

## 7 Literature

- Allen, C.F.H., 1930. The identification of carbonyl compounds by use of 2, 4-dinitrophenylhydrazine. *J. Am. Chem. Soc.* 344, 2955–2959.
- Anthon, G.E., Barrett, D.M., 2004. Comparison of three colorimetric reagents in the determination of methanol with alcohol oxidase. Application to the assay of pectin methylesterase. *J. Agric. Food Chem.* 52, 3749–3753.
- Arakawa, T., Goddette, D., 1985. The mechanism of helical transition of proteins by organic solvents. *Arch. Biochem. Biophys.* 240, 21–32.
- Aranda, J., Cerqueira, N.M.F.S.A., Fernandes, P.A., Roca, M., Tunon, I., Ramos, M.J., 2014. The catalytic mechanism of carboxylesterases: a computational study. *Biochemistry* 53, 5820–5829.
- Arpigny, J.L., Jaeger, K., 1999. Bacterial lipolytic enzymes: classification and properties. *Biochem. J.* 343, 177–183.
- Bailey, A.L., Wortley, G., Southon, S., 1997. Measurement of aldehydes in low density lipoprotein by high performance liquid chromatography. *Free Radic. Biol. Med.* 23, 1078–1085.
- Beasley, R.K., Hoffmann, C.E., Rueppel, M.L., Worley, J.W., 1980. Sampling of formaldehyde in air with coated solid sorbent and determination by high performance liquid chromatography. *Anal. Chem.* 52, 1110–1114. doi:10.1021/ac50057a026
- Beilen, J.B. van, Li, Z., 2002. Enzyme technology: an overview. *Curr. Opin. Biotechnol.* 13, 338–344. doi:10.1016/S0958-1669(02)00334-8
- Bornscheuer, U., Kazlauskas, R.J., 2011. Survey of protein engineering strategies. *Curr. Protoc. Protein Sci.* 1, 1–14. doi:10.1002/0471140864.ps2607s66
- Bornscheuer, U.T., 2002. Microbial carboxyl esterases: classification, properties and application in biocatalysis. *FEMS Microbiol. Rev.* 26, 73–81.
- Bornscheuer, U.T., Pohl, M., 2001. Improved biocatalysts by directed evolution and rational protein design. *Curr. Opin. Chem. Biol.* 5, 137–143. doi:10.1016/S1367-5931(00)00182-4
- Böttcher, D., Bornscheuer, U.T., 2010. Protein engineering of microbial enzymes. *Curr. Opin. Microbiol.* 13, 274–282. doi:10.1016/j.mib.2010.01.010
- Boyce, S., Tipton, K.F., 2001. Enzyme Classification and Nomenclature. *Encycl. life Sci.* 1–11. doi:10.1002/9780470277577.ch6
- Brady, O.L., 1931. The use of 2,4-dinitrophenylhydrazine as a reagent for carbonyl compounds. *J. Chem. Soc.* 756–759.
- Brink, L.E.S., Tramper, J., 1985. Optimization of organic solvent in multiphase biocatalysis. *Biotechnol. Bioeng.* 27, 1258–1269.
- Buchholz, K., Kasche, V., 2006. Biocatalysts and enzyme technology. *Focus Catal.* 2006, 8.
- Cadwell, R.C., Joyce, G.F., 1992. Randomization of genes by PCR mutagenesis. *Genome Res.* 2, 28–33.
- Carrea, G., Ottolina, G., Riva, S., 1995. Role of solvents in the control of enzyme selectivity in organic media. *Trends Biotechnol.* 13, 63–70. doi:10.1016/S0167-7799(00)88907-6
- Dickinson, R.G., Jacobsen, N.W., 1970. A new sensitive and specific test for the detection of aldehydes: Formation of 6-Mercapto-3-substituted-s-triazolo(4,3-b)-s-tetrazines. *Chem. Commun.* 1719–1720.
- Dordick, J.S., 1989. Enzymatic catalysis in monophasic organic solvents. *Enzyme Microb. Technol.* 11, 194–211.
- Dröge, M.J., Bos, R., Boersma, Y.L., Quax, W.J., 2005. Comparison and functional characterisation of three homologous intracellular carboxylesterases of *Bacillus subtilis*. *J. Mol. Catal. B Enzym.* 32, 261–270. doi:10.1016/j.molcatb.2004.12.010
- Eberhardt, M.A., Sieburth, J.M., 1985. A colorimetric procedure for the determination of aldehydes in seawater and in cultures of methylotrophic bacteria. *Mar. Chem.* 17, 199–212.
- Faber, K., 2011. *Biotransformations in organic chemistry: a textbook.* Springer Science & Business Media.



- Fleming, C.D., Bencharit, S., Edwards, C.C., Hyatt, J.L., Tsurkan, L., Bai, F., Fraga, C., Morton, C.L., Howard-Williams, E.L., Potter, P.M., Redinbo, M.R., 2005. Structural insights into drug processing by human carboxylesterase 1: Tamoxifen, mevastatin, and inhibition by benzil. *J. Mol. Biol.* 352, 165–177. doi:10.1016/j.jmb.2005.07.016
- Frackman, S., Kobs, G., Simpson, D., Storts, D., 1998. Betaine and DMSO: Enhancing agents for PCR. *Promega Notes* 65, 27–30.
- Gandolfi, R., Gualandris, R., Zanchi, C., Molinari, F., 2001. Resolution of (RS)-2-phenylpropanoic acid by enantioselective esterification with dry microbial cells in organic solvent. *Tetrahedron Asymmetry* 12, 501–504. doi:10.1016/S0957-4166(01)00033-7
- Grosjean, D., Fung, K., 1982. Collection efficiencies of cartridges and microimpingers for sampling of aldehydes in air as 2,3-dinitrophenylhydrazones. *Anal. Chem.* 54, 1221–1224.
- Gutteridge, A., Thornton, J.M., 2005. Understanding nature's catalytic toolkit. *Trends Biochem. Sci.* 30, 622–629.
- Hauser, T., Cummins, R., 1964. Increasing sensitivity of 3-methyl-2-benzothiazolone hydrozone test for analysis of aliphatic aldehydes in air. *Anal. Chem.* 36, 679–681.
- Holley, A.E., Walker, M.K., Cheeseman, K.H., Slater, T.F., 1993. Measurement of n-alkanals and hydroxyalkenals in biological samples. *Free Radic. Biol. Med.* 15, 281–289.
- Hünig, S., Fritsch, K. oxydative K.I.-T. und D.H., 1957. Azofarbstoffe durch oxydative Kupplung III. *Liebigs Ann. Chem.* 609, 172–180.
- Inada, Y., Takahashi, K., Yoshimoto, T., Ajima, A., Matsushima, A., Saito, Y., 1986. Application of polyethylene glycol-modified enzymes in biotechnological processes: organic solvent-soluble enzymes. *Tibtech* 190–194.
- Ingalls, R.G., Squires, R.G., 1975. Reversal of enzymatic hydrolysis: Rate and extent of ester synthesis as catalyzed by chymotrypsin and subtilisin Carlsberg at low water concentrations 17, 1627–1637.
- Ivancic, M., Valinger, G., Gruber, K., Schwab, H., 2007. Inverting enantioselectivity of *Burkholderia gladioli* esterase EstB by directed and designed evolution. *J. Biotechnol.* 129, 109–122.
- Jacobsen, N.W., Dickinson, R.G., 1974. Spectrometric assay of aldehydes as 6-mercapto-3-substituted-s-triazolo(4,3-b)-s-tetrazines. *Anal. Chem.* 46, 298–299.
- Jaeger, K.E., Reetz, M.T., 1998. Microbial lipases form versatile tools for biotechnology. *Trends Biotechnol.* 16, 396–403.
- Jakubke, H.D., Kuhl, P., Könnicke, A., 1985. Basic principles of protease-catalyzed peptide bond formation. *Angew. Chem. Int. Ed. Engl.* 24, 85–93.
- Janssen, F.W., Ruelius, H., 1968. Alcohol oxidase, a flavoprotein from several basidiomycetes species - crystallisation by fractional precipitation with polyethylene glycol. *Biochim. Biophys. Acta* 151, 330–342.
- Jendral, J. a, Monakhova, Y.B., Lachenmeier, D.W., 2011. Formaldehyde in Alcoholic Beverages: Large Chemical Survey Using Purpald Screening Followed by Chromotropic Acid Spectrophotometry with Multivariate Curve Resolution. *Int. J. Anal. Chem.* 2011, 1–11. doi:10.1155/2011/797604
- Kazlauskas, R.J., 2000. Molecular modeling and biocatalysis: Explanations, predictions, limitations, and opportunities. *Curr. Opin. Chem. Biol.* 4, 81–88. doi:10.1016/S1367-5931(99)00056-3
- Kazlauskas, R.J., Bornscheuer, U.T., 2009. Finding better protein engineering strategies. *Nat. Chem. Biol.* 5, 526–9. doi:10.1038/nchembio0809-526
- Keeseey, J., 1987. *Biochemica Information*, 1st ed. Boehringer Mannheim Biochemicals, Indianapolis.
- Khmelnitsky, Y.L., Levashov, A. V., Klyachko, N.L., Martinek, K., 1988. Engineering biocatalytic systems in organic media with low water content. *Enzym. Microb. Technol.* 10, 710–724.
- Klibanov, A.M., 1989. Enzymatic catalysis in anhydrous organic solvents. *TIBS* 141–144.
- Koizumi, H., Suzuki, Y., 1988. High-performance liquid chromatography of aliphatic aldehydes by means of post-column extraction with fluoromeric detection. *J. Chromatogr. Elsevier Sci. Publ. B.V* 457, 299–307.

- Konarzycka-Bessler, M., Bornscheuer, U.T., 2003. A high-throughput-screening method for determining the synthetic activity of hydrolases. *Angew. Chemie - Int. Ed.* 42, 1418–1420.
- Konopińska, D., Muzalewski, F., 1983. Proteolytic enzymes in peptide synthesis. *Mol. Cell. Biochem.* 51, 165–175.
- Kuntz, I.D., Kauzmann, W., 1974. Hydration of proteins and polypeptides, in: C.B. Anfinsen, J.T.E., Richards, F.M. (Eds.), *Advances in Protein Chemistry*. Academic Press, pp. 239–345.
- Laane, C., Boeren, S., Vos, K., Veeger, C., 1987. Rules for optimization of biocatalysis in organic solvents. *Biotechnol. Bioeng.* 30, 81–87.
- Lee, M.Y., Dordick, J.S., 2002. Enzyme activation for nonaqueous media. *Curr. Opin. Biotechnol.* 13, 376–384.
- Li, G., Wang, K., Liu, Y.H., 2008. Molecular cloning and characterization of a novel pyrethroid-hydrolyzing esterase originating from the Metagenome. *Microb. Cell Fact.* 7, 38. doi:10.1186/1475-2859-7-38
- Li, Q., Sriharathikhun, P., Motomizu, S., 2007. Development of novel reagent for Hantzsch reaction for the determination of formaldehyde by spectrophotometry and fluorometry. *Anal. Sci.* 23, 413–7. doi:10.2116/analsci.23.413
- Lutz, S., Ostermeier, M., Moore, G.L., Maranas, C.D., Benkovic, S.J., 2001. Creating multiple-crossover DNA libraries independent of sequence identity. *Proc. Natl. Acad. Sci. U. S. A.* 98, 11248–11253. doi:10.1073/pnas.201413698
- Mateos-Díaz, E., Rodríguez, J.A., Camacho-Ruiz, M. de los Á., Mateos-Díaz, J.C., 2012. High-throughput screening method for Lipases/Esterases - *Methods and Protocols*, in: Sandoval, G. (Ed.), *Lipases and Phospholipases*. Springer Science & Business Media, pp. 89–100.
- Mine, Y., Fukunaga, K., Itoh, K., Yoshimoto, M., Nakao, K., Sugimura, Y., 2003. Enhanced enzyme activity and enantioselectivity of lipases in organic solvents by crown ethers and cyclodextrins. *J. Biosci. Bioeng.* 95, 441–447.
- Nash, T., 1953. The colorimetric estimation of formaldehyde by means of the Hantzsch reaction. *Biochem. J.* 55, 416–421.
- Nebel, G., 1981. Determination of total aliphatic aldehydes in auto exhaust by a modified 2-methyl-2-benzothiazolinone hydrazone method 53, 1708–1709.
- Ollis, D.L., Cheah, E., Cyglerl, M., Dijkstra, B., Frolow, F., Franken, S.M., Harel, M., Remington, S.J., Silman, I., Schragl, J., Sussman, J.L., Goldmans, A., 1992. The  $\alpha / \beta$  hydrolase fold 5, 197–211.
- Ostermeier, M., Shim, J.H., Benkovic, S.J., 1999. A combinatorial approach to hybrid enzymes independent of DNA homology. *Nat. Biotechnol.* 17, 1205–1209. doi:10.1038/70754
- Panda, T., Gowrishankar, B.S., 2005. Production and applications of esterases. *Appl. Microbiol. Biotechnol.* 67, 160–169. doi:10.1007/s00253-004-1840-y
- Patsch, R., Höhne, C., 1971. Der Einfluss verschiedener organischer Lösungsmittel auf das Wachstum von Bakterien. *Zeitschrift für Allg. Mikrobiol.* 11, 49–56.
- Persson, M., Mladenoska, I., Wehtje, E., Adlercreutz, P., 2002a. Preparation of lipases for use in organic solvents. *Enzyme Microb. Technol.* 31, 833–841.
- Persson, M., Wehtje, E., Adlercreutz, P., 2002b. Factors governing the activity of lyophilised and immobilised lipase preparations in organic solvents. *ChemBioChem* 3, 566–571.
- Petek, S.M., 2015. Development of a colorimetric screening assay for aldehyde detection.
- Petersen, E.I., Valinger, G., Sölkner, B., Stubenrauch, G., Schwab, H., 2001. A novel esterase from *Burkholderia gladioli* which shows high deacetylation activity on cephalosporins is related to  $\beta$ -lactamases and DD-peptidases. *J. Biotechnol.* 89, 11–25.
- Pickard, A.D., Clark, E.R., 1984. The determination of traces of formaldehyde. *Talanta* 31, 763–771.
- Pohn, B., 2005. Screening systems for directed evolution of enzymes. Applied Biocatalysis Research Centre.
- Quax, W.J., Broekhuizen, C.P., 1994. Development of a new *Bacillus carboxyl* esterase for use in the resolution of chiral drugs. *Appl. Microbiol. Biotechnol.* 41, 425–431.

- Quesenberry, M.S., Lee, Y.C., 1996. A rapid formaldehyde assay using Purpald reagent: application under periodation conditions. *Anal. Biochem.* 234, 50–55.
- Quinney, S.K., Sanghani, S.P., Davis, W.I., Hurley, T.D., Sun, Z., Murry, D.J., Bosron, W.F., 2005. Hydrolysis of capecitabine to 5'-deoxy-5-fluorocytidine by human carboxylesterases and inhibition by loperamide. *J. Pharmacol. Exp. Ther.* 313, 1011–1016. doi:jpet.104.081265 [pii]r10.1124/jpet.104.081265
- Redinbo, M.R., Potter, P.M., 2005. Mammalian carboxylesterases: From drug targets to protein therapeutics. *Drug Discov. Today* 10, 313–325. doi:10.1016/S1359-6446(05)03383-0
- Romano, A., Gandolfi, R., Molinari, F., Converti, A., Zilli, M., Del Borghi, M., 2005. Esterification of phenylacetic and 2-phenylpropionic acids by mycelium-bound carboxylesterases. *Enzyme Microb. Technol.* 36, 432–438. doi:10.1016/j.enzmictec.2004.08.042
- Romano, D., Bonomi, F., de Mattos, M.C., de Sousa Fonseca, T., de Oliveira, M. da C.F., Molinari, F., 2015. Esterases as stereoselective biocatalysts. *Biotechnol. Adv.* 33, 547–565.
- Ru, M.T., Hirokane, S.Y., Lo, A.S., Dordick, J.S., Reimer, J.A., Clark, D.S., 2000. On the salt-induced activation of lyophilized enzymes in organic solvents: Effect of salt kosmotropicity on enzyme activity. *J. Am. Chem. Soc.* 122, 1565–1571.
- Rupley, J.A., Gratton, E., Careri, G., 1983. Water and globular proteins 18–22.
- Sangster, J., 1997. Octanol-water partition coefficients: fundamentals and physical chemistry. John Wiley & Sons.
- Sanishvili, R., Yakunin, A.F., Laskowski, R.A., Skarina, T., Evdokimova, E., Doherty-Kirby, A., Lajoie, G.A., Thornton, J.M., Arrowsmith, C.H., Savchenko, A., Joachimiak, A., Edwards, A.M., 2003. Integrating structure, bioinformatics, and enzymology to discover function: BioH, a new carboxylesterase from *Escherichia coli*. *J. Biol. Chem.* 278, 26039–26045. doi:10.1074/jbc.M303867200
- Satoh, T., Hosokawa, M., 2006. Structure, function and regulation of carboxylesterases. *Chem. Biol. Interact.* 162, 195–211. doi:10.1016/j.cbi.2006.07.001
- Sawicki, E., Carnes, R.A., 1968. Spectrophotofluorimetric determination of aldehydes with dimedone and other reagents. *Microchim. Acta* 56, 148–159.
- Sawicki, E., Hauser, T.R., Stanley, T.W., Elbert, W., 1961. The 3-methyl-2-benzothiazolone hydrazone test - Sensitive new methods for the detection, rapid estimation, and determination of aliphatic aldehydes. *Anal. Chem.* 33, 93–96.
- Schlacher, A., Stanzer, T., Osprian, I., Mischitz, M., Klingsbichel, E., Faber, K., Schwab, H., 1998. Detection of a new enzyme for stereoselective hydrolysis of linalyl acetate using simple plate assays for the characterization of cloned esterases from *Burkholderia gladioli*. *J. Biotechnol.* 62, 47–54.
- Schmidt, M., Bornscheuer, U.T., 2005. High-throughput assays for lipases and esterases. *Biomol. Eng.* 22, 51–56.
- Serdakowski, A.L., Dordick, J.S., 2008. Enzyme activation for organic solvents made easy. *Trends Biotechnol.* 26, 48–54.
- Sieber, V., Martinez, C.A., Arnold, F.H., 2001. Libraries of hybrid proteins from distantly related sequences. *Nat. Biotechnol.* 19, 456–460. doi:10.1038/88129
- Simon, L.M., László, K., Vértesi, A., Bagi, K., Szajáni, B., 1998. Stability of hydrolytic enzymes in water-organic 177.
- Singh, R., Gupta, N., Goswami, V.K., Gupta, R., 2006. A simple activity staining protocol for lipases and esterases. *Appl. Microbiol. Biotechnol.* 70, 679–682. doi:10.1007/s00253-005-0138-z
- Stemmer, W.P., 1994. Rapid evolution of a protein in vitro by DNA shuffling. *Nature.* doi:10.1038/370389a0
- Stubenrauch, G., 1991. Klonierung von Esterase-Genen aus *Pseudomonas marginata* und *Xanthomonas campestris*, sowie detaillierte Analyse des *Pseudomonas marginata* estA Gens und dessen Genprodukts (Esterase EP10). Technical University of Graz, Austria.
- Uchiyama, S., Santa, T., Okiyama, N., Fukushima, T., Imai, K., 2001. Fluorogenic and fluorescent labeling reagents with a benzofurazan skeleton. *Biomed. Chromatogr.* 15,

- 295–318.
- Uzu, S., Kanda, S., Imai, K., Nakashima, K., Akiyama, S., 1990. Fluorogenic reagents: 4-aminosulphonyl-7-hydrazino-2,1,3-benzoxadiazole, 4-(N,N-dimethylaminosulphonyl)-7-hydrazino-2,1,3-benzoxadiazole and 4-hydrazino-7-nitro-benzoxadiazole hydrazine for aldehydes and ketones. *Analyst* 115, 1477–1482.
- Valinger, G., Hermann, M., Wagner, U.G., Schwab, H., 2007. Stability and activity improvement of cephalosporin esterase EstB from *Burkholderia gladioli* by directed evolution and structural interpretation of muteins. *J. Biotechnol.* 129, 98–108.
- Vidal, N., Cavaille, J.P., Graziani, F., Robin, M., Ouari, O., Pietri, S., Stocker, P., 2014. Redox Biology High throughput assay for evaluation of reactive carbonyl scavenging capacity. *Redox Biol.* 2, 590–598.
- Vogel, R.M., Karst, U., 2000. Hydrazine reagents as derivatizing agents in environmental analysis – a critical review 781–791.
- Wagner, U.G., Petersen, E.I., Schwab, H., Kratky, C., 2002. EstB from *Burkholderia gladioli*: a novel esterase with a beta-lactamase fold reveals steric factors to discriminate between esterolytic and beta-lactam cleaving activity. *Protein Sci.* 11, 467–78.
- Wescott, C.R., Klibanov, A.M., 1994. The solvent dependence of enzyme specificity. *Biochim. Biophys. Acta (BBA)/Protein Struct. Mol.* 1206, 1–9.
- Wheelock, C.E., Phillips, B.M., Anderson, B.S., Miller, J.L., Miller, M.J., Hammock, B.D., 2008. Applications of carboxylesterase activity in environmental monitoring and toxicity identification evaluations (TIEs). *Rev. Environ. Contam. Toxicol.* 195, 117–178.
- Wong, T.S., Tee, K.L., Hauer, B., Schwaneberg, U., 2004. Sequence saturation mutagenesis (SeSaM): a novel method for directed evolution. *Nucleic Acids Res.* 32, e26. doi:10.1093/nar/gnh028
- Zaks, A., Klibanov, A.M., 1988. Enzymatic catalysis in nonaqueous solvents. *J. Biol. Chem.* 263, 3194–3201.
- Zaks, A., Klibanov, A.M., 1985. Enzyme-catalyzed processes in organic solvents. *Proc. Natl. Acad. Sci.* 82, 3192–3196.
- Zhao, H., Giver, L., Shao, Z., Affholter, J.A., Arnold, F.H., 1998. Molecular evolution by staggered extension process (StEP) in vitro recombination. *Nature* 395, 258–261.
- Zheng, J., Fu, X., Ying, X., Zhang, Y., Wang, Z., 2014. A sensitive colorimetric high-throughput screening method for lipase synthetic activity assay. *Anal. Biochem.* 452, 13–15.
- Zurek, G., Karst, U., 1997. Microplate photometric determination of aldehydes in disinfectant solutions. *Anal. Chim. Acta* 351, 247–257.